Insights into Molecular Mechanisms of Carotenoid Properties

Mendes Pinto, M.M.

2013

document version
Publisher's PDF, also known as Version of record

INSIGHTS INTO MOLECULAR MECHANISMS OF CAROTENOID PROPERTIES

Maria Manuela Mendes Pinto

2013

INSIGHTS INTO MOLECULAR MECHANISMS OF CAROTENOID PROPERTIES

Maria Manuela Mendes Pinto

INSIGHTS INTO MOLECULAR MECHANISMS OF CAROTENOID PROPERTIES

Maria Manuela Mendes Pinto

The research presented in this thesis was financially supported by the EU program Marie Curie (FP7 Initial Training Network HARVEST), by the ERC funding agency (PHOTPROT project), by the CEA interdisciplinary program Technology for Health (MEDIASPEC project), and by the National Research Agency (ANR, Cyanoprotect Project).

This thesis was reviewed and approved by

Dr. George Britton,	University of Liverpool, UK
Prof. Dr. Harry Frank,	University of Connecticut, USA
Dr. Andrew Pascal,	CEA-Saclay, France
Prof. Dr. Rienk van Grondelle,	VU University Amsterdam, The Netherlands

ISBN: 978-90-9027-735-6

Printed by Salima-Artes Gráficas, Lda - S. M. Feira

VRIJE UNIVERSITEIT

Insights into Molecular Mechanisms of Carotenoid Properties

ACADEMISCH PROEFSCHRIFT

ter verkrijging van de graad Doctor aan
de Vrije Universiteit Amsterdam,
op gezag van de rector magnificus
prof.dr. F.A. van der Duyn Schouten,
in het openbaar te verdedigen
ten overstaan van de promotiecommissie
van de Faculteit der Exacte Wetenschappen
op woensdag 16 oktober 2013 om 13.45 uur
in de aula van de universiteit
De Boelelaan 1105

door

Maria Manuela Mendes Pinto

geboren te Marco de Canaveses, Portugal

promotor: prof.dr. B. Robert

Aos meus pais

CONTENTS

CHAPTER 1	General Introduction…….	9
CHAPTER 2	Electronic absorption and ground state structure of carotenoid molecules……..	35
CHAPTER 3	Variation in carotenoid-protein interaction in bird feather proteins produces novel plumage coloration……..	53
CHAPTER 4	Mechanisms underlying carotenoid absorption in oxygenic photosynthetic proteins…….	79
CHAPTER 5	Carotenoid breakdown products- the norisoprenoids- in wine aroma..	99
	Summary……...	127
	Samenvatting……	131
	Acknowledgments……	135

CHAPTER 1

GENERAL INTRODUCTION

1. 1. Overview

Carotenoids are a group of widespread naturally occurring pigments characterized by an isoprenoid motif in their structure. Carotenoids are biosynthesised in photosynthetic organisms, whilst in animals and humans they are acquired from the diet. They are notable molecules that perform a range of vital biological functions either as intact molecules or as degraded compounds (apocarotenoids, norisoprenoids) [1]. In humans the best known attribute of carotenoids is their activity as pro-vitamin A, but they are also associated with reduced risk of several chronic health disorders and with photoprotection [2]. In plants, algae and in some bacteria, carotenoids are essential in the process of photosynthesis, performing different roles in light-harvesting [see *e.g.* 3-6] and photoprotection, having the ability to quench singlet oxygen species [see *e.g.* 7-12], to ensure the best balance between the beneficial uses of light energy and protection against light damage. Colors of carotenoids are seen in both the plant and animal kingdoms and are typically displayed in fruits, vegetables, flowers and birds. Carotenoid coloration has been considered to be essential for signalling functions, particularly in birds, where carotenoids are thought to be important for communication in many species [13-17].

The biological functions of carotenoids are strictly related to their structure. The characteristic structural feature of carotenoids is a linear conjugated polyene chain, which absorbs light in the visible region of the electromagnetic spectrum (400-500 nm). The electronic properties of the conjugate polyene chain of carotenoids are the basis of those biological functions of carotenoids that involve interactions with light, such as coloration and in photosynthesis [1].

The interest in understanding how carotenoids carry out such biological functions has driven researchers to study the electronic properties of these molecules, as has been reported extensively in the literature for four decades [18-21,26,29]. From these studies

it was possible, for instance, to establish the direct relationship between the energy of the main absorption transition $S_0 \rightarrow S_2$ and the number of C=C double bonds in the polyene chain [18-20], and to show that the absorption properties of carotenoids are influenced by the properties of the solvent, primarily the refractive index, *n*, [21-26]. New low-energy excited states have been proposed [27,28]; however, there is still controversy about the nature and dynamics of these, as reviewed recently by [29]. The complete picture of the electronic structure of carotenoids is thus very complex, making it difficult to predict with accuracy the electronic and vibrational properties of carotenoids [30].

In biological systems, carotenoids are associated with sub-cellular structures and are often present as aggregates or associated with other molecules, usually proteins [31]. Many of the biological functions of carotenoids are performed when carotenoid molecules are bound to a particular protein [32], which has specific carotenoid binding sites, interactions with which further complicate the characterization of the electronic properties of the carotenoid *in vivo*. Molecular interactions between the carotenoid and the binding site can influence the electronic properties of carotenoids and lead to a pronounced red-shift (bathochromic shift) in the absorption of the bound carotenoid compared to the absorption of the isolated carotenoid. This effect is observed with many different carotenoid molecules and in very different biological systems [32]. However, in spite of spectroscopic studies and detailed information about the carotenoid binding site provided by X-ray crystallography studies, *e.g.* of the carotenoid binding sites in photosynthetic tissues [33-39], and of crustacyanin, the blue protein in the shell of the lobster [40,41], clear descriptions of the molecular mechanism responsible for the observed carotenoid absorption shifts have not yet emerged. How these properties are tuned *in vivo*, and what are the relationships between structural features and specific function remain a challenge.

The aim of this thesis is to contribute to the understanding of such phenomenon by the identification of the molecular factors that control the light absorption properties of carotenoids in *vivo*.

In addition, a review of carotenoid molecules as precursors of important aroma coumpounds- the norisoprenoids- with high sensorial impact on wine aroma, is presented.

1.2. Carotenoid chemical structure

Carotenoids are built from an assembly of isoprenoid units, -CH=CH-CCH_3=CH-, to form a linear polyene chain, a π-electron conjugated system as the backbone of the molecular structure. Displaying an extraordinary structural diversity- chemical structures of about 700 of these molecules have been fully elucidated- they include molecules containing only carbon and hydrogen (carotenes) and molecules with enzymatically incorporated oxygen functions (xanthophylls) [42]. They can have different carbon skeletons, they can be linear or cyclic molecules, with triple and allenic bonds and with different functional groups, mainly oxygen-containing, which may or may not be conjugated with the polyene chain [42]. Such multiplicity of carotenoid structures is translated into molecules having chromophores with different structures and with different conjugation chain length, N. Structures of representative carotenoid molecules, including the carotenoids studied in this thesis, are shown in Figure 1.1.

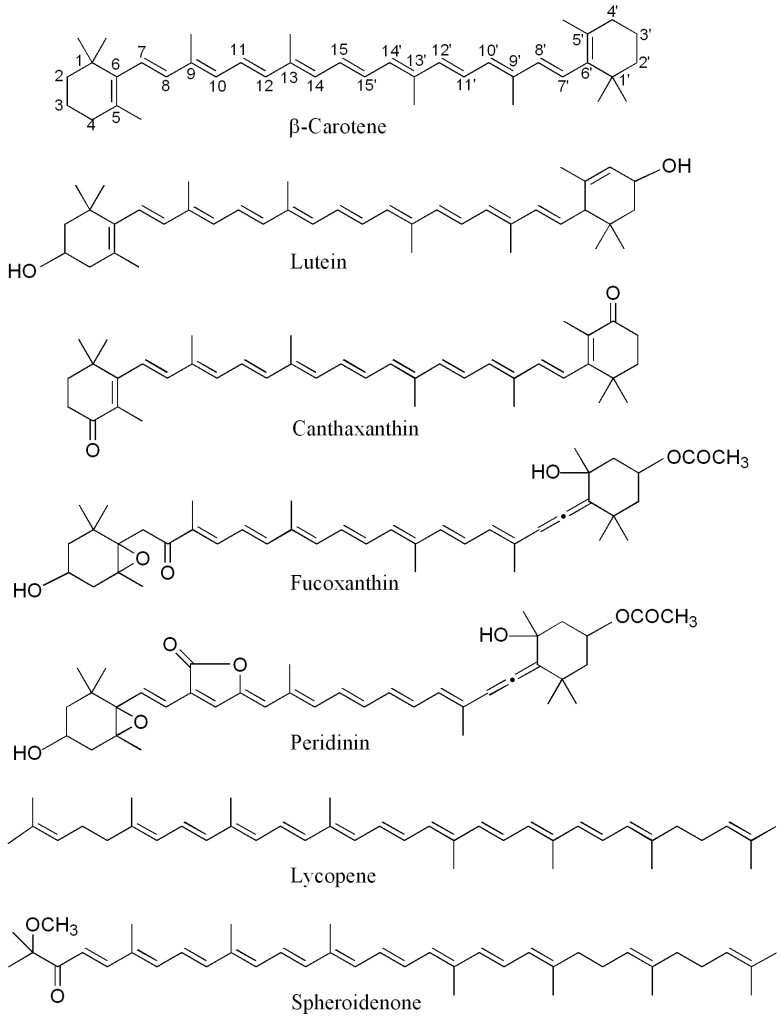

Figure 1.1. Typical structures of carotenoid molecules.

Carotenoids: three-dimensional shape and low-energy conformation

Carotenoids are three-dimensional structures and can exist in a number of configurations due to geometrical (*trans/cis* or *E/Z*) and optical (*R/S*) isomerism, and in multiple conformations due to rotations about C-C single bonds [43]. However, low-energy conformations are preferably adopted by the molecules. X-Ray crystallographic studies of carotenoid structures revealed some typical features of specific preferred low-energy conformations of carotenoid structures [44]. A*ll-trans* carotenoids are not strictly

linear molecules but have a slight bowing, and S-shape of the zig-zag polyene chain, possibly due to steric hindrance involving the methyl groups along the chain [43,45]. In cyclic carotenoids, the ring-chain conformation of the β-ring (see *e.g.* β-carotene in Figure 1.1) has been found to be in a modified *6-s-cis* conformation, in which the C(6,7) single bonds has undergone ~ 55º rotation from the *s-cis*; in some cases, even a modified *s-trans* conformation is preferred. The twisting about the C(6,7) or C(6',7') single bonds (Figure 1.2.) relieves the steric hindrance, particularly between the methyl groups at C(5) of the ring, and the hydrogen atom at C(8) of the chain, which would result from a planar arrangement, whether 6-*s-cis* or 6-*s-trans*, about the C(6,7) single bond [43] (Figure 1.2).

Figure 1.2. The extreme conformations due to twisting around the C(6,7) single bond.

1.3. Electronic structure of carotenoids

Based on pioneering theoretical studies on linear conjugated polyenes [46-54], the interpretation of the electronic structure of carotenoids followed a three-state model consisting of the ground electronic state S_0 and two low-lying excited singlet states S_1 and S_2. This description appears, however, no longer sufficient to fully describe the electronic structure of carotenoids. This follows the discovery of additional low-lying excited states that are difficult to observe by one-photon optical absorption [27,28], and are known as the dark-states, which have been proposed to lie between or in the vicinity of S_2 and S_1 [20,27,28,29,55,56]. A triplet state T_1 can also be generated within the $S_0 \rightarrow S_1$ gap, and in photosynthetic organisms can be formed by energy transfer from chlorophyll triplets [54,57].

The allowedness of transitions between electronic states is determined by symmetry considerations which give rise to selection rules. One-photon transitions between electronic states that involve a change in the symmetry designation g ↔ u or a change in

the pseudoparity sign - ↔ + are allowed, otherwise they are forbidden [56]. The use of the idealized C_{2h} point group symmetry of linear polyenes, and the symmetry of individual π-orbitals assigns the ground state S_0, as $1A_g^-$, the first excited state S_1 as $2A_g^-$, and another excited state as $1Bu^+$. Therefore, the strongest allowed π-π* transition is not to the lowest excited single state S_1 ($2A_g^-$), which is only allowed by two-photon absorption, but to the excited state denoted S_2 ($1B_u^+$) [54,55]. In contrast, the transition from the ground state to S_2 ($1B_u^+$), $S_0 \rightarrow S_2$, ($1A_g^- \rightarrow 1B_u^+$), is strongly allowed and is the electronic transition that is responsible for the color of carotenoids [58]. Both the S_1 and S_2 states function as energy donors in photosynthetic organisms, depending on the conjugation chain length N that determines their energy [55,59]. Also the triplet state has a photoprotective role by quenching chlorophyll triplets and scavenging of oxygen singlets [60,61]. The suggested role of the new dark states, assigned as $1B_u^-$, $3A_g^-$ and S* (of unknown symmetry) in the light-harvesting functions of carotenoids is still controversial [29,59]. The energy-level scheme of a carotenoid molecule can be represented as depicted in Figure 1.3. For the case of asymmetric carbonyl carotenoids, however, an intramolecular charge transfer state (ICT) is coupled to the S_1 state and induced by the conjugated carbonyl group [55,62-64]. This state is responsible for the characteristic polarity dependence of the excited states of carbonyl-containing carotenoids.

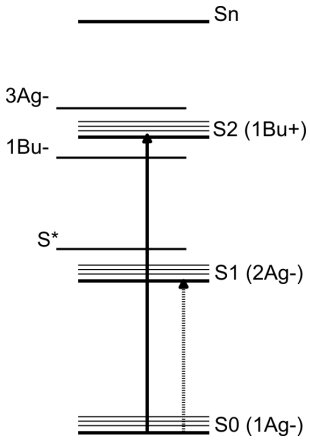

Figure 1.3. A general energy-level diagram of a carotenoid molecule. The solid arrow indicates the strongly allowed $S_0 \rightarrow S_2$ transition; the dotted arrow indicates a forbidden transition.

1.4. The $S_0 \rightarrow S_2$ transition: the carotenoid absorption spectrum

The $S_0 \rightarrow S_2$ electronic transition is responsible for the strongly allowed absorption from the ground state (S_0) to second lowest energetic excited state (S_2). This transition typically corresponds to light absorption in the visible region of the electromagnetic spectrum, and is the origin of the color of the carotenoids [58]. In the minimum energy structure or ground state S_0 ($1A_g^-$), all bonding molecular orbitals are doubly occupied. The promotion of one electron from the highest-energy occupied molecular orbital (HOMO) to the lowest energy-unoccupied molecular orbital (LUMO), generates the excited state S_2 ($1B_u^+$) [53]. This π-π* transition is the strongest allowed transition because it occurs between states with different symmetry. The fact that the conjugated π-electrons are highly delocalised along the chain, makes it easier to promote an electron to the excited state, *i.e.,* the energy required to generate the transition is relatively low and corresponds typically to light in the visible rather than the UV region of the spectrum.

The carotenoid absorption spectrum shows, in most cases, a strong absorption band in the blue-green region (400-500 nm) or, in some cases, in the UV region. The strong absorption band can appear as a single band, or as a more defined three-peaked shape from vibrational structure (or spectral fine structure), which arises from transitions from the lowest vibrational level of the ground state to the vibrational levels 0, 1 and 2, of the excited state [53,58]. The transition between zero-point vibrational level, the (0-0) transition is also referred as vibrational band or spectral origin, and corresponds to the lowest energy band, occuring at the longest wavelength in the absorption spectrum. Figure 1.4 shows typical absorption spectra of carotenoid molecules in hexane.

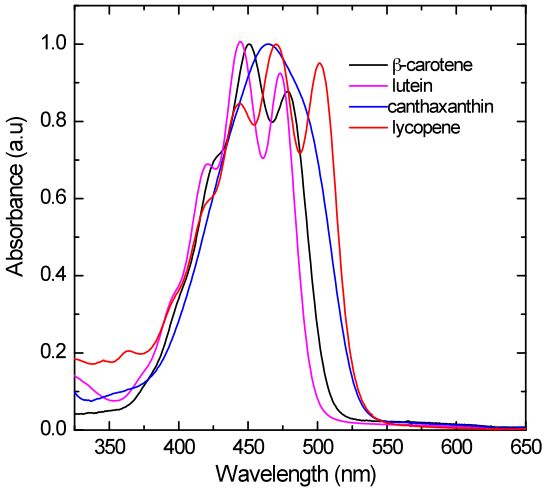

Figure 1.4. Room temperature absorption spectra of some carotenoids in hexane.

The position of the absorption band, *i.e.*, the energy of the electronic transition $S_0 \rightarrow S_2$, and resolution of the vibrational structure, indicate specific carotenoid structural features of the chromophore. They are both dependent on N and are affected by the electrostatic properties of the solvent.

Conjugation chain length N

The evidence that the number of C=C double bounds is directly related to the position of the absorption maximum was provided by Araki G. and T. Murai in the early 1950's. [65]. Based on studies of linear polyenes, it was established that the position of the absorption maximum for linear carotenoids is related to the number of C=C double bonds in the polyene chain [18-20]. The simple versions of the theoretical models describing π-π* transitions (molecular orbital theory or by the free-electron model ('particle in a box') explain why the position of the $S_0 \rightarrow S_2$, transition shifts to longer wavelength with increasing conjugation chain length N [54].

An empirical relation between the energy of the electronic transition $S_0 \rightarrow S_2$ and the conjugation chain length was established from studies on linear homologous series [53,54] These studies with molecules with $4 \leq N \leq 10$ showed that the energy of the $S_0 \rightarrow S_2$ electronic transition can be predicted by the dependence A + B /N, where N is the

number of conjugated C=C double bonds, A and B are adjustable parameters (A is the (0-0) vibrational band of the electronic transition for the $S_0 \rightarrow S_2$ transition for an infinite carotenoid). Different empirical relations from several series of homologues of polyenes and carotenoid molecules with different N have been established, providing different extrapolated values for the energy of the $S_0 \rightarrow S_2$ (0-0) transition [54,55 and references therein]. For example, for the natural carotenoids of photosynthetic systems, with $9 \leq N \leq 13$, the (0-0) transitions are located between 475 and 525 nm (21200 and 19000 cm^{-1}) [55]. Experimental data suggest an asymptotic limit of ~ 700 nm (~ 14,000 cm^{-1}) of infinite polyenes and carotenoids.

However, the conjugation chain length N is not always exclusively the number of conjugated C=C bonds in the polyene chain ("nominal" N). For non-linear molecules the "effective" conjugation length N should be estimated taking into account the effect of the ring C=C double bonds or substituents [53,67]. Whilst for β-ring cyclic carotenoids the effective conjugation chain length is shorter than that expected from their chemical structure due to decrease of orbital overlap between the π-orbital of the ring double bond and those of the polyene chain, caused by twisting of the β-ring [43,58], in carbonyl carotenoids the presence of the carbonyl group extends the conjugated part of the chromophore, resulting in a spectral shift to longer wavelengths [58]. In the case of aryl carotenoids the additional C=C double bonds in the ϕ-ring do not contribute to the conjugation chain length [43,66].

The spectral vibrational structure is also influenced by the presence of β-rings or carbonyl groups. The reduction of the vibrational structure of β-ring cyclic carotenoids compared to equivalent linear molecules [42] is a consequence of the large number of conformers differing in the angle of twist of the C(6,7) or C(6',7') single bonds [67]. For carbonyl carotenoids there is a characteristic lack of vibrational structure, as in canthaxanthin; in the case of asymmetric molecules such as peridinin, the vibrational structure is solvent dependent [64].

In Chapter 2 it is shown that, for several *all-trans* β-ring molecules in hexane solution, the C=C double bond on the β-ring accounts for only a fraction of a full C=C double bond, with an average of 0.3 for all the molecules studied. This shortening of the effective conjugation chain length is rationalized in terms of steric hindrance between the methyl group at C(5) of the β-ring and the hydrogen atom at C(8) of the chain, which induces the molecule to adopt an out-of-plane *cis*-like conformation [43,58].

Solvent effects

The effect of solvent properties, namely refractive index, n, and dielectric constant, ε, on the position of the absorption transition of carotenoid molecules has been studied extensively [21-26]. It has been shown that the position of the (0-0) band of the $S_0 \rightarrow S_2$ electronic transition in solution depends primarily on the refractive index, n. When expressed as function of the solvent polarizability, $R(n) = (n^2-1) / (n^2+2)$, the 0-0 transition of a carotenoid molecule shifts to longer wavelength as the refractive index, n, increases [26]. Dispersive interactions between the solvent environment and the carotenoid large transition dipole moment are considered to be the major factor responsible for these shifts. The absorption shifts caused by polarity are of smaller magnitude [26].

Asymmetric carbonyl carotenoids show a particular behaviour in relation to solvent. The absorption spectrum is shown to be a single broad band in polar solvents such as methanol, whereas in some non-polar solvents, *e.g.* petrol or hexane, a well defined spectral fine structure is observed [58,62]. Although this effect has been suggested to be due to the polarity induced by the carbonyl group, the nature of the ICT sate, and how it affects the dynamic and electronic properties of these carbonyl carotenoids is not yet clear [68,69].

1.5. Carotenoid-protein complexes

In Nature, many carotenoids with different chemical structures are non-covalently bound to proteins [32]. By such binding, the solubility of the carotenoid in the aqueous cellular environment is enhanced, and their electronic properties and conformation can change according to the specific conditions of the binding site. The result of such

carotenoid-protein interactions is often a red-shift of the carotenoid absorption maximum. The most impressive absorption shift for a carotenoid in biological tissues is the shifted absorption of astaxanthin from 480 to 630 nm in crustacyanin, the blue carotenoid-protein complex in the shell of the lobster *Homarus gammarus* or *Homarus americanus* [32,40,41,70-73]. Many other carotenoid-protein complexes have been found in widely different biological tissues, including some bacteria, algae, plants, starfish, salmon, and skin and feathers of birds. In humans, it was recently proposed that a 'xanthophyll-binding protein' (XBP) isolated from the retina is involved in the specific delivery of xanthophylls to the macula lutea [74].

In this thesis, the absorption properties of carotenoid molecules in two very distinct biological systems have been studied, namely the carotenoid in keratin proteins of bird feathers and carotenoids in in oxygenic photosynthetic proteins (higher plants)

Case study A: Carotenoid absorption in bird feathers

Carotenoids contribute to the color of bird feathers, giving typical yellow, red and orange colors [14] and, in combination with structural colors, to green color [75-77]. Interactions between carotenoid and the keratin protein in bird feathers can produce novel plumage coloration. Moreover, due to the highly heterogeneous amino acid composition that can vary even in the same feathers, a single type of carotenoid can have different colors in the plumage of birds because of differences in interactions with the keratin [78,79]. Carotenoid colors in feathers are associated with signalling functions, which are believed to be important for communication in many birds in, for example, species recognition and health quality status [13-17]. The electronic properties of carotenoids bound to the structural proteins have been reported only for the red and yellow feathers of the European goldfinch (*Carduelis carduelis*) pigmented by the canary xanthophylls (ε,ε-carotene-3,3'-dione and 3'-hydroxy-ε,ε-caroten-3-one) [77]. How the same carotenoid can produce the two different colors is not clear. Knowledge of the absorption properties of carotenoids in bird feathers is extremely limited.

A spectroscopic study of different colored feathers of three bird species containing canthaxanthin as their primary pigment is presented in Chapter 3. Figure 1.5 shows the

plumage of the birds: the brilliant red scarlet ibis (*Eudocimus ruber*, Threskiornithidae), the orange-red summer tanager (*Piranga rubra*, Cardinalidae) and the violet-purple feathers of the white-browed purpletuft (*Iodopleura isabellae*, Tityridae).

Figure 1.5. Plumages coloration of the A: scarlet ibis *Eudocimus ruber* (Threskiornithidae, image courtesy of G. Armistead/VIREO); B: the male summer tanager *Piranga rubra* (Cardinalidae, image courtesy of R. Nussbaumer/VIREO), and C: the white-browed purpletuft *Iodopleura isabellae* (Tityridae, photograph courtesy of Nick Athanas).

Case study B: Carotenoids in oxygenic photosynthetic proteins (higher plants)

Carotenoids are ubiquitous in photosynthetic organisms where they are associated with pigment-protein complexes in the membranes and perform vital roles in light-harvesting by complementing the weak chlorophyll absorption in the blue-green region of the spectrum [see *e.g.* 3-6] and in photoprotection either by quenching chlorophyll triplet states [1,8,9], by scavenging singlet oxygen directly [7] or by dissipating excess energy [10-12].

The electronic properties of carotenoids in photosynthetic tissues have been studied extensively in many pigment-protein complexes, which involve various carotenoid structures: (i) linear molecules in purple bacteria (*e.g.* spheroidene, neurosporene and spirilloxanthin) [80-82], (ii) cyclic molecules *(e.g.* β-carotene, lutein, and xanthophylls cycle pigments in higher plants [5,83-86], and (iii) carbonyl carotenoids, mostly highly substituted, in marine algae, (*e.g.* 3-hydroxyechinenone [87,88], peridinin [89] and fucoxanthin [90,91].

However, in spite of the many spectroscopic studies, and molecular information about the carotenoid binding site provided by the X-ray crystallography structures [33-39], the

cause of the absorption shifts of carotenoids bound in photosynthetic complexes has not yet been elucidated.

In order to know more about the light absorption properties of carotenoids, we selected the case of the two β-carotenes in the photosystem II reaction centers (PSII-RC) and the two luteins in light-harvesting complex II (LHCII). The spectroscopic study and possible relation with specific structural features for all four carotenoid molecules is presented in Chapter 4. The localization of the binding pockets of the two luteins (LHCII) and the two β-carotenes in (PSII-RC) are shown in Figures 1.6 and 1.7 respectively.

The PSII-RC binds two β-carotene molecules, which at low temperature have their main absorption transition at 489 nm and 507 nm, respectively [83-85] the former being perpendicular and the latter parallel to the membrane plane [36,83].

LHCII is assembled into a trimeric form in the photosynthetic membrane, with each monomer containing two lutein molecules (lut1, lut2) whose binding sites are related by pseudosymmetry. Whilst in LHCII monomers these luteins both absorb at 495 nm, in LHCII trimers one of them (lut2) has its absorption shifted to 510 nm; lut1 absorption remains at 495 nm [5,86].

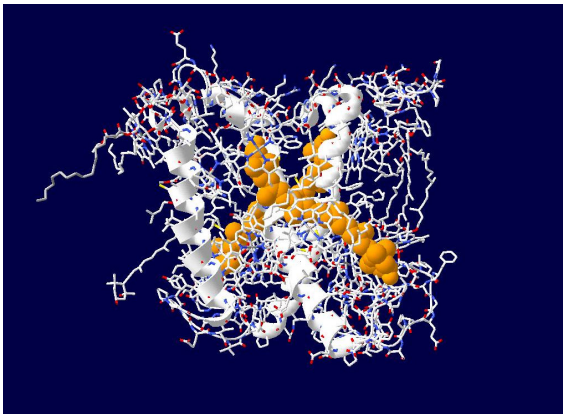

Figure 1.6. Lutein molecules (in orange) in the LHCII monomer from spinach *(Spinacia oleracea)*.

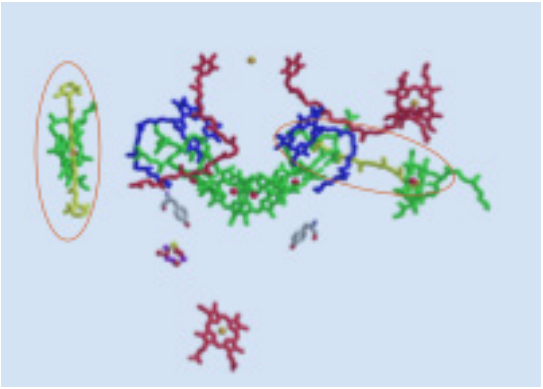

Figure 1.7. β-Carotene molecules (in the ovals) of PSII reaction center complex from the cyanobacterium *T. elongatus*.

1.6 Theory on the basis of carotenoid absorption shifts *in vivo*

Advanced spectroscopic approaches and theoretical calculations associated with the high-resolution X-ray crystallography structure of the carotenoid binding site have the potential to allow spectroscopic information to be related with structural features. Although few three-dimensional structures of the carotenoid-proteins complexes are available, most of what is known about carotenoid behaviour related to detailed structural features *in vivo* has been obtained from the extensive research on astaxanthin in the blue crustacyanin proteins of the lobster [32,40,41,70-73]. On the other hand, early research work on carotenoids that function in photosynthesis speculated about possible mechanisms for the carotenoid absorption shift in those pigment-protein complexes [23,92].

Specific carotenoid location, orientation and distances from other molecules such as chlorophylls, water molecules, amino acid residues, and other carotenoid molecules, in the protein environment define potentially the role of each factor, which can act *per se* or in combination with other factors. The proposed theories on how the electronic properties of carotenoid molecules are tuned are:

1- Conformational changes between free carotenoid and that bound to protein.

2- Increase of conjugation chain length N due to increased coplanarity of the β-end rings with the polyene chain.
3- Polarization effect due to protein environment mediated by polar aminoacid residues or bound water molecules.
3- Excitonic coupling arising from the close proximity of the chromophores of different carotenoid molecules in the protein binding site.
4- Average polarizability of the carotenoid binding site.

Chapters 3 and 4 present the contribution of β-rings to the conjugation chain length of canthaxanthin bound to the feather proteins, and for both red-absorbing β-carotene and lutein molecules in oxygenic photosynthetic proteins, respectively. It is also proposed that the average polarizability of the carotenoid binding site can explain the absorption shift in *vivo*, either *per se* as for the photosynthetic blue-absorbing carotenoids β-carotene and lutein (Chapter 4), or in combination with other factors as in the case of canthaxanthin in bird feathers (Chapter 3). It is proposed as well that head-to tail aggregation of bound canthaxanthin can be an additional factor accounting for the absorption shift of the purple feather.
From the information in Chapter 2, average polarizability of the carotenoid binding site is proposed to account for the absorption shifts of carotenoids bound to light-harvesting (LH) proteins in purple photosynthetic bacteria.

1.7. Experimental

Resonance Raman spectroscopy associated with electronic absorption is an experimental approach used for the analysis of carotenoid structure. As a vibrational technique, resonance Raman provides direct information of the structure of the electronic ground state of the carotenoid molecule [93-95]. By matching the energy of incident light that is scattered by the molecule with the energy of its electronic transition (resonance effect), it allows selective probing of a given molecule in a complex medium but also makes it possible to distinguish the same carotenoid molecule in a different protein environment. It is thus possible to characterize the specific carotenoid structure *in vivo* [93,96]. It yields structural information including the conjugation length of the

conjugated double bond chain, the geometric configuration (*cis-trans*), and the degree of distortion of the conjugated double bond chain [94,95,97].

Principle of resonance Raman spectroscopy

The Raman effect is the phenomenon of an exchange of energy between a polyatomic molecule and a photon, during scattering (Figure 1.8A). When a photon of light (thick grey arrow) collides with a molecule (turquoise box), the scattered light can be of three types: (i) Rayleigh: the majority of scattered light has same energy as the incident light and thus the same wavelength (green arrow); after the collision, the molecule returns to its ground state; (ii) anti-Stokes Raman: the molecule starts from a higher vibrational level than the one it reaches in after collision. In this case the emitted photon is of higher energy (shorter wavelength, toward the blue end of the spectrum, blue arrow); and (iii) lower energy (Stokes Raman) where the molecule can be moved to a higher vibrational energy level after the collision. Here scattered photon will be of lower energy (longer wavelength, towards the red end of the spectrum, red arrow). This is the case of classical Raman spectroscopy that is performed under Stokes conditions, since high energy vibrational levels are usually less populated at room temperature.

The Raman spectrum is a plot of the intensity of Raman scattered light as a function of the difference between the frequency of the incident light provided by the excitation laser beam and the frequency of the scattered light. This difference, expressed usually in units of wavenumber cm^{-1}, is called the Raman shift.

Figure 1.8. Principle of resonance Raman spectroscopy. A: Energy level diagrams involved in the Raman scattering phenomenon. B: Raman and resonance Raman [92].

The resonance effect occurs when the energy of the incoming photon (excitation light) matches that of an electronic absorption transition of the molecule (Figure 1.8B). This effect results in a dramatic enhancement of the Raman scattering. The Raman-active modes can be enhanced by as much as six orders of magnitude provided that the energy of the absorption transition matches the energy of the photon used to produce the Raman effect. Under such conditions the Raman-active modes are those coupled to the electronic transition, *i.e.* they involve only the atoms involved in that transition and the modes it affects. For carotenoid molecules resonance Raman-active modes will involve the atoms that make up the effective conjugated polyene chain length in their electronic ground state. These modes are structure-sensitive, meaning that changes in their frequencies, or the appearance of new vibrational modes or bands, indicate changes in the structure of the molecule.

Resonance Raman spectrum of carotenoid molecules

The resonance Raman spectrum of a carotenoid contain four main groups of bands denoted ν_1 to ν_4 (Figure 1.9; [95,97]). These bands are designed Raman or resonance Raman bands througout this thesis. The strongest ν_1 Raman band occurs at ~ 1550-1500

cm^{-1} and arises from the stretching modes of the conjugated C=C double bonds, mainly those near the centre of the molecule [98]. Its frequency depends on the length of the π-electron conjugated chain of the carotenoid and its configuration*, i.e.,* the existence and position of *cis/trans* isomerisation and the position of twisting along the carbon backbone of the molecule [94,99-103]. This band is a direct reflection of the C=C bond order of the conjugated chain, which itself depends on the effective conjugated chain length, N. The group of ν_2 bands between ~ 1400-1100 cm^{-1} arises mainly from stretching vibrations of C-C single bonds coupled with C-H in-plane bending modes [100]. The features of this group of bands is also sensitive to the position of twisting along the carbon backbone; this is the so called "fingerprint region" used for the assignment of carotenoid configurations. The ν_3 band at ~ 1010 cm^{-1} arises from in-plane rocking vibrations of the methyl groups attached to the conjugated chain coupled with the in-plane bending modes of the adjacent C-H bonds [95,97]. The ν_4 band at ~ 960 cm^{-1} arises from out-of-plane wagging motions of the C-H groups coupled with C=C torsional modes. For symmetry reasons these are not coupled with the electronic transition when the molecule is planar and are thus not expected to be resonance active [95,97]. However, in the case of distortions around C-C single bonds, this band can be strongly resonance enhanced [104].

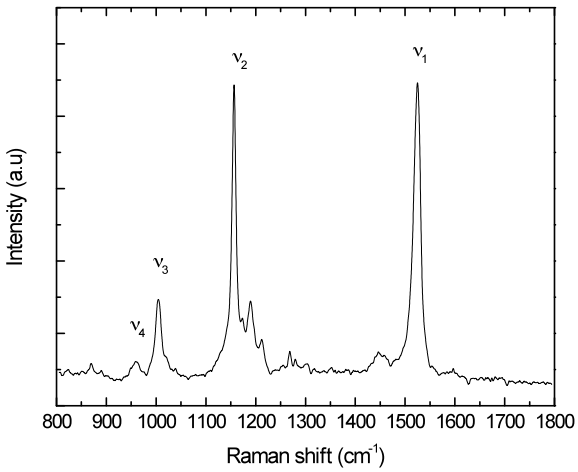

Figure 1.9. Room temperature resonance Raman spectrum of *all-trans* β-carotene in hexane.

1.8. Outline of the work presented in this thesis

In this thesis, the factors involved in the molecular mechanisms underlying carotenoid absorption shifts were investigated. The background of the research topic and the experimental strategy is given in the Introduction.

In Chapter 2 is presented a systematic study on the electronic properties of nine relatively simple linear and β-ring cyclic carotenoids *in vitro*. The correlations between the position of the $S_0 \rightarrow S_2$ electronic transition, the frequency of ν_1 Raman band and the conjugation chain length N were determined. The effect of solvent polarizability on the two spectroscopic parameters for four of these molecules was investigated. It is shown to be possible to discriminate between the change in the conjugation chain length and polarizability effects as probable mechanisms responsible for the absorption shifts of carotenoid molecules. This chapter provides groundwork for the subsequent two chapters, which examine the electronic properties of carotenoids in two very distinct biological systems.

In Chapter 3 the different colors of feathers of three bird species- scarlet ibis, summer tanager and the white-browed purpletuft, which all contain the carotenoid canthaxanthin as their primary pigment, are investigated. Results show that the significant differences in the coloration of their plumage may be due to a combination of factors associated with differences in carotenoid-protein interactions.

In Chapter 4 the absorption shifts of the two β-carotene molecules in PSII-RC and those of the two lutein molecules in LHCII are investigated in order to examine the molecular factors of the carotenoid binding pocket that may be responsible for the different electronic properties. The mechanism underlying these differences is determined and attempts are made to relate it to the three-dimensional structure of these proteins as determined by X-ray crystallography.

An additional chapter present a review on carotenoid breakdown products- the norisoprenoids- in wine aroma (Chapter 5).

REFERENCES

[1] Britton, G., Liaaen-Jensen, S., Pfander, H. (eds). 2008. *Carotenoids: natural fucntions, vol. 4* Basel, Switzerland; Boston, MA; Berlin, Germany: Birkhäuser.

[2] Britton, G., Liaaen-Jensen, S., Pfander, H. (eds). 2009. *Carotenoids: nutrition and health, vol. 5* Basel, Switzerland; Boston, MA; Berlin, Germany: Birkhäuser.

[3] Cogdell, R. J., Gillbro, T., Andersson, P. O., Liu, R. S. H., and Asato, A. E. 1994. Carotenoids as accessory light-harvesting pigments. *Pure Appl. Chem.* 66, 1041-1046.

[4] Horton, P., Ruban, A. V., Walters, R. G. 1996. Regulation of light harvesting in green plants. *Annu. Rev. Plant Physiol. Plant Molec. Biol.* 47**,** 655-684.

[5] Ruban, A. V., Pascal., A. A., Robert B. 2000. Xanthophylls of the major photosynthetic light-harvesting complex of plants: identification, conformation and dynamics. *FEBS* 477, 181-185.

[6] Polivka, T., Frank, H. A. 2010. Molecular factors controlling photosynthetic light harvesting by carotenoids. *Accounts Chem. Res.* 43, 1125-1134.

[7] Foote, C. S. 1976. Photosensitized oxidation and singlet oxygen: consequences in biological systems. In: *Free radicals in biology.* (ed. William Pryor), pp. 85-133. New York, NY: Academic Press.

[8] Truscott, T. G., Land, E. J., Sykes, A. 1973. *In-vitro* photochemistry of biological molecules. 3. Absorption-spectra, lifetimes and rates of oxygen quenching of triplet-states of β-carotene, retinal and related polyenes. *Photochem. Photobiol.* 17**,** 43-51.

[9] Niyogi, K. K., Bjorkman, O.,Grossman, A. R. 1997. The roles of specific xanthophylls in photoprotection. *Proc. Natl. Acad. Sci. USA* 94**,** 14162-14167.

[10] Ruban, A. V., Berera, R., Ilioaia, C., van Stokkum, I. H. M., Kennis, J. T. M., Pascal, A. A., van Amerongen, H., Robert, B., Horton, P., van Grondelle, R. 2007. Identification of a mechanism of photoprotective energy dissipation in higher plants. *Nature* 450, 575-578.

[11] Ahn, T. K., Avenson, T. J., Ballottari, M., Cheng, Y. C., Niyogi, K. K., Bassi, R., Fleming, G. R. 2008. Architecture of a charge-transfer state regulating light harvesting in a plant antenna protein. *Science* 320, 794-797.

[12] Wilson, A., Punginelli, C., Gall, A., Bonetti, C., Alexandre, M., Routaboul, J. M., Kerfeld, C. A., van Grondelle, R., Robert, B., Kennis, J. T. M., Kirilovsky, D. 2008. A photoactive carotenoid protein acting as light intensity sensor. *Proc. Natl. Acad. Sci. USA* 105, 12075-12080.

[13] Blount, J. D., McGraw, K. J. 2008. Signal functions of carotenoid coloration. In: *Carotenoids vol 4: natural functions*. (eds. G. Britton, S. Liaaen-Jensen, H. Pfander), pp. 213-232. Basel, Switzerland; Boston, MA; Berlin, Germany: Birkhäuser.

[14] McGraw, K. J. 2006. Mechanics of carotenoid-based coloration. In: *Bird coloration vol 1: mechanisms and measurements*. (eds. G. E. Hill, K. J. McGraw), pp. 177-242. Cambridge, MA: Harvard University Press.

[15] Stoddard, M. C., Prum, R. O. 2011. How colorful are birds? Evolution of the avian plumage color gamut. *Behav. Ecol.* 22, 1042-1052.

[16] Hill, G. E., McGraw, K. J. (eds). 2006. *Bird coloration, volume 1: mechanisms and measurements*. Cambridge, MA: Harvard University Press.

[17] Hill, G. E., McGraw, K. J. (eds). 2006. *Bird coloration, volume 2: function and evolution*. Cambridge, MA: Harvard University Press.

[18] Dale, J. 1954. Empirical relationships of the minor bands in the absorption spectra of polyenes. *Acta Chem. Scand.* 8, 1235-1256.

[19] Hemley, R., Kohler, B. E. 1977. Electronic-structure of polyenes related to visual chromophore. A simple model for the observed band shapes. *Biophys. J.* 20**,** 377-382.

[20] Christensen, R. L., Barney, E. A., Broene, R. D., Galinato, M. G. I., Frank, H. A. 2004. Linear polyenes: models for the spectroscopy and photophysics of carotenoids. *Arch. Biochem. Biophys.* 430, 30-36.

[21] Le Rosen, A. L., Reid, C. E. 1952. An investigation of certain solvent effect in absorption spectra. *J. Chem. Phys.* 20, 233-236.

[22] Hirayama, K. 1955. Absorption spectra and chemical structure. II. Solvent effect. *J. Am. Chem. Soc.* 77, 379-381.

[23] Andersson, P. O., Gillbro, T., Ferguson, L., Cogdell, R. J. 1991. Absorption spectral shifts of carotenoids related to medium polarizability. *Photochem. Photobiol.* 54, 353-360.

[24] Kuki, M., Nagae, H., Cogdell, R. J., Shimada, K., Koyama, Y. 1994. Solvent effect on spheroidene in nonpolar and polar solutions and the environment of spheroidene in the light-harvesting complexes of *Rhodobacter sphaeroides* 2.4.1 as revealed by the energy of the $^1Ag^- \rightarrow {}^1Bu^+$ absorption and the frequencies of the vibronically coupled C=C stretching Raman lines in the $^1Ag^-$ and 2^1Ag^- states. *Photochem. Photobiol.* 59, 116-124.

[25] Chen, Z. G., Lee, C., Lenzer, T., Oum, K. 2006. Solvent effects on the S_0 (1^1Ag^-) → S_2 (1^1Bu^+) transition of beta-carotene, echinenone, canthaxanthin, and astaxanthin in supercritical CO_2 and CF_3H. *J. Phys. Chem. A* 110, 11291-11297.

[26] Renge, I., Sild, E. 2011. Absorption shifts in carotenoids-influence of index of refraction and submolecular electric fields. *J. Photochem. Photobiol. A- Chem.* 218, 156-161.

[27] Papagiannakis, E., Kennis, J. T. M., van Stokkum, I. H. M., Cogdell, R. J., van Grondelle, R. 2002. An alternative carotenoid-to-bacteriochlorophyll energy transfer pathway in photosynthetic light harvesting. *Proc. Natl. Acad. Sci. USA* 99, 6017-6022.

[28] Wang, P., Nakamura, R., Kanematsu, Y., Koyama, Y., Nagae, H., Nishio, T., Hashimoto, H., Zhang, J. P. 2005. Low-lying singlet states of carotenoids having 8-13 conjugated double bonds as determined by electronic absorption spectroscopy. *Chem. Phys. Lett.* 410, 108-114.

[29] Polívka, T., Sundström, V. 2009. Dark excited states of carotenoids: Consensus and controversy. *Chem. Phys. Lett.* 477, 1-11.

[30] Wirtz, A., C., van Hermert, M. C., Lugtenburg, J., Frank, H. A., Groen, E. J. J. 2007. Two stereoisomers of spheroidene in the *Rhodobacter sphaeroides* R26 reaction center: A DFT analysis of resonance Raman spectra. *Biophys. J.* 93, 981-991.

[31] Britton, G. 1995. Structure and propertie sof carotenoids in relation to function. *FASEB J.* 9, 1551-1558.

[32] Britton, G., Helliwell, J. R. 2008. Carotenoid-protein interactions. In: *Carotenoids vol 4: natural functions*. (eds. G. Britton, S. Liaaen-Jensen, H. Pfander), pp. 99-117. Basel, Switzerland; Boston, MA; Berlin, Germany: Birkhäuser.

[33] McDermott, G., Prince, S. M., Freer, A. A., Hawthornwaite-Lawless, A. M., Papiz, M. Z., Codgell, R. J., Isaacs, N. W. 1995. Crystal structure of an integral membrane light-harvesting complex from photosynthetic bacteria. *Nature* 374, 517-521.

[34] Hofmann, E., Wrench, P., Sharples, F. P., Hiller, R. G., Welte, W., Diederichs, K. 1996. Structural basis of light harvesting by carotenoids: peridinin-chlorophyll-protein from *Amphidinium carterae*. *Science* 272, 1788- 1791.

[35] Kerfeld, C.A., Sawaya M. R., Brahmandam, V., Cascio, D., Ho, K. K., Trevithick-Sutton, C. C., Krogmann, D. W., Yeates, T. O. 2003. The crystal structure of cyanobacterial water-soluble carotenoid binding protein. *Structure* 11, 55-66.

[36] Umena, Y., Kawakami, K., Shen, J. R., and Kamiya, N. 2011. Crystal structure of oxygen-evolving photosystem II at a resolution of 1.9Å. *Nature* 473, 55-60.

[37] Liu, Z., Yan, H., Wang, K., Kuang, T., Zhang, J., Gui, L., An, X., Chang, W. 2004. Crystal structure of spinach major light-harvesting complex at 2.72 Å resolution. *Nature* 418, 287-292.

[38] Standfuss, R., van Scheltinga, A. C. T., Lamborghini, M., Kühlbrandt, W. 2005. Mechanisms of photoprotection and nonphotochemical quenching in pea light-harvesting complex at 2.5 Å resolution. *Embo J.* 24, 919-928.

[39] Yan, H., Zhang, P., Wang, C., Liu, Z., Chang, W. 2007. Two lutein molecules in LHCII have different conformations and functions: insights into the molecular mechanism of thermal dissipation in plants. *Biochem. Biophys. Res. Commun.* 355, 457-463.

[40] Cianci, M., Rizkallah, P. J., Olczak, A., Raftery, J., Chayen, N. E., Zagalsky, P. F., Helliwell, J. R. 2002. The molecular basis of the coloration mechanism in lobster shell: β-Crustacyanin at 3.2-Å resolution. *Proc. Natl. Acad. Sci. USA* 99, 9795-9800.

[41] Ilagan, R. P., Christensen, R. L., Chapp, T. W., Gibson, G. N., Pascher, T., Polivka, T., Frank, H. A. 2005. A femtosecond time-resolved absorption spectroscopy of astaxanthin in solution and in α-crustacyanin. *J. Phys. Chem. A* 109, 3120-3127.

[42] Britton, G., Liaaen-Jensen S., Pfander, H. 2004. *Carotenoids handbook*. Basel, Switzerland; Boston, MA; Berlin, Germany: Birkhäuser.

[43] Weedon, B. C. L., Moss, G. P. 1995. Structure and nomenclature. In: *Carotenoids vol 1A: isolation and analysis* (eds. G. Britton, S. Liaaen-Jensen, H. Pfander), pp. 27-70. Basel, Switzerland; Boston, MA; Berlin, Germany: Birkhäuser.

[44] Mo, F. 1995. X-ray cristallography studies. In: *Carotenoids vol 1B: spectroscopy* (eds. G. Britton, S. Liaaen-Jensen, H. Pfander), pp. 321-342. Basel, Switzerland; Boston, MA; Berlin, Germany: Birkhäuser.

[45] Britton, G., Helliwell, J. R. 2008. Three-dimensional structures of carotenoids by X-ray crystallography. In: *Carotenoids vol 4: natural fucntions*. (eds. G. Britton, S. Liaaen-Jensen, H. Pfander), pp. 37-52. Basel, Switzerland; Boston, MA; Berlin, Germany: Birkhäuser.

[46] Hudson, B. S., Kohler, B. E., 1972. A low lying weak transition in the polyene α,ω-diphenyloctatetraene. *Chem. Phys. Lett*. 14, 299-304.

[47] Hudson, B. S., Kohler, B. E., 1973. Polyene spectroscopy: the lowest energy excited single state of diphenyloctatetraene and other linear polyenes. *J. Chem. Phys.* 59, 4894-5002.

[48] Christensen, R. L., Kohler, B. E., 1973. Low resolution optical spectroscopy of retynil polyenes: low lying electronic levels and spectral broadness. *Photochem. Photobiol.* 18, 293-301.

[49] Hudson, B. S., Kohler, B. E., 1974. Linear polyene electronic structure and spectroscopy. *Ann. Rev. Phys. Chem*. *25*, 437-460.

[50] Christensen, R. L., Kohler, B. E., 1975. Vibronic coupling in polyenes: high resolution optical spectroscopy of 2,10-dimethylundecapentaene. *J. Chem. Phys.* 63, 1837-1846.

[51] Hudson, B. S., Kohler, B. E., Shulten, K. 1982. Linear polyene electronic structure and potential surfaces. In: *Excited states vol 6* (ed. E. C. Lim), pp. 1-95. New York, NY: Academic press.

[52] Shulten, K. Karplus, M. 1972. On the origin of a low- lying forbidden transition in polyenes and related molecules. *Chem. Phys. Lett*. 14, 305-309.

[53] Kohler, B. E. 1995. Electronic structure of carotenoids. In: *Carotenoids vol 1B: spectroscopy* (eds. G. Britton, S. Liaaen-Jensen, H. Pfander), pp. 1-12. Basel, Switzerland; Boston, MA; Berlin, Germany: Birkhäuser.

[54] Christensen, R. L. 1999. The electronic states of carotenoids. In: *The photochemistry of carotenoids* (eds. H. A. Frank, A. J. Young, G. Britton, R. J. Cogdell), pp. 137-159. Dordrecht, The Netherlands; Boston, MA; London, UK: Kluwer Academic Publishers.

[55] Polívka, T., Sundström, V. 2004. Ultrafast dynamics of carotenoids excited states- from solution to natural and artificial systems. *Chem. Rev*. 104, 2021-2071.

[56] Frank, H. A., Christensen, R. L. 2008. Excited electronic states, photochemistry and photophysics of carotenoids. In: *Carotenoids vol 4: natural fucntions* (eds. G. Britton, S. Liaaen-Jensen, H. Pfander), pp. 167-188. Basel, Switzerland; Boston, MA; Berlin, Germany: Birkhäuser

[57] Frank, H. A., Codgell, R. J. 1993. Photochemistry and function of carotenoids in photosynthesis. In: *Carotenoids in photosynthesis*. (eds. A. Young, G. Britton), pp. 252-326. London, UK: Chapman and Hall.

[58] Britton, G. UV/Visible spectroscopy. 1995. In: *Carotenoids vol 1B: spectroscopy* (eds. G. Britton, S. Liaaen-Jensen, H. Pfander), pp. 13-62. Basel, Switzerland; Boston, MA; Berlin, Germany: Birkhäuser.

[59] Polívka, T., Frank, H. A. 2010 Molecular factors controlling photosynthetic light harvesting by carotenoids. *Accounts. Chem. Res.* 43, 1125-1134.

[60] Frank, H., A., Codgell R., J. 1996. Carotenoids in photosynthesis. *Photochem. Photobiol*. 63, 257-264.

[61] Andrew, G., Berera, R., Alexandre, T. A., Pascal, A. A., Bordes, L., Mendes-Pinto, M. M., Andrianambininstsoa, S., Stoitchkova, K. V., Marin, A., Valkunas, L., Horton, P., Kennis, J. T. M., van Grondelle, R., Ruban, A., Robert, B. 2011. *Biophys. J.* 101, 934-942.

[62] Frank, H., A., Bautista, J., A., Josue, J., Pendon, Z., Hiller, R. G., Sharples, F. P., Gosztola, D., Wasielewski, M., R. 2000. Effect of the solvent environment on the spectroscopic properties and dynamics of the lowest excited states of carotenoids. J. *Phys. Chem. B* 104, 4569-4577.

[63] Zigmantas, D., Hiller, R. G., Sharples, F. P., Frank, H. A, Sundström, V., Polívka, T. 2004. Effect of a conjugated carbonyl group on the photophysical properties of carotenoids. *Phys. Chem. Chem. Phys*. 6, 3009-3016.

[64] James, A. Bautista, J. A., Connors, B. E., Raju, B. B., Hiller, R. G., Sharples, F. P., Gosztola, D., Wasielewski, M. R., Frank, H. A. 1999. Excited state properties of peridinin: observation of a solvent dependence of the lowest excited singlet state lifetime and spectral behavior unique among carotenoids. *J. Phys. Chem. B* 103, 8751-8758.

[65] Araki, G., Murai, T. 1952. Molecular structure and absorption spectra of carotenoids. *Prog. Theorec. Phys*. 6, 639-654.

[66] Fuciman, M., Chávera, P., Župčanová, A., Hrřbek, P., Arellano J. B., Vácha, F., Pšenčik, J., Polívka, T. 2010. Excited states of aryl carotenoids. *Phys. Chem. Chem. Phys.* 12, 3112-3120.

[67] Hemley, R., Kohler, B. E. 1977. Electronic structure of polyenes related to the visual chromophore: a simple model for the observed band shapes. *Biophys. J*. 20, 377-382.

[68] Enriquez, M. M., Fuciman, M., Lafountain, A. M., Wagner, N. L., Birge, R. R., Frank, H. A. 2010. The intramolecular charge transfer state in carbonyl-containing polyenes and carotenoids. *J. Phys. Chem. B* 114, 38, 12416-12426.

[69] Polívka, T., Kaligotla, S., Cháver, P., Frank, H., A. 2011. An intramolecular charge transfer state of carbonyl carotenoids: implications for excited state dynamics of apo-carotenals and retinal. *Phys. Chem. Chem. Phys*. 2011, 13, 10787–10796.

[70] Buchwald, M., Jencks, W. P. 1968. Properties of crustacyanins and the yellow lobster shell pigment. *Biochem.* 7, 844- 859.

[71] Britton, G., Wessie, R. J., Askin, D., Warburton, J. D., Gallardo-Guerreo, L., Jansen, F. J., de Groot, J. M., Lugtenburg, J., Cornard, J. -P., Merlin J. C. 1997. Carotenoid blues: structural studies on carotenoproteins. *Pure & Appl. Chem*. 69, 10, 2075-2084.

[72] Weesie, R. J., Merlin, J. C., de Groot, H. J. M., Britton, G., Lugtenburg, J., Jansen, J. H. M., Cornard, J. -P. 1999. Resonance Raman spectroscopy and quantum chemical modelling studies of protein-astaxanthin intercationn in α- crustacyanin (major blue carotenoprotein complex in carapace of lobster, *Homarus gammarus*). *Biospectrosc*. 5, 358-370.

[73] Neugbauer, J., Veldstra, J., Buda, F. 2011. Theorectical spectroscopy of astaxanthin in crustacyanin proteins: absorption, circular dichroism, and Nuclear Magnetic Resonance. *J. Phys. Chem. B* 115, 3216-3225.

[74] Bhosale, P., Binxing, L., Sharifzadeh, M., Gellermann, W., Frederick, J. M., Tsuchida, K., Berstein, P. S. 2009. Purification and partial characterization of a lutein-binding protein from Human retina. *Biochem.* 48, 4798-4807.

[75] Prum, R. O. 2006. Anatomy, physics, and evolution of avaian structural colors. In: *Bird coloration vol 1: mechanisms and measurements*. (eds. G. E. Hill, K. J. McGraw), pp. 295-353. Cambridge, MA: Havard University Press.

[76] Shawkey, M. D., Hill, G. E. 2005. Carotenoids need structural colours to shine. *Biol. Letters* 1, 121-124.

[77] Stradi, R., Celentano, G., Rossi E., Rovati G., Pastore, M. 1995 Carotenoids in bird plumage: the carotenoid pattern in a series of *Paleartic Carduelinae*. *Comp. Biochem. Physiol.* 110 B, 131-143.

[78] Brush, A. H. 1972. Correlation of protein electrophoretic pattern with morphology of normal and mutant feathers. *Biochem. Genet.* 7, 87-93.

[79] Brush, A. H. 1986. Tissue specific protein heterogeneity in keratin structures. *Biochem. Syst. Eco.l* 14, 547-551.

[80] Niedzwiedzki, D., Koscielecki, J. F., Cong, H., Sullivan, J. O., Gilbson, N. G., Birge, R. R., Frank, A. H. 2007. Ultrafast dynamics and excited state spectra of open-chain carotenoids at room and low temperatures. *J. Physic. Chem. B* 111, 5984-5998.

[81] Angerhofer, A., Bornhäuser, F., Gall, A., Cogdell, R. J. 1995. Optical and optically detected magnetic resonance investigation on purple photosynthetic bacterial antenna complexes. *Chem. Phys*. 194, 259-274.

[82] Takaichi, S. 1999. Carotenoids and carotenogenesis in anoxygenic photosynthetic bacteria. In: *The photochemistry of carotenoids*. (eds. H. A. Frank, A. J. Young, G. Britton, R. J. Cogdell), pp. 39-69. Dordrecht, The Netherlands; Boston, MA; London, UK: Kluwer Academic Publishers.

[83] Van Dorssen, R. J., Breton, J., Plijter, J. J., Satoh, K., van Gorkom, H. J., Amesz, J. 1987. Spectroscopic properties of the reaction center and of the 47 kDa chlorophyll protein of photosystem II. *Biochim. Biophys. Acta* 893, 267-274.

[84] Kwa, S. L. S., Newell, W. R., van Grondelle, R., Dekker, J. P. 1992. The reaction center of photosystem-II studied with polarized fluorescence spectroscopy. *Biochim. Biophys. Acta* 1099, 193-202.

[85] Tomo, T., Mimuro, M., Iwaki, M., Kobayashi, M., Itoh, S., Satoh, K. 1997. Topology of pigments in the isolated photosystem II reaction center studied by selective extraction. *Biochim. Biophys. Acta-Bioenerg.* 1321, 21-30

[86] Caffarri, S., Croce, R., Breton, J., Bassi, R. 2001. The major antenna complex of photosystem II has a xanthophyll binding site not involved in light harvesting. *J. Biol. Chem.* 276, 35924-35933.

[87] Polivka, T., Kerfeld, C. A., Pascher, T., Sumdstrom, V. 2005. Spectroscopic properties of the carotenoid 3'-hydroxyechinenone in the orange carotenoid protein from the cyanobacterium *Arthrospira maxima*. *Biochem.* 44, 3994-4003.

[88] Polivka, T., Chávera, P., Kerfeld, C. A. 2012. Carotenoid-protein interactions alters the S_1 energy of hydroxyechinenone in the orange carotenoid protein. *Biochem. Biophys. Acta-Bioenergetics,* 3, 248-254.

[89] Shima, S., Ilagan, R. P. Gillespie, N., Sommer, B. J., Hiller, R. G., Sharples, F. P., Frank, H. A., Birge, R. R. 2003. Two-photon and fluorescence spectroscopy and the sffect of environment on the photochemical properties of peridinin in solution and in the peridinin-chlorophyll-protein from *Amphidinium carterae. J. Phys. Chem. A* 107, 8052-8066.

[90] Büchel, C. 2003. Fucoxanthin-Chlorophyll Proteins in Diatoms: 18 and 19 kDa Subunits Assembleinto Different Oligomeric States. *Biochem*. 42, 13027-13034.

[91] Premvardhan, L., Bordes, L., Beer, A., Büchel, C., Robert, B. 2009. Carotenoid structures and environments in trimeric and oligomeric fucoxanthin chlorophyll a/c_2 proteins from resonance Raman spectroscopy. *J. Phys. Chem. B* 113, 12565-12574.

[92] Mimuro, M., Katok, T. 1991. Carotenoids in photosynthesis: absoprtion, transfer and energy dissipation. *Pure & Appl. Chem*. 63, 123, 123-130.

[93] Robert, B., Horton P., Pascal A. A., Ruban A. V. 2004. Insights into the molecular dynamics of plant light-harvesting proteins *in vivo*. *Trends Plant Sci.* 9, 1360-1385.

[94] Koyama, Y. 1995. Resonance Raman spectroscopy. In: *Carotenoids vol 1B: Spectroscopy*. (eds. G. Britton, S. Liaaen-Jensen, H. Pfander), pp. 135-146. Basel, Switzerland; Boston, MA; Berlin, Germany: Birkhäuser.

[95] Robert, B. 1999. The electronic structure, stereochemistry and resonance Raman spectroscopy of carotenoids. In: *The photochemistry of carotenoids*. (eds. H. A. Frank, A. J. Young, G. Britton, R. J. Cogdell), pp. 189-201. Dordrecht, The Netherlands; Boston, MA; London, UK: Kluwer Academic Publishers.

[96] Ruban, A. V., Pascal A. A., Robert, B., Horton, P. 2001. Configuration and dynamics of xanthophylls in light-harvesting antennae of higher plants: spectroscopic analysis of isolated light-harvesting complex of photosystem II and thylakoid membranes. *J. Biol. Chem.* 276, 24862-24870.

[97] Robert, B. 2009. Resonance Raman spectroscopy. *Photosynth. Res.* 101, 147-155.

[98] Saito, S., Tasumi, M. 1983. Normal-coordinate analysis of retinal isomers and assignments of Raman and Infrared bands. *J. Raman Specrosc*. 14, 4, 236-245.

[99] Rimai, L., Heyde, M. E., Gill D. 1973. Vibrational spectra of some carotenoids and related linear polyenes. A Raman spectroscopy study. *J. Am. Chem. Soc*. 95, 4493-4501.

[100] Salares, V. R., Young N. M., Carey, P. R., Bernstein, H. J. 1977. Excited state (exciton) interactions in polyene aggregates. *J. Raman Spectrosc.* 6, 282-288.

[101] Koyama, Y., Kito, M., Takii, T., Saiki, K., Tsukida, K., Yamashita, J. 1982. Configuration of the carotenoid in the reaction centers of photosynthetic bacteria. Comparison of the resonance Raman spectrum of the reaction centers of *Rhodopseudomonas sphaeroides* G1C with those of *cis-trans* isomers of ß-carotene. *Biochim. Biophys. Acta* 680, 109-118.

[102] Koyama, Y., Takii, T., Saiki, K., Tsukida, K. 1983. Configuration of the carotenoid in the reaction centers of photosynthetic bacteria. 2) Comparison of the resonance Raman lines of the reaction centers with whose of the 14 different *cis-trans* isomers of β-carotene. *Photobiochem. Photobiophys*. 5, 139-150.

[103] Koyama, Y., Takatsuka, I., Nakata, M., Tasumi, M. 1988. Raman and infra-red spectra of the *all-trans*, *7-cis*, *9-cis*, *13-cis* and *15-cis* isomers of β-carotene: key bands distinguishing stretched or terminal bent configurations from central-bent configurations. *J. Raman Spectrosc.* 19, 37-49.

[104] Lutz, M., Szponarski, W., Berger, G., Robert, B., Neumann, J. -M. 1987. The stereoisomerization of bacterial, reaction-center-bound carotenoids revisited: an electronic absorption, resonance Raman and NMR study. *Bochem. Biophys. Acta* 894, 423-433.

CHAPTER 2

ELECTRONIC ABSORPTION AND GROUND STATE STRUCTURE OF CAROTENOID MOLECULES

Predicting the complete electronic structure of carotenoid molecules remains an extremely complex problem, particularly in anisotropic media such as proteins. In this paper, we address the electronic properties of nine relatively simple carotenoids by the combined use of electronic absorption and resonance Raman spectroscopies. Linear carotenoids exhibit an excellent correlation between (i) the inverse of their conjugation chain length N, (ii) the energy of their $S_0 \rightarrow S_2$ electronic transition, and (iii) the position of their ν_1 Raman band (corresponding to the stretching mode of their conjugated C=C double bonds). For β-ring cyclic carotenoids such as β-carotene, this correlation is also observed between the latter two parameters ($S_0 \rightarrow S_2$ energy and ν_1 frequency), whereas their "nominal" conjugation length N does not follow the same relationship. We conclude that β-carotene and β-ring cyclic carotenoids in general exhibit a shorter effective conjugation length than that expected from their chemical structure. In addition, the effect of solvent polarizability on these molecular parameters was investigated for four of the carotenoids used in this study. We demonstrate that resonance Raman spectroscopy can discriminate between the different effects underlying shifts in the $S_0 \rightarrow S_2$ transition of carotenoid molecules.

This chapter is based on the following publication:
Mendes-Pinto, M. M., Sansiaume, E., Hashimoto, H., Pascal, A. A., Gall, A., Robert, B. 2013. *J. Phys. Chem. B.*

INTRODUCTION

Carotenoids are natural organic molecules built from the assembly of isoprenoid units (Figure 2.1), which play a number of essential roles in biology (for a comprehensive review of these functions, see Britton G. *et al.* [1]). During the first steps of the photosynthetic process, in addition to their role as light-harvesters [see *e.g.* 2-5] they also act as photoprotective molecules *via* a number of different mechanisms. Carotenoids quench the excited singlet and triplet states of chlorophyll molecules [1,6-11], which could otherwise induce the formation of singlet oxygen ($^1O_2$), one of the most harmful reactive oxygen species [12]. They are more generally able to quench the latter $^1O_2$ molecule to ground state triplet oxygen. Finally, carotenoids add their touch to the world- the color of a wide range of organisms (algae, animals, plants…) is acquired through carotenoid accumulation in their tissues, enabling a number of complex biological signalling processes [1]. Carotenoids achieve all these roles through their electronic properties, which arise from their linear conjugated polyene chain, and more precisely through their lower energy electronic excited states. The main absorption transition of carotenoid molecules, which corresponds to a transition from the ground state to the second excited state, $S_0 \rightarrow S_2$, tightly depends on the number of conjugated C=C double bonds present in this chain [13,14].

Because of the apparent simplicity of their structure, one should expect the electronic states of carotenoid molecules to be easily predictable through modern molecular physics. For instance, the relationship between carotenoid absorption maximum and the extent of their conjugated chain was established directly from polyene studies [15-17]. Carotenoid absorption properties have been shown to depend on the solvent refractive index [18-23]. The existence of their lower, absorption-silent, excited state was predicted in the 1972 [24]. However, predicting the full electronic structure of carotenoid molecules has proven extremely complex. No less than three, low-energy excited states have been proposed in the literature for these molecules [25,26]. Precise calculations of their electronic and vibrational properties are still difficult to perform, although considerable progress has been achieved in this field [27]. Prediction even of the behaviour of their electronic properties according to the surrounding solvent requires complex approaches [23,28]. As a result, even simple questions do not find an

immediate answer. For instance, while the electronic absorption transitions of most carotenoids appear sharply-defined in non-polar solvents, with the characteristic vibronic sub-bands clearly resolved, this is often not the case in more polar solvents where the bandwidths are seen to increase significantly. Although this issue has been addressed fairly recently, no clear explanation could be derived from the experimental work performed [29].

Natural carotenoids also display significant structural diversity. Their carbon skeletons may be purely linear or include cycles (*e.g.* β-carotene, where the conjugated chain extends into both cycles; Figure 2.1), and they may contain several functional groups which may or may not be conjugated with the isoprenoid chain (such as carbonyl groups in the case of fucoxanthin and spheroidenone [30]). In biology the situation is even more daunting as carotenoid molecules are generally present in highly anisotropic environments, most often bound to proteins. Predicting the electronic properties of carotenoids *in vivo*, which is essential if we are to understand how these molecules perform their biological function, becomes extremely difficult and often impossible to perform with accuracy.

In this paper, we study the electronic properties of nine relatively simple carotenoid molecules by the combined use of electronic absorption and resonance Raman spectroscopies. Resonance Raman is ideally suited to the study of carotenoid molecules [31]. As a vibrational technique, it yields direct information on the molecular properties of their electronic ground state. Resonance Raman spectra of carotenoids contain four main groups of bands, termed ν_1 to ν_4 (Figure 2.2). The ν_1 band arises from the stretching modes of the -mainly central [32]- conjugated C=C double bonds. It thus gives direct access to the structure of the conjugated chain- its frequency is a direct measurement of the C=C bond order of this chain, which in turn depends directly on the conjugation length. Measuring in parallel the frequency of this band and the position of the $S_0 \rightarrow S_2$ electronic absorption transition for these molecules gives access both to the structure of the carotenoid electronic ground state and to the energy of the $S_0 \rightarrow S_2$ transition. From this, we can dissect the molecular parameters which underlie the tuning

of the $S_0 \rightarrow S_2$ transition. Thus we provide a means for assessing the mechanism(s) tuning the functional properties of carotenoids *in vivo*.

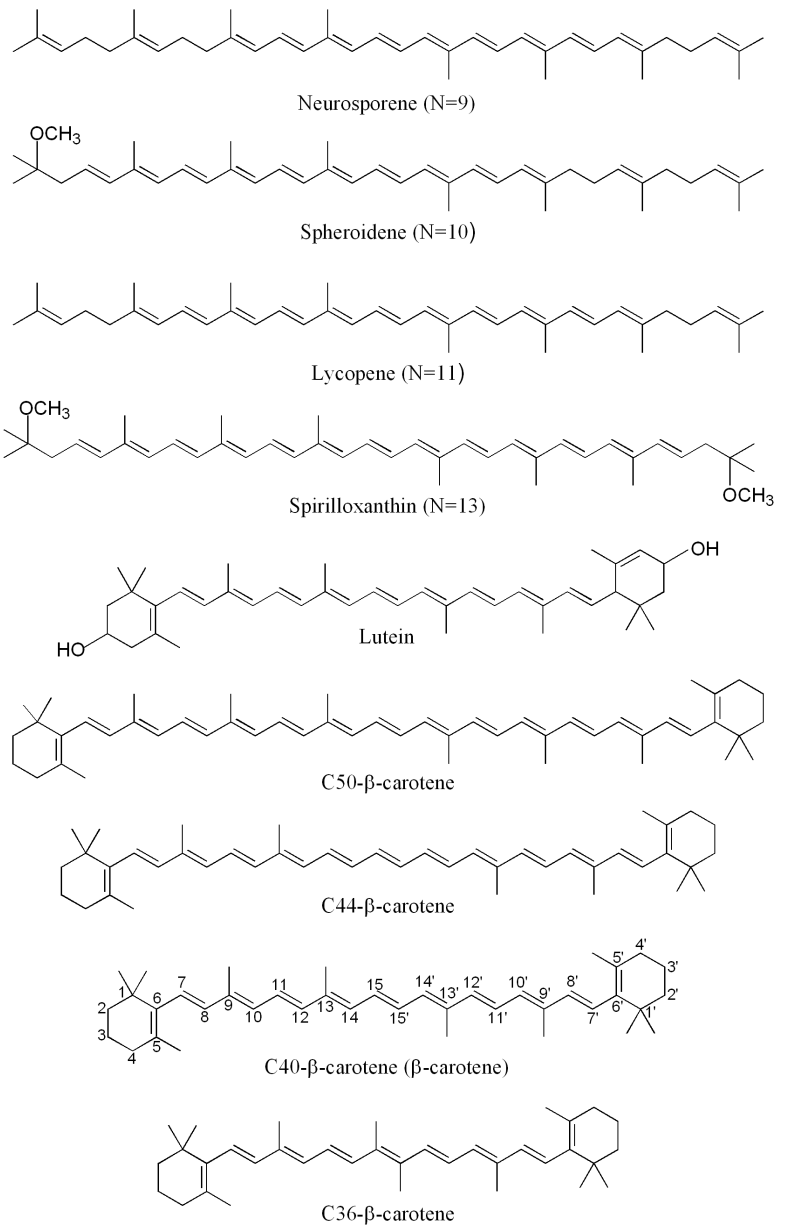

Figure 2.1. Molecular structure of the carotenoids studied in this work.

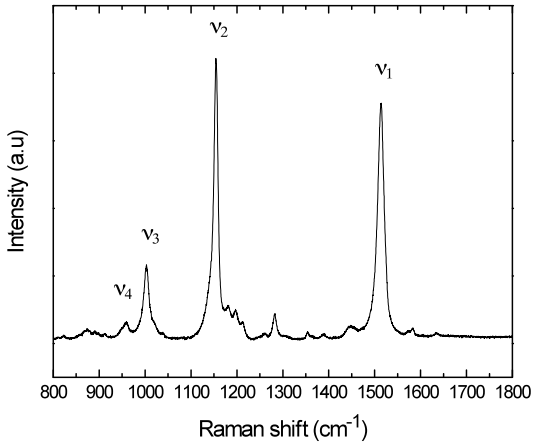

Figure 2.2. Typical resonance Raman spectrum of a carotenoid molecule (lycopene in hexane).

MATERIAL AND METHODS

Carotenoids

Lycopene (L-9879, from tomato) and β-carotene (β,β-carotene synthetic type I, C-9750) were obtained from Sigma-Aldrich (St. Louis, MO, USA). Neurosporene, spheroidene and spirilloxanthin were isolated from *Rhodobacter* (*Rba.*) *sphaeroides* strain GA, *Rba. sphaeroides* strain 2.4.1, and *Rhodospirillum rubrum* strain S1, respectively, and purified according to Niedzwiedzki *et al.* [33]. Lutein (β,ε-carotene-3,3'-diol) was isolated and purified as previously described [34]. C50-, C44-, C40- and C36-β-carotene homologues were synthesized as described by Yanagi *et al*. 2005 [35]. Based on their chromatographic and spectroscopic characteristics, namely retention times and absence of the *cis*-peak, all the carotenoids studied were *all-trans* (*all-E*) isomers.

Solvents

The solvents used in this study were tetrahydrofuran (THF), hexane, cyclohexane and acetonitrile (all absolute grade, ≥ 99.5 % GC), 1,2-dichloroethane (DCE), toluene, pyridine and methanol (anhydrous, 99.8 %), chloroform and carbon disulfide (CS_2) (anhydrous, ≥ 99 %), diethyl ether (≥ 99.8 % GC) and nitrobenzene (≥ 99,5 % GC), all purchased from Sigma-Aldrich (St. Louis, MO, USA).

Protein isolation

The major light-harvesting (LH) pigment-protein complexes from *Rba. sphaeroides* strain G1C (neurosporene bound to LH2), *Rba. sphaeroides* strain 2.4.1 (spheroidene bound to LH2), and *Rhodospirillum rubrum* strain S1S (spirilloxanthin bound to LH1), were purified from membranes in the presence of detergent, as previously described [36,37].

Spectroscopy

Room temperature absorption spectra were collected using a Varian Cary E5 double-beam scanning spectrophotometer. As the $S_0 \rightarrow S_2$ electronic transition of carotenoid molecules generally displays three clear vibrational levels, the position of the 0-0 level was used in this paper to define the position of this transition. Resonance Raman spectra (in resonance with this transition) were obtained using excitations provided by a 24 W Ar^+ Sabre laser (Coherent, Palo Alto, CA, USA), and recorded at room temperature with 90° signal collection using a two-stage monochromator (U1000, Jobin Yvon, Longjumeau, France), equipped with a front-illuminated, deep-depleted CCD detector (Jobin Yvon, Longjumeau, France). Typically, less than 20 mW reached the sample during the measurement, and sample integrity was verified by following the evolution of the spectra during the experiment. The Raman spectra of carotenoid-containing LH complexes were obtained by FT-Raman spectroscopy, in pre-resonance with the $S_0 \rightarrow S_2$ transition, using a Bruker IFS 66 infrared spectrophotometer coupled to a Bruker FRA 106 Raman module equipped with a continuous Nd:YAG laser, as previously described by Mattioli *et al.* [38].

RESULTS

Figure 2.3 displays the linear correlation between the position of the $S_0 \rightarrow S_2$ electronic transition and the inverse of the conjugation chain length N for neurosporene (N = 9), spheroidene (N = 10), lycopene (N = 11) and spirilloxanthin (N = 13) in hexane. Restricting the study to carotenoid molecules with no conjugated substituents yields a much better correlation for the linear fit (compare Figure 2.3 with *e.g.* Figure 2 in Araki G. and Murai T. [13]). This relationship is well established in the literature [15-17]. β-

carotene and lutein are also plotted, but excluded from the correlation calculation. These two carotenoids have cyclic end groups containing C=C double bonds, which are expected to be conjugated with the 9 double bonds in the linear chain (in lutein, only one of these C=C bonds is conjugated with the polyene chain, while for β-carotene both the C=Cs present in the cycles are conjugated). Thus the "nominal" conjugated chain length is 10 and 11 C=Cs for lutein and β-carotene, respectively (Figure 2.1). As seen in Figure 3, the electronic properties of β-carotene and lutein do not strictly follow the correlation observed for the other carotenoid molecules used here (as already noticed for several other carotenoids with conjugated cycles [39]. Panel B of the same Figure displays the correlation between the frequency of the ν_1 Raman band with the inverse of the carotenoid conjugation length. This linear relationship is also well established in the literature [40,41]. Once again, restricting the study to carotenoid molecules bearing no substituents yields a much better correlation between these parameters, and again β-carotene and lutein clearly deviate from the observed correlation (R^2 = 0.9492 for displayed correlation of linear carotenoids only; including β-carotene and lutein gives R^2 = 0.7608).

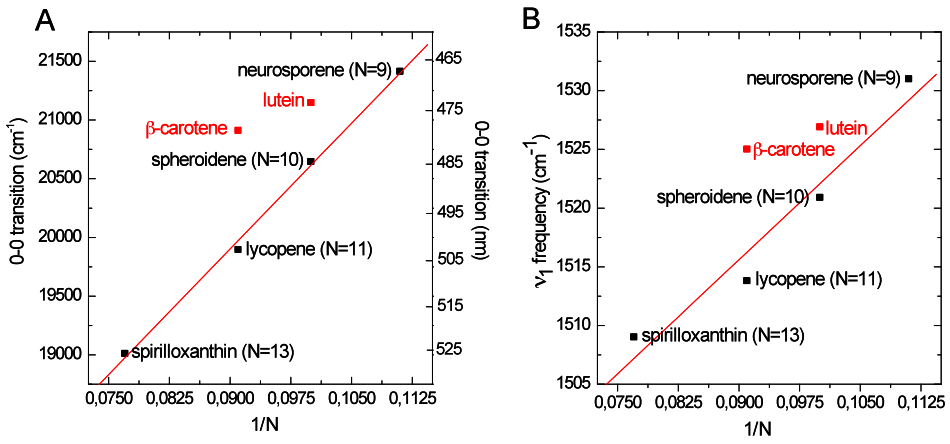

Figure 2.3. A: Correlation between the position of the $S_0 \rightarrow S_2$ electronic transition and the inverse of the number of conjugated double bonds, N, for linear carotenoids (black symbols). Measurements performed in hexane. β-Carotene and lutein are also plotted (red symbols) but excluded from the correlation calculation. B: Correlation between the frequency of the ν_1 Raman band (in hexane) and 1/N.

In Figure 2.4 the above data was redrawn to investigate the relationship between the position of the carotenoid $S_0 \rightarrow S_2$ electronic transition and the frequency of its ν_1 Raman band, *i.e.* we relate the energy difference between the ground and first allowed excited states with the electronic structure of the conjugated chain in the ground state [40,42]. An excellent correlation is obtained, this time for all the carotenoids studied - including β-carotene and lutein, indicating that for all these molecules the position of the electronic absorption position strictly correlates with the structure of the electronic ground state of the molecules. The ν_1 frequency observed for β-carotene and lutein corresponds to that expected for molecules having a shorter conjugated chain length than that expected from their structure. This band arises from the frequency of the Raman ν_1 band and is a direct reflection of the C=C bond order of the conjugated chain in the electronic ground state of the molecules, which itself depends on the effective conjugation length of the molecules. Accurate values for the effective conjugation chain length N of these molecules can be thus be readily inferred from the frequency of this band, using the correlation obtained in Figure 2.3. This gives a value of N = 9.6 for β-carotene and N = 9.3 for lutein (Figure 2.3).

Note that theoretical models have already been used to infer an effective N for β-ring cyclic carotenoids [16], but the models were not robust enough to give consistent values [43]. Thus taking into account the 9 conjugated double bonds in the central, linear part of their structure, the C-5,6 (& C-5′,6′) double bond(s) in the β-ring(s) are only partially conjugated, adding 0.3 to the effective N in each case.

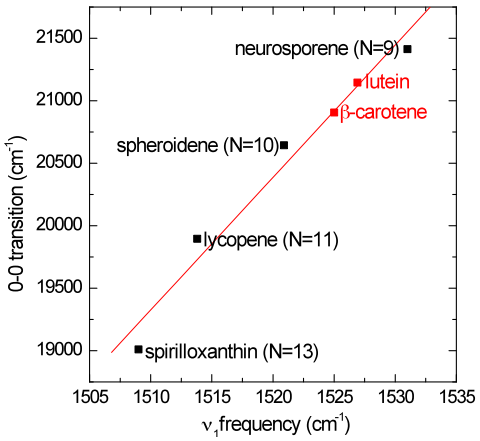

Figure 2.4. Correlation between the position of the $S_0 \rightarrow S_2$ electronic transition and the frequency of the ν_1 Raman band for each carotenoid studied (performed in hexane). The correlation calculation includes β-carotene and lutein.

In order to confirm the above observation, we studied a series of β-carotene homologues containing different conjugated chain-lengths of nominally 15, 13, 11 and 9 C=C double bonds, termed C50-, C44-, C40- and C36-β-carotene respectively (Figure 2.1). The position of the $S_0 \rightarrow S_2$ electronic transition according to the inverse of the chain length is plotted in Figure 2.5, and compared to the relationship observed in Figure 2.3. The β-carotene homologues do exhibit a direct correlation for these values, but with a different slope. However, this relationship should actually be the same for every carotenoid-like molecule, independent of its structure. Taking into account the shorter apparent conjugation length found for β-carotene and lutein than their nominal N value (see above), we therefore infer a similarly shorter conjugation length for the whole series of β-carotene-derived molecules. The ν_1 frequency measured for each of these β-carotene homologues yields an effective conjugation for these molecules of 13.7, 11.3, 9.6 and 7.8 instead of 15, 13, 11 and 9, respectively (Figure 2.5).

With this correction, all the values obtained for this series of molecules fit perfectly with the correlation found for linear carotenoids (Figure 2.5). We thus conclude that the apparent shortening of the conjugation length is a general property of β-carotene-derived molecules. Additionally, considering that we also observe an apparent shortening of the conjugation chain length of lutein, it is likely that such shortening occurs in other β-ring cyclic carotenoids.

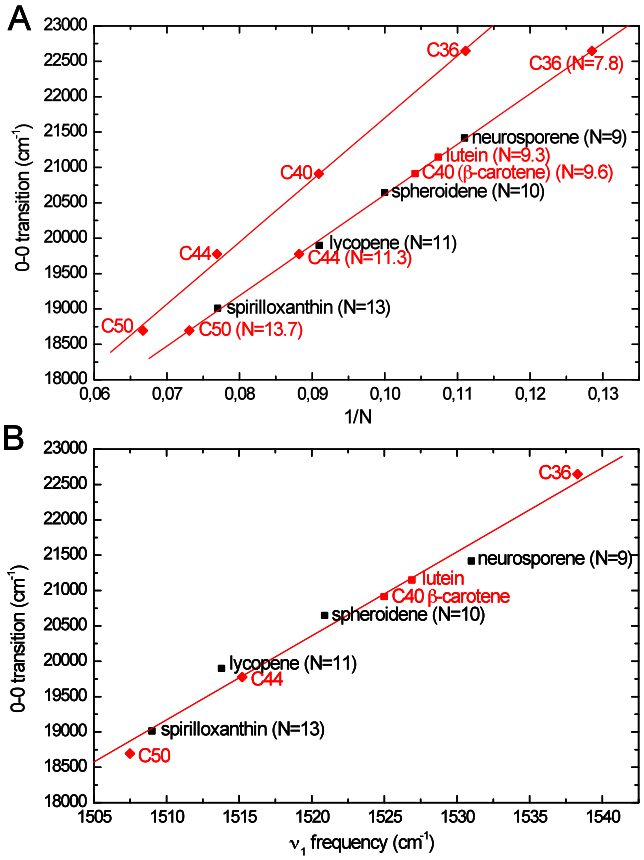

Figure 2.5. A: Correlation between the position of the $S_0 \rightarrow S_2$ electronic transition and 1/N for lutein and the β-carotene homologues C50, C44, C40 and C36 (red symbols) compared with the same correlation for the linear carotenoid molecules from Figure 2.3 (black symbols). For lutein and the β-carotene homologues, the data are also plotted using the deduced "effective" N (red symbols with red legends).
B: Correlation between the position of the $S_0 \rightarrow S_2$ electronic transition and the frequency of the ν_1 Raman band observed for all carotenoids studied- linear carotenoids, lutein and the β-carotene homologues.

Subsequently we employed resonance Raman to study β-carotene, lutein, spheroidene and lycopene for a range of solvents and compared the data to that obtained in hexane. The dependence of the position of the absorption transition of carotenoid molecules according to the properties of the solvent has been extensively studied [13,14,18-23,29]. To a first approximation, it primarily depends on the refractive index, *n*, of the

considered solvent [18-23]. A small, but significant correlation was found between the frequency of the ν_1 Raman band and the polarizability of the solvent, R(*n*), for lutein, β-carotene, spheroidene and lycopene (Figure 2.6), representing the effect of the solvent polarizability on the carotenoid ground state. This correlation appears similar for the four carotenoids studied. It is worth noting at this point that no such correlation could be found between the frequency of this Raman band and the solvent polarity (dielectric constant, ε; data not shown).

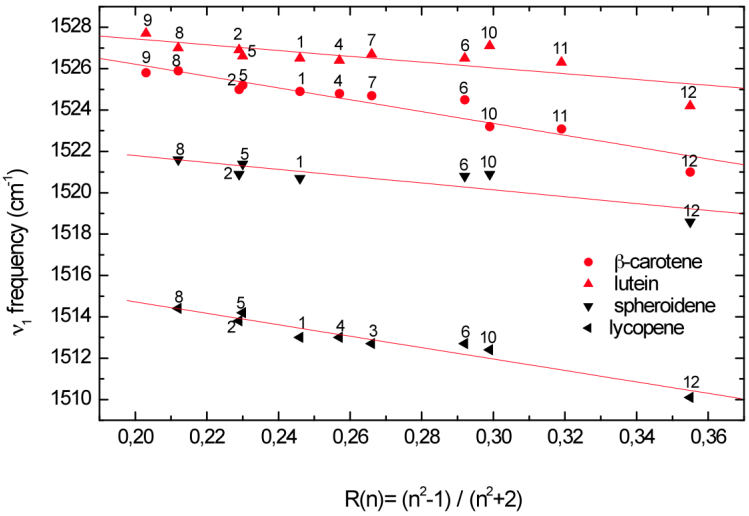

Figure 2.6. Correlation between the frequency of the ν_1 Raman band and the solvent polarizability for β-carotene, lutein, spheroidene and lycopene in different solvents (1- THF; 2- hexane; 3- DCE; 4- cyclohexane; 5- diethylether; 6- toluene; 7- chloroform; 8- acetonitrile; 9- methanol; 10- pyridine; 11- nitrobenzene; 12- CS_2). Note that symbol 2 for hexane corresponds to the data in the previous figures.

As a consequence, a linear relationship for each carotenoid can be found when plotting the correlation between the $S_0 \rightarrow S_2$ transition and the ν_1 frequency expressed as a function of solvent polarizability (Figure 2.7, red lines), but it is not the same relationship as that between carotenoids of different conjugation length in the same solvent - the points do not lie on the same line as that from Figures 2.4 and 2.5 (reproduced in Figure 2.7, black line). The relatively greater effect on the absorption transition (resulting in these points not lying on the black line) indicates that, as

expected, polarizability affects both the ground and excited electronic states of the carotenoid molecule (S_0 and S_2, respectively). Thus ν_1 reflects polarizability-induced changes in the ground state only, while the absorption shift results from the combined (actually entangled) effects on both S_0 and S_2. It is also of note that the dependence on polarizability appears to be similar for all four carotenoid molecules- the red lines in Figure 2.7 exhibit comparable trends, albeit the slopes are not identical.

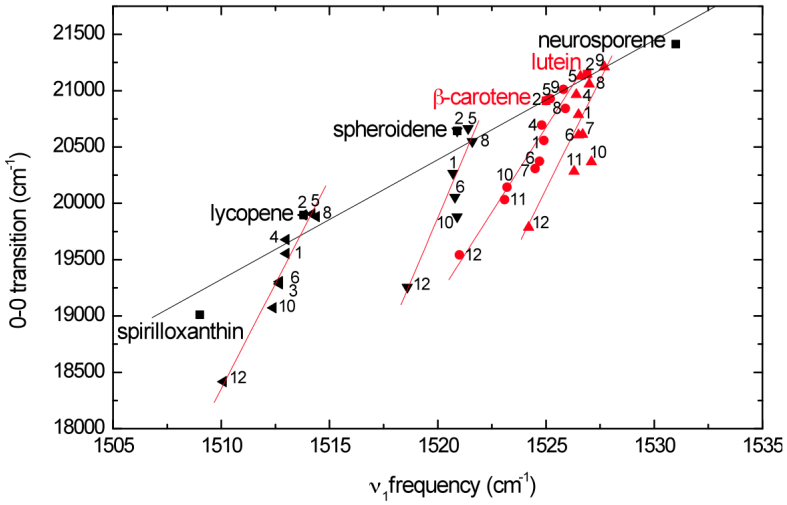

Figure 2.7. Correlation between the position of the $S_0 \rightarrow S_2$ electronic transition and the ν_1 band frequency as a function of solvent polarizability for *β*-carotene, lutein, spheroidene and lycopene. (1- THF; 2- hexane; 3- DCE; 4- cyclohexane; 5- diethylether; 6- toluene; 7- chloroform; 8- acetonitrile; 9- methanol; 10- pyridine; 11- nitrobenzene; 12- CS_2). For comparison, the relationship between carotenoids of different conjugation length in the same solvent (hexane) is indicated by the black line (*c.f.* Figures 2.4 and 2.5).

DISCUSSION

In this paper we have studied, using resonance Raman spectroscopy, the ground state electronic structure of different carotenoid molecules, in relation to changes in the position of their $S_0 \rightarrow S_2$ electronic transition. For linear carotenoids (spirilloxanthin, lycopene, spheroidene and neurosporene) a very good correlation is observed between the inverse of their conjugation chain length N and the energy of their $S_0 \rightarrow S_2$ transition, as well as with the position of their ν_1 Raman band. This is not true (as

already stressed *e.g.* in Angerhofer *et al*. [39]) for cyclic carotenoids such as β-carotene, β-carotene derivatives and lutein. However, an excellent correlation between the stretching modes of the C=C double bonds (*i.e.* position of ν_1) and the energy of the $S_0 \rightarrow S_2$ transition is observed for all carotenoids, including the above-mentioned cyclic ones. We may thus conclude that, in terms of the structure of their electronic ground states, β-carotene, β-carotene derivatives and lutein exhibit a shorter effective conjugation length N than expected from their chemical structures (9.6 and 9.3 C=C for β-carotene and lutein, respectively). The conjugated C=C double bond on the β-ring thus accounts for only a fraction of a C=C bond (an average of 0.3 C=C for all the studied molecules).

This phenomenon could be due to the *cis*-conformation of the ring. However, end-chain *trans-cis* isomerisation in linear carotenoids has been reported to shift the ν_1 Raman band by only 1-2 cm^{-1}, and thus cannot fully account for the observed effects. Steric hindrance between the methyl at C-5 of the β-ring and the hydrogen at C-8 of the chain, inducing the molecule to adopt an out-of-plane *cis*-like conformation, is more probably behind this phenomenon [44,45]. This out-of-plane twisted conformation of the β-rings of β-carotene and lutein should lead to a significant reduction of the conjugation of their C=C double bond(s) with the rest of the isoprenoid chain.

Much experimental and theoretical attention has been given to the effect of solvent refractive index and permittivity on the position of the (0-0) band of the $S_0 \rightarrow S_2$ absorption transition of carotenoids [13,14,18-23,29]. Dispersive forces were recently concluded to be the major factor driving the transition energy change, the red-shifts caused by polarity being one order of magnitude smaller [23]. Our data reveal an important parameter for such studies. The apparent conjugation length of carotenoid molecules slightly extends as solvent polarizability increases, reflecting the response of the ground state (S_0) electronic structure to the properties of the surrounding medium.

Altogether, this study reveals how resonance Raman spectroscopy can discriminate between the different effects underlying the shifts in the $S_0 \rightarrow S_2$ transition of carotenoid molecules. In particular, polarizability effects and changes in the effective conjugation length of these molecules can easily be distinguished due to the different correlations

between the frequency of the ν_1 Raman band and the position of the carotenoid absorption electronic transition. This should be helpful in disentangling these different mechanisms that may underlie the shifts in $S_0 \rightarrow S_2$ observed in complex media, and in particular *in vivo*. Indeed, biological systems display many examples of shifts in carotenoid absorption, the parameter which largely determines those functions of carotenoid molecules which involve interaction with light. From the data reported here, a combined Raman/absorption study of these carotenoids may help in discriminating between polarizability effects and changes in the effective conjugation length (due, for instance, to changes in the conformation of the β-end cycles induced by steric hindrance). As an example, in Figure 2.8 we report the effect of protein binding on these two spectroscopic parameters for three *all-trans*-carotenoids, spirilloxanthin, spheroidene and neurosporene. The proteins chosen are all light-harvesting (LH) pigment-protein complexes of purple photosynthetic bacteria- spheroidene and neurosporene bind to LH2 from *Rhodobacter sphaeroides* 2.4.1 and G1C, respectively, while spirilloxanthin binds to LH1 from *Rhodospirillum rubrum* S1S [37,38,39,46].

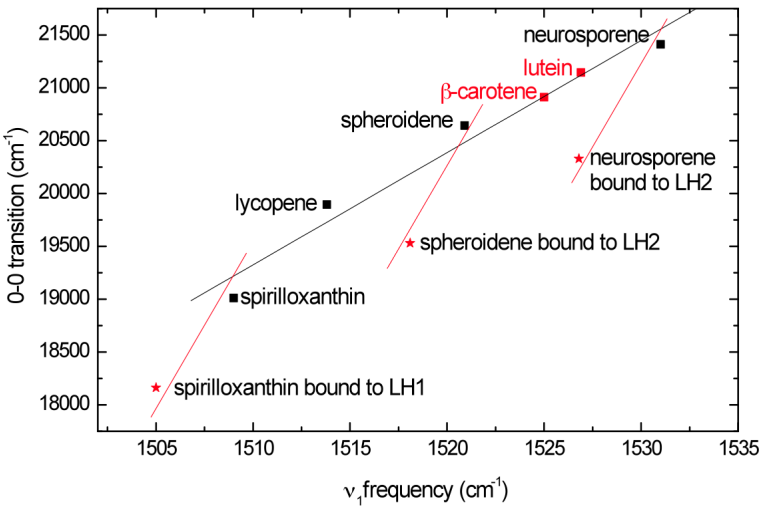

Figure 2.8. Correlation between the position of the $S_0 \rightarrow S_2$ electronic transition and the ν_1 band frequency for spirilloxanthin, spheroidene and neurosporene, in hexane and bound to LH proteins. For comparison, the relationship between carotenoids of different conjugation length in the same solvent (hexane) is added from Figure 2.4 and 2.5 (black line), as well as the relationship as a function of solvent polarizability (red lines, using an average of the four slopes from Figure 2.7).

The correlation between ν_1 frequency and the position of the $S_0 \rightarrow S_2$ transition, for each carotenoid *in vitro* and upon protein binding, is compared to the correlation found for varying carotenoid conjugation length (black line, taken from Figure 2.4) and to the correlation upon varying solvent polarizability (red lines, using an average of the four slopes in Figure 2.7). It clearly appears that the relationship between the ν_1 frequency and the position of the $S_0 \rightarrow S_2$ transition for these three LH-bound carotenoids follows the correlation seen when varying the polarizability of the solvent. Thus the average polarizability of the protein binding pocket is enough by itself to explain the shift in carotenoid $S_0 \rightarrow S_2$ transition upon binding to their light-harvesting protein host. This average polarizability, which appears to be nearly identical for the three proteins studied, corresponds to a value, R(*n*), of 0.334, slightly lower than that found in carbon disulphide (R(*n*) = 0.355). It should be noted that these three proteins form part of the same LH family, and the carotenoids are bound to equivalent positions in these homologous proteins, and so their binding sites would be expected to exhibit similar electrostatic properties. It is also of note that the deduced polarizability of the carotenoid binding pocket is high. LH-bound carotenoids are in close contact with bacteriochlorophyll molecules, which may provide them a highly polarizable environment [47]. From this example, we may hope that the information reported in this work will constitute a valuable contribution to the understanding of carotenoid absorption properties *in vivo*. A huge diversity of carotenoid species is involved in a wide range of very different biological systems, including many examples where their absorption properties are modified for a specific purpose [1].

REFERENCES

[1] Britton, G., Liaaen-Jensen S., Pfander H. (eds). 2008. *Carotenoids: natural fucntions, vol. 4* Basel, Switzerland; Boston, MA; Berlin, Germany: Birkhäuser.

[2] Cogdell, R. J., Gillbro, T., Andersson, P. O., Liu, R. S. H., Asato, A. E. 1994. Carotenoids as accessory light-harvesting pigments. *Pure Appl. Chem.* 66, 1041-1046.

[3] Horton, P., Ruban, A. V., Walters, R. G. 1996. Regulation of light harvesting in green plants. *Annu. Rev. Plant Physiol. Plant Molec. Biol.* 47, 655-684.

[4] Ruban, A. V., Pascal., A. A., and Robert B. 2000. Xanthophylls of the major photosynthetic light harvesting complex of plants: identification, conformation and dynamics. *FEBS* 477, 181-185.

[5] Polivka, T., Frank, H. A. 2010. Molecular factors controlling photosynthetic light harvesting by carotenoids. *Accounts Chem. Res.* 43**,** 1125-1134.

[6] Truscott, T. G., Land, E. J., Sykes, A. 1973. *In-vitro* photochemistry of biological molecules .3. Absorption-spectra, lifetimes and rates of oxygen quenching of triplet-states of β-carotene, retinal and related polyenes. *Photochem. Photobiol.* 17**,** 43-51.

[7] Palozza, P., Krinsky, N. I. 1992. Antioxidant effect of carotenoids in vivo and in vitro: an overview. *Methods Enzymol*. 213, 403-420.

[8] Niyogi, K. K., Bjorkman, O., Grossman, A. R. 1997. The roles of specific xanthophylls in photoprotection. *Proc. Natl. Acad. Sci. USA* 94**,** 14162-14167.

[9] Pascal, A. A. Liu, Z. Broess, K. van Oort, B. van Amerongen, H., Wang, C., Horton, P., Robert, B., Chang, W., Ruban, A. 2005. Molecular basis of photoprotection and control of photosynthetic light-harvesting. *Nature* 436, 134-137

[10] Ruban, A. V., Berera, R., Ilioaia, C., van Stokkum, I. H. M., Kennis, J. T. M., Pascal, A. A., van Amerongen, H., Robert, B., Horton, P., van Grondelle, R. 2007. Identification of a mechanism of photoprotective energy dissipation in higher plants. *Nature* 450, 575-578.

[11] Ishikita, H., Loll, B., Biesiadka, J., Kern, J., Irrgang, K. -D., Zouni, A., Saenger, W., Knapp, E. -W. 2007. Function of two β-carotenes near D1 and D2 proteins in photosystem II dimmers. *Biochim. Biophys. Acta-Bioenergetics*. 1767, 79-87.

[12] Foote, C. S. 1976. Photosensitized oxidation and singlet oxygen: consequences in biological systems. In: *Free radicals in biology.* (ed. William Pryor), pp. 85-133. New York, NY: Academic Press.

[13] Araki, G., Murai, T. 1952. Molecular structure and absorption spectra of carotenoids. *Prog. Theorec. Phys*. 6, 639-654.

[14] Suzuki, H., Mizuhuashi, S. 1964. π-Electronic structure and absorption spectar of carotenoids. *J. Phys. Soc. Japan*. 19, 724-738.

[15] Dale, J. 1954. Empirical relationships of the minor bands in the absorption spectra of polyenes. *Acta Chem. Scand.* 8, 1235-1256.

[16] Hemley, R., Kohler, B. E. 1977. Electronic-structure of polyenes related to visual chromophore. A simple model for the observed band shapes. *Biophys. J.* 20**,** 377-382.

[17] Christensen, R. L., Barney, E. A., Broene, R. D., Galinato, M. G. I., Frank, H. A. 2004. Linear polyenes: models for the spectroscopy and photophysics of carotenoids. *Arch. Biochem. Biophys.* 430, 30-36.

[18] Le Rosen, A. L., Reid, C. E. 1952. An investigation of certain solvent effect in absorption spectra. *J. Chem. Phys.* 20, 233-236.

[19] Hirayama, K. 1955. Absorption spectra and chemical structure .II. Solvent effect. *J. Am. Chem. Soc.* 77, 379-381.

[20] Andersson, P. O., Gillbro, T., Ferguson, L., Cogdell, R. J. 1991. Absorption spectral shifts of carotenoids related to medium polarizability. *Photochem. Photobiol.* 54, 353-360.

[21] Kuki, M., Nagae, H., Cogdell, R. J., Shimada, K., Koyama, Y. 1994. Solvent effect on spheroidene in nonpolar and polar solutions and the environment of spheroidene in the light-harvesting complexes of *Rhodobacter sphaeroides* 2.4.1 as revealed by the energy of the $^1Ag^- \rightarrow {}^1Bu^+$ absorption and the frequencies of the vibronically coupled C=C stretching Raman lines in the $^1Ag^-$ and 2^1Ag^- states. *Photochem. Photobiol.* 59, 116-124.

[22] Chen, Z. G., Lee, C., Lenzer, T., Oum, K. 2006. Solvent effects on the S_0 (1^1Ag^-) $\rightarrow S_2$ (1^1Bu^+) transition of beta-carotene, echinenone, canthaxanthin, and astaxanthin in supercritical CO_2 and CF_3H. *J. Phys. Chem. A* 110, 11291-11297.

[23] Renge, I., Sild, E. 2011. Absorption shifts in carotenoids-influence of index of refraction and submolecular electric fields. *J. Photochem. Photobiol. A- Chem.* 218, 156-161.

[24] Shulten, K., Karplus, M. 1972. On the origin of a low- lying forbidden transition in polyenes and related molecules. *Chem. Phys. Lett*. 14, 305-309.

[25] Papagiannakis, E., Kennis, J. T. M., van Stokkum, I. H. M., Cogdell, R. J., van Grondelle, R. 2002. An alternative carotenoid-to-bacteriochlorophyll energy transfer pathway in photosynthetic light harvesting. *Proc. Natl. Acad. Sci. USA* 99, 6017-6022.

[26] Wang, P., Nakamura, R., Kanematsu, Y., Koyama, Y., Nagae, H., Nishio, T., Hashimoto, H., Zhang, J. P. 2005. Low-lying singlet states of carotenoids having 8-13 conjugated double bonds as determined by electronic absorption spectroscopy. *Chem. Phys. Lett.* 410, 108-114.

[27] Wirtz, A. C., van Hermert, M. C., Lugtenburg, J., Frank, H. A., Groen, E. J. J. 2007. Two stereoisomers of spheroidene in the *Rhodobacter sphaeroides* R26 reaction center: A DFT analysis of resonance Raman spectra. *Biophys. J*. 93, 981-991.

[28] Nagae, H., Kuki, M., Codgell R. J., Koyama, Y. *J.* 1994. Shifts of the $^1Ag^- \rightarrow {}^1Bu^+$ electronic absorption of carotenoids in nonpolar and polar solvents. *Chem. Phys*. 101, 8, 6750-6765.

[29] Frank, H. A., Bautista, J. A., Josue, J., Pendon, Z., Hiller, R. G., Sharples, F. P., Gosztola, D. Wasielewski, M., R. 2000. Effect of the solvent environment on the spectroscopic properties and dynamics of the lowest excited states of carotenoids. J. *Phys. Chem. B* 104, 4569-4577.

[30] Britton, G., Liaaen-Jensen S., Pfander, H. 2004. (eds). *Carotenoids handbook*. Basel, Switzerland; Boston, MA; Berlin, Germany: Birkhäuser.

[31] Robert, B. 1996. Resonance Raman studies in photosynthesis- chlorophyll and craotenoid molecules. In: *Biophysical Techniques in Photosynthesis* (eds. J. Amesz, A. J. Hoff), pp. 161-176. Amsterdam, The Netherlands: Kluwer Academic Publishers.

[32] Saito, S., Tasumi M. 1983. Normal-coordinate analysis of retinal isomers and assignments of Raman and Infrared bands. *J. Raman Specrosc*. 14, 4, 236-245.

[33] Niedzwiedzki, D., Koscielecki, J., F., Cong, H., Sullivan, J., O., Gilbson, N., G., Birge, R., R., Frank, A., H. 2007. Ultrafast dynamics and excited state spectra of open-chain carotenoids at room and low temperatures. *J. Physic. Chem. B* 111, 5984-5998.

[34] Phillip, D., Ruban, A. V.; Horton, P., Asato, A., Young, A. J. 1996. Quenching of chlorophyll fluorescence in the major light-harvesting complexes of photosystem II: a systematic study of the effect of carotenoid structure. *Proc. Natl. Acad. Sci. USA* 93, 1492-1497.

[35] Yanagi, K., Gardiner, A. T., Codgell, R. J., Hashimoto, H. 2005. Electroabsorption spectroscopy of β-carotene homologues: anomalous enhancement of $\Delta\mu$. *Phys. L Rev. B* 71, 195118-1-9.

[36] Gall, A., Robert, B. 1999. Characterization of the different periphereal light-harvesting complexes from light and low-light grown cells from *Rhodopseudomonas palustris*. *Biochem*. 38, 5185-5190.

[37] Seguin, J., Ajlani, G., Verbavatz, J. M., Gobin, R., Gall, A., Paternostre, M., Robert, B. 2005. LHI antenna complexes of *Rhodospirillum rubrum*: a model for study of polypetides in the membrane. *Febs J*. 272, 453.

[38] Mattioli, T. A., Hoffman, A., Sockalingum, D. G., Schrader, B., Robert, B., Lutz, M. 1993. Application of near IR-fourier transform resonance Raman spectroscopy to the study of photosynthetic proteins. *Spectrochim. Acta Part A* 49, 785-799.

[39] Angerhofer, A., Bornhäuser, F., Gall, A., Cogdell, R. J. 1995. Optical and optically detected magnetic resonance investigation on purple photosynthetic bacterial antenna complexes. *Chem. Phys*. 194, 259-274.

[40] Merlin, J. C. 1985. Resonance Raman spectroscopy of carotenoids and carotenoid-containing sustems. *Pure & Appl. Chem*. 5, 785-792.

[41] Withnall, R., Babur, Z. C., Silver, J., Howell, G. E., de Oliveira, L. C.2003. Raman spectra of carotenoids in natural products. *Spectrochim. Acta Part A* 2207-2212.

[42] Rimai, L., Heyde, M. E., Gill D. 1973. Vibrational spectra of some carotenoids and related linear polyenes. A Raman spectroscopy study. *J. Am. Chem. Soc*. 95, 4493-4501.

[43] Kohler, B. E. 1995. Electronic structure of carotenoids. In: *Carotenoids vol 1B: spectroscopy* (eds. G. Britton, S. Liaaen-Jensen, H. Pfander), pp. 1-12. Basel, Switzerland; Boston, MA; Berlin, Germany: Birkhäuser.

[44] Weedon, B. C. L., Moss, G. P. 1995. Structure and nomenclature. In: *Carotenoids vol 1A: isolation and analysis* (eds. G. Britton, S. Liaaen-Jensen, H. Pfander), pp. 27-70. Basel, Switzerland; Boston, MA; Berlin, Germany: Birkhäuser.

[45] Britton, G. UV/Visible spectroscopy. 1995. In: *Carotenoids vol 1B: spectroscopy* (eds. G. Britton, S. Liaaen-Jensen, H. Pfander), pp. 13-62. Basel, Switzerland; Boston, MA; Berlin, Germany: Birkhäuser.

[46] Takaichi, S. 1999. Carotenoids and carotenogenesis in anoxygenic photosynthetic bacteria. In: *The photochemistry of carotenoids*. (eds. H. A. Frank, A. J. Young, G. Britton, R. J. Cogdell), pp. 39-69. Dordrecht, The Netherlands; Boston, MA; London, UK: Kluwer Academic Publishers.

[47] McDermott, G., Prince, S. M., Freer, A. A., Hawthornwaite-Lawless, A. M., Papiz M. Z., Codgell R. J., Isaacs, N. W. 1995. Crystal structure of an integral membrane light-harvesting complex from photosynthetic bacteria. *Nature* 374, 517-521.

CHAPTER 3

VARAIATION IN CAROTENOID-PROTEIN INTERACTION IN BIRS FEATHERS PRODUCES NOVEL PLUMAGE COLORATION

Light absorption by carotenoids is known to vary substantially with the shape or conformation of the pigment molecule induced by the molecular environment, but the role of interactions between carotenoid pigments and the proteins to which they are bound, and the resulting impact on organismal coloration, remain unclear. Here, we present a spectroscopic investigation of feathers from the brilliant red Scarlet Ibis (Eudocimus ruber, Threskiornithidae), the orange-red summer tanager (Piranga rubra, Cardinalidae) and the violet-purple feathers of the white-browed purpletuft (Iodopleura isabellae, Tityridae). Despite their striking differences in color, all three of these feathers contain canthaxanthin (β,β-carotene-4,4'-dione) as their primary pigment. Reflectance and resonance Raman spectroscopy were used to investigate the induced molecular structural changes and carotenoid-protein interactions responsible for the different coloration in these plumage samples. The results demonstrate a significant variation between species in the peak frequency of the strong ethylenic vibration (ν_1) peak in the resonance Raman spectra, the most significant of which is found in I. isabellae feathers and is correlated with a red-shift in canthaxanthin absorption that results in violet reflectance. Neither polarizability of the protein environment nor planarization of the molecule upon binding can entirely account for the full extent of the color shift. Therefore, we suggest that head-to-tail molecular alignment (i.e. J-aggregation) of the protein-bound carotenoid molecules is an additional factor.

This chapter is based on the following publication:
Mendes-Pinto, M. M., LaFountain, A. M, Stoddard, M. C., Prum, R. O., Frank, H. A., Robert, B. 2012. *J. R. Soc. Interface* 77, 3338-3350.

INTRODUCTION

Carotenoid pigments contribute to color of feathers, and are thought to be important for communication in many bird species [1-5]. Coloration in feathers can arise from light scattering by nanostructures, or from the presence of pigments that absorb light in particular regions of the electromagnetic spectrum [2,6,7]. Nanostructures usually produce UV-to-turquoise, white or iridescent colors [6,8]. Melanins are associated with black and browns [6,7,9]. Carotenoids give rise to yellow, orange and red coloration [2]. Green colors in feathers often results from a combination of yellow pigmentation and blue structural colors [6,10,11]. All of these factors contribute to make bird feather coloration of one of the most striking displays in all of nature.

Birds do not synthesize carotenoids *de novo*, and therefore must ingest them with their diet [2,12,13]. After ingestion, carotenoids are transported to various body tissues where they accumulate and carry out their biological roles [2,13]. Common carotenoids in bird diets are β-carotene, lutein, zeaxanthin and β-cryptoxanthin [13-16]. Coloration in feathers may arise directly from deposition of dietary carotenoids [2,17]. Alternatively, ingested carotenoids may be metabolically-modified before deposition *e.g.* by ketolase activity at the β- and ε-rings [2,18,19].

It is known that carotenoids incorporated during feather development bind strongly to proteins in the structures [11,13,20]. The proteins have a heterogeneous amino acid composition that can vary even in the same feather depending on the required physical properties [21,22]. Due to different pigment-protein interactions, the same carotenoid composition can give rise to different colors in feathers from various species or to different colored patches of feathers in the same species [11,20]. A similar phenomenon has been observed for the coloration of exoskeletons of crustaceans [11,20,23-27].

Resonance Raman spectroscopy provides direct, selective information regarding the structure of the electronic ground state of carotenoid molecules [28-30]. By matching the energy of incident light with the energy of the electronic absorption of a given carotenoid, selective probing of a subpopulation of molecules in a complex mixture may be achieved [28,31], thus allowing structural characterizations *in situ*. Resonance Raman spectra of carotenoids are characterized by four distinct bands denoted ν_1 through ν_4 whose frequencies vary with the effective conjugation length of the π-

electron double bond chain in the molecule, geometric isomeric configuration, and degree of distortion [27,29,30,32]. In an analysis of yellow and red colored patches of the European goldfinch (*Carduelis carduelis*), which are pigmented by canary xanthophylls (ε,ε-carotene-3,3'-dione and 3'-hydroxy-ε,ε-caroten-3-one), Stradi *et al.* [11] documented variation in the energy of the strongly allowed $S_0 \rightarrow S_2$ electronic transition by resonance Raman spectroscopy. This variation was due to an apparent change in the bond alternation of the conjugated polyene chain of the protein-bound carotenoids, suggesting an influence of the molecular environment on the binding of the pigments [11].

In *C. carduelis,* the effect of feather protein binding was to shift the color from yellow to red- two plumage colors that are also easily produced independently by changes in carotenoid molecular structure. So, it is not clear that association with the protein can contribute to novel plumage colors. In the present study we employed resonance Raman spectroscopy to investigate carotenoid-protein interactions responsible for the coloration of brilliant red and purple plumages of the scarlet ibis *Eudocimus ruber* (Threskiornithidae), summer tanager *Piranga rubra* (Cardinalidae), and white-browed purpletuft *Iodopleura isabellae* (Tityridae). All these plumage patches contain canthaxanthin (β,β-carotene-4,4'-dione) as the primary carotenoid [33-35] (see Figure 1.5 presented in Chapter 1). The violet color of male *I. isabellae* is very rare in bird plumages, and nothing is known about its production in *Iodopleura*.

In this study, resonance Raman and absorption spectra deduced from reflectance spectra of canthaxanthin bound *in situ* were compared with those recorded from canthaxanthin in solution to evaluate the molecular basis for the different spectral shifts that result in distinct colors of the feathers. We predict that the spectral differences of these three birds can be attributed to novel modes of binding canthaxanthin within the keratin matrix of the feathers, and postulate the involvement of specific factors including polarizability of the molecular environment and binding-induced configurational changes (*e.g.* planarization of the terminal β-rings). It should be noted that the nature of the bond between the carotenoid pigment and the specific structural component of the feather were not explored herein, and while it is possible that the pigment could bind to

lipid components of the feather, it is generally accepted that carotenoids are bound directly to keratin or to other proteins in the feather [11,20]. The characterization of the molecular factors responsible for these differences will further elucidate how birds have evolved to use variation in the molecular environment of pigment binding to tune the electronic properties of specific carotenoid molecules.

MATERIAL AND METHODS

Extraction and analysis of carotenoids

Red back feathers of a male *E. ruber* (YPM 26570; collected March 1951), red-orange belly feathers of a male *P. rubra* (YPM 7362, collected June 1957; YPM 3771, no collection data), and feathers from the purple pectoral tufts of a male *I. isabellae* (YPM 77812, no collection data; AMNH 494716, collected in 1886) were obtained from the Yale Peabody Museum of Natural History, Yale University, New Haven, CT, USA and the American Museum of Natural History, New York, NY, USA. Specimens were chosen for the high quality of color preservation based on visual evaluation by ROP. *All-trans*-canthaxanthin (β,β-carotene-4,4'-dione) was obtained from Roche. Carotenoids were extracted from the feathers as previously described by LaFountain *et al*. [36]. HPLC analysis was conducted using a Waters 600E multi-solvent delivery system with an in-line Waters 2996 photodiode array detector and a Phenomenex Luna 5 μm silica column (250 x 4.6 mm). The mobile phase consisted of a linear gradient from 90:10 to 80:20 hexanes/acetone (Fisher Scientific, Pittsburgh, PA, USA) over a period of 40 minutes, with a flow rate of 1.5 mL/min. The injection solvent was 14 % acetone and 86% hexanes.

Spectroscopy

Reflectance spectra of the feathers were measured using procedures previously described [37]. Briefly, the measurements were carried using an Ocean Optics S2000 spectrometer with an Ocean Optics DH-2000-BAL deuterium-halogen light source. Measurements were integrated for 500 ms at a distance of ~ 6 mm from the plumage with a perpendicular incident light, resulting in a ~ 3mm^2 illumination field. The probe

was secured in an aluminum block to obscure ambient light. The following formula was used to calculate percent reflectance (%R):

$$\%R = [\ (S-D) / (W-D)\ ] \times 100$$

where S is the reflectance of the specimen, D is the reflectance of the dark standard, and W is the reflectance of the white standard. The white standard was determined by measuring the reflectance of a white Spectralon tablet from Ocean Optics, while the dark standard was measured using ambient light in a darkened room [37].

Absorption spectra of *all-trans*-canthaxanthin in methanol, acetonitrile, tetrahydrofuran (THF), hexane, diethylether, cyclohexane, toluene, and carbon disulfide (CS_2) (all purchased from Sigma-Aldrich, St. Louis, MO, USA) were recorded at room temperature using a Varian Cary E5 double-beam scanning spectrophotometer. These solvents were chosen to represent a wide range of polarizabilities. Resonance Raman spectra of canthaxanthin were obtained in all solvents at room temperature, using a Jobin-Yvon U1000 Raman spectrophotometer equipped with a front-illuminated, deep-depleted CCD detector (Synapse Horiba, Jobin Yvon, France). Excitation at 457.9, 488.0, 514.5 and 528.7 nm was provided by a Sabre argon ion laser (Coherent, Palo Alto, CA, USA) and at 568.2 nm by an Innova 90 krypton ion laser (Coherent). For *in situ* resonance Raman spectroscopic experiments, a confocal microscope Olympus BX41 was coupled to the spectrometer. The same slit-width (200 μm) and grating were used for both systems, thereby achieving the same spectral resolution. The excitation beam was defocused and kept at a sufficiently low power (typically less than 20 mW) to prevent degradation of the sample by the absorbed light energy. Systematic comparison of resonance Raman spectra was performed throughout the time duration of each experiment to confirm sample integrity.

Avian color space modeling

Avian perception of color was modeled using a tetrahedral color space [3,37], which provides a quantitative representation of sensory experience, using the computer program TETRACOLORSPACE 1.0 for MATLAB 7 [3,37] (available for free from the

authors). The idealized stimulus, Q_I, of each single cone type was estimated by the reflectance spectrum of a plumage patch:

$$Q_I = \int_{300}^{700} R(\lambda) C_r(\lambda) d\lambda$$

where $R(\lambda)$ is the reflectance spectrum of the plumage patch, and $C_r(\lambda)$ is the spectral sensitivity function of each cone type *r*. For each plumage color, the idealized stimulation values of the four single cones - Q_I - were normalized to sum to one, yielding relative [*uv/ v s m l*] values. The [*uv/ v s m l*] values were converted to a color point with spherical coordinates θ, ϕ, and *r,* which defines a color vector pointing from the achromatic point is at the origin. Hue is the direction of the vector, given by the angles θ and ϕ, and saturation is the length of the vector, *r*, [3,37].

We modeled *E. ruber, P. rubra,* and *I. isabellae* reflectance spectra in avian tetrahedral color space using a standard violet (VS) cone-type visual system [38], which is the ancestral condition in birds [39,40]. We further compared the color space distribution of *E. ruber, P. rubra,* and *I. isabellae* reflectance spectra to a diverse sample of avian orders and families (including data from Stoddard and Prum [3] on all non-cotinga species having plumage coloration either inferred or identified as carotenoid-based).

RESULTS

Both the feather reflectance spectra (Figure 3.1A) and the inferred absorption spectra (Figure 3.2B) are broad and relatively structureless, which is typical of keto-carotenoids [41]. The absorption spectra of the feathers from *E. ruber* and *P. rubra* are very similar, and have an absorption maximum (reflectance minimum) centered at 495 nm. However, the absorption spectra of *E. ruber* feathers are much broader than *P. rubra,* resulting in a substantially redder reflectance and the near elimination of the *P. rubra* reflectance peak in the near ultraviolet at 361 nm. The spectra of the purple feathers of *I. isabellae* display a maximum absorbance (minimum reflectance) shifted to longer wavelengths, peaking at approximately 570 nm. Consequently, the high-energy reflectance peak of *I. isabellae* is shifted well into the human visible spectrum, resulting in a blue reflectance

peak at 426 nm. Combined with the long wavelength reflectance above 600 nm (on from the far side of the 570 nm absorbance peak), the blue and red reflectance create an entirely pigmentary violet color.

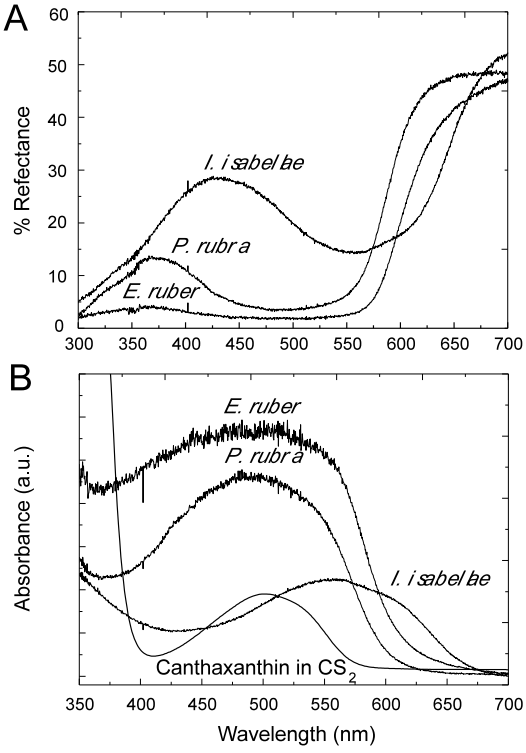

Figure 3.1. A: Single reflectance spectra of the red back feathers of *E. ruber* (YPM 26570), the red-orange belly feathers of a male *P. rubra* (YPM 7362), and the purple breast feathers of male *I. isabellae* (YPM 77812); B: Optical absorption spectra of the feathers computed from the reflectance spectra using A = -log (R) where R = Reflectance.

HPLC analysis of the carotenoids extracted from feathers of *E. ruber*, *P. rubra,* and *I. isabellae* demonstrated the presence of a single major carotenoid in all three samples (Figure 3.2). Based on the absorption spectra and retention times, the carotenoid was unambiguously identified as *all-trans*-canthaxanthin (β,β-carotene-4,4'-dione) (Figure 3.2). This identification was confirmed by mass spectrometry as well as by the HPLC of a heated *bona fide* canthaxanthin standard run under the same conditions (Figure 3.3D). This sample also demonstrated that the smaller peaks eluting in proximity to the major peaks are associated with *cis*-canthaxanthin formed during the heating and extraction process. The absorption spectrum of *cis*-canthaxanthin is confirmed by a slight blue-

shift in the absorption spectrum relative to that of *all-trans*-canthaxanthin and the large cis-band appearing at ~ 360 nm (dashed traces in Figure 3.2). These findings confirm previous reports that canthaxanthin is the primary pigment of *E. ruber* and *P. rubra* [33-35]. While canthaxanthin was found to be the dominant pigment in all three birds, *E. ruber and P. rubra* were also found to contain small amounts of other carotenoids. A pigment isolated from *E. ruber* with a retention time of 5.0 min displayed a blue-shifted absorption spectrum suggestive of a shortened conjugated chain (Figure 3.2C). This pigment was found to have a mass of 568 m/z, which is consistent with bis-dihydrocanthaxanthin, a carotenoid previously reported in *E. ruber* plumage by Fox and Hopkins [33]. *P. rubra* plumage was found to contain a minor pigment which eluted at 9.7 min and had a featureless absorption spectrum consistent with a keto-carotenoid, and a mass of 580 m/z. Additional small peaks were observed in the HPLC chromatograms of these two birds, however further analysis of these pigments was precluded due to lack of material. Some of the minor peaks in each chromatogram could be attributed to cis-isomers of canthaxanthin that were formed during the extraction procedure.

Saranathan *et al*. [42] have used small angle X-ray scattering (SAXS) to assay the nanoscale variation in refractive index in structurally colored and pigmented feathers. Unlike structurally colored feathers with spongy β-keratin nanostructures [43-46], the azimuthal average of the SAXS data from *I. isabellae* shows no peaks for any optically relevant spatial frequencies, or q values [42]. Rather, the azimuthal average has a slope that is closely congruent to Porod's Law (q^{-4}), the expectation for a random heterogeneous mixture of two materials with well-defined interface [47]. In the absence of any nanostructure that could enhance the coherent scattering of blue light, the purple feathers of male *I. isabellae* are produced by pigmentary absorption.

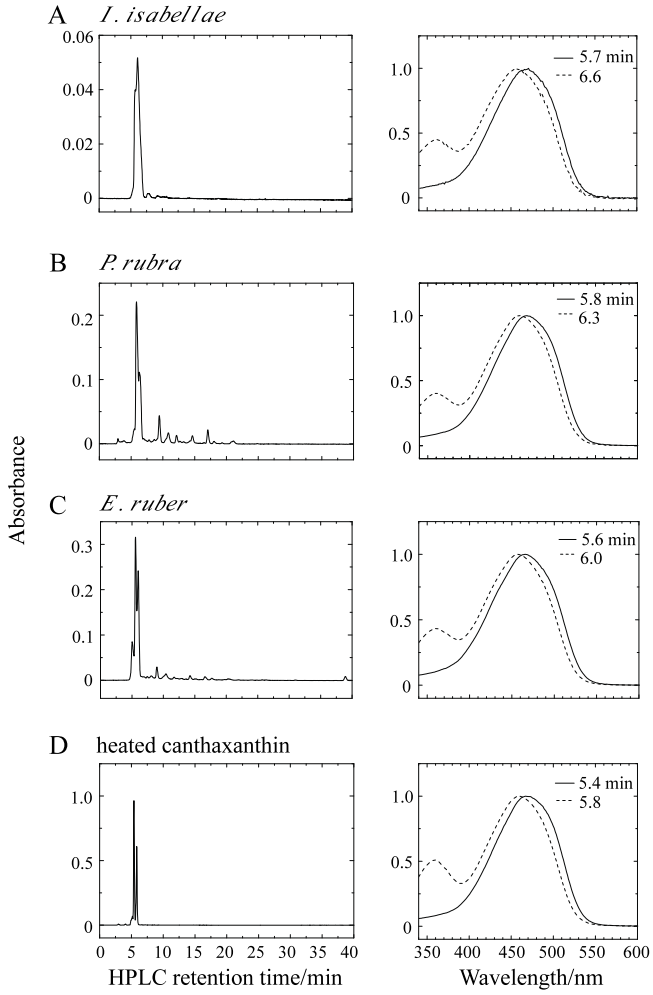

Figure 3.2. Normal-phase HPLC chromatogram of the extracts from feathers of *E. ruber*, *P. rubra* and *I isabellae* carried out as described in the text. The chromatograms were detected at 470 nm. A- *I. isabellae*: solid line, 5.7 min; dashed line, 6.6 min; B- *P. rubra*: solid line 5.8 min; dashed line, 6.3 min; C- *E. rubber*: solid line, 5.6 min; dashed line, 6.0 min; D- heated canthaxanthin solid line, 5.7 min; dashed line, 6.6 min.

The absorption spectrum of canthaxanthin in solution exhibits only small modulations within the spectrum, and appears as a single, broad band (see the spectrum of canthaxanthin in CS_2, Figure 3.1B). This type of broad band corresponds to the strongly-allowed $S_0 \rightarrow S_2$ electronic transition which gives carotenoids their

characteristic visible coloration [48]. The position of the spectral origin (0-0) of the $S_0 \rightarrow S_2$ transition can be determined from the longest-wavelength minimum of the second derivative of the absorption spectrum. The energy of this (0-0) band in solution depends primarily on the refractive index, *n*, of the solvent, and there is a small influence of the solvent dielectric constant [49]. As *n* increases, the polarizability, R(*n*), of the solvent expressed as $R(n) = (n^2-1) / (n^2+2)$ also increases, and the position of the $S_0 \rightarrow S_2$ transition shifts to longer wavelength. In the present work we evaluated the effect of solvent polarizability on the position of the (0-0) spectral origin band of the $S_0 \rightarrow S_2$ electronic transition of canthaxanthin in solution (Figure 3.3). The spectral origin varies linearly over ~ 40 nm for a variety of solvents with a wide range of R(*n*) (Figure 3.3).

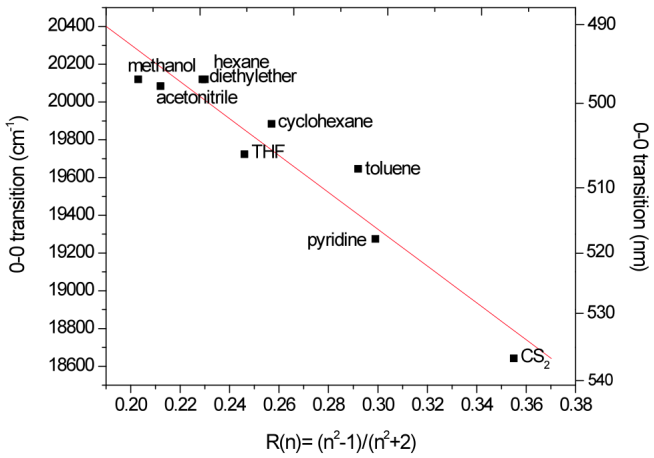

Figure 3.3. Position of the (0-0) band of the $S_0 \rightarrow S_2$ electronic transition of canthaxanthin as a function of polarizability in different solvents.

Room temperature resonance Raman spectra of canthaxanthin dissolved in hexane and diethylether contain the four main groups of bands, denoted ν_1 through ν_4, that are typical of carotenoid molecules (Figure 3.4) [30,32]. The ν_1 band at ~ 1520 cm^{-1} arises from stretching vibrations of C=C double bonds, and its frequency depends on both the length of the π-electron conjugated chain of the carotenoid and its configuration; *i.e.* the extent and position of twisting along the carbon backbone of the molecule [29,50,51].

The ν_2 band at ~ 1160 cm^{-1} is due mainly to stretching vibrations of C-C single bonds coupled with C-H in-plane bending modes [29,32]. The resonance Raman bands in the vicinity of ν_2 are also sensitive to the position of twisting along the carbon backbone and this constitutes the "fingerprint region" for the assignment of carotenoid configurations [50]. The ν_3 band at ~ 1010 cm^{-1} arises from the coupling of the in-plane rocking vibration of the methyl groups attached to the conjugated chain with the adjacent C-H in-plane bending modes [30,32]. The ν_4 band around 960 cm^{-1} arises from C-H out-of-plane wagging motions coupled with C=C torsional modes which are out-of-plane twists of the carbon backbone [30,32]. If the π-electron conjugated system in the carotenoid is symmetric, as it is in canthaxanthin, the out-of-plane ν_4 modes will not be coupled with the electronic transition when the molecule is planar. Accordingly these bands will not be resonance-enhanced upon excitation and will exhibit very low intensity in the resonace Raman spectra. However, they will increase in intensity when distortions around C-C single bonds occur [52]. For canthaxanthin in solution (Figure 3.4), the ν_4 band exhibits two weak overlapping components between 955 and 964 cm^{-1}. This result indicates that the average relaxed state of canthaxanthin in solution corresponds to a geometry deviating slightly from completely planar. An X-ray structure analysis of crystalline canthaxanthin supports the view that the terminal rings in the molecule are asymmetrically twisted out of the plane of the conjugated π-electron C=C chain by ~ 55º [53].

The resonance Raman spectra of *E. ruber*, *P. rubra,* and *I. isabellae* were measured by resonance Raman microspectroscopy using excitation of 457.9, 488.0, 514.5, 528.7 and 568.2 nm which span the carotenoid absorption transition (Figure 3.5). For *P. rubra* feathers (Figure 3.5A), the resonance Raman spectra are not dependent on the excitation wavelength and resemble that of *all-trans*-canthaxanthin in solution. The ν_1 band is positioned at precisely 1514.3 cm^{-1} for all excitation wavelengths (Table 3.1), but its full-width at half-maximum (fwhm) is 21.4 cm^{-1} for excitation at 457.9 nm compared to 21.6 cm^{-1} at 514.5 nm which is suggestive of a slight variation in carotenoid binding. However, the spectra indicate little out-of plane distortion upon binding canthaxanthin to the protein. From a structural point of view, the strong similarity in the spectra taken using the different excitation wavelengths are suggestive of a single pool of *all-trans*-

canthaxanthin molecules in these feathers. Thus, little difference in canthaxanthin absorption is predicted between *P. rubra* and canthaxanthin in solution except for the widening of the absorbance due to slight variation shown by the width of ν_1.

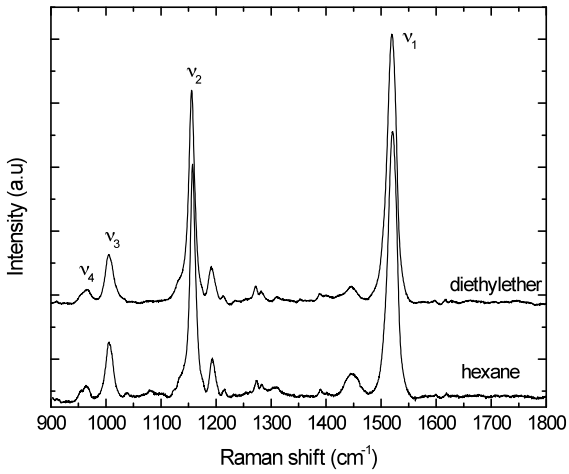

Figure 3.4. Room temperature resonance Raman spectra of canthaxanthin in diethylether and hexane. Excitation wavelength, 514.5 nm. Four distinct bands denoted ν_1 to ν_4 are observed in the spectra whose frequencies vary as described in the text.

The resonance Raman spectra of *E. ruber* feathers (Figure 3.5B) are typical of *all-trans*-canthaxanthin, but the frequency of the ν_1 band varies between 1512.1 cm^{-1} and 1519.7 cm^{-1} depending on the excitation wavelength. In addition, the fwhm of the ν_1 band is 3 cm^{-1} larger than observed for *P. rubra*. The fwhm of the ν_1 band is largest (~ 28 cm^{-1}) when the shortest wavelength (457.9 nm) excitation is used. This is suggestive of a heterogeneous population of twisted, but not fully isomerized, *all-trans*-canthaxanthin molecules in *E. ruber* feathers. These results are consistent with the reflectance and absorption spectra obtained from these feathers (Figure 3.1), which show that the electronic absorption transition of *E. ruber* feathers is even broader than that observed from *P. rubra*. In *E. ruber* feathers, the overall intensity in the ν_4 band region compared to that of the ν_3 bands, is higher than for *P. rubra* feathers. This is particularly true for

excitation longer than 488.0 nm and indicates distortion of the relaxed geometric state of canthaxanthin in the feathers from *E. ruber*.

Resonance Raman spectra of *I. isabellae* feathers recorded using different excitation wavelengths were very similar (Figure 3.6C), indicating the presence of a single pool *all-trans*-canthaxanthin molecules with some differences in the frequencies compared to the spectra taken from the other feathers and from canthaxanthin in solution. The frequency of the ν_1 band, which occurs between 1507.5 cm^{-1} and 1509.6 cm^{-1} is substantially lower than that observed in the feathers from the other two species and from canthaxanthin in solution (Figures 3.4 and 3.5, Table 3.1). The frequency of the ν_1 band is ~ 7 cm^{-1} lower than the ν_1 peak from *P. rubra* and *E. ruber* (at an excitation of 488.0 nm) and up to 12.5 cm^{-1} lower than the ν_1 peak of canthaxanthin in solution. Given that ν_1 is associated with the stretching of C=C double bonds [29,50], this result is associated with a physical extension of the effective π-electron conjugated chain within the molecular backbone of canthaxanthin in *I. isabellae* which is functionally correlated with the observed red-shift in its absorbance.

Also, the structure of the ν_2 band in *I. isabellae* is rather unusual for carotenoid molecules in organisms. Typically the satellite bands associated with the intense band at ~ 1160 cm^{-1} appear as two distinct bands (see *e.g.* spectra of lutein in the work by Ruban et *al.*) [54]. This is also the case for the feathers from *P. rubra* and *E. ruber* (Figures 3.5A and 3.5B, respectively). For *I. isabellae*, the ν_2 band at ~ 1155 cm^{-1} displays only one satellite band at 1209 cm^{-1}. Purified canthaxanthin in solution also exhibits only one satellite band in that region, however at a lower frequency (~ 1190 cm^{-1}, Figure 3.4). Lastly, the ν_4 band in the resonance Raman spectra from *I. isabellae* feathers (Figure 3.5C) has a significantly high intensity compared to that seen from canthaxanthin in solution (Figure 3.4). This result is indicative of molecular distortion.

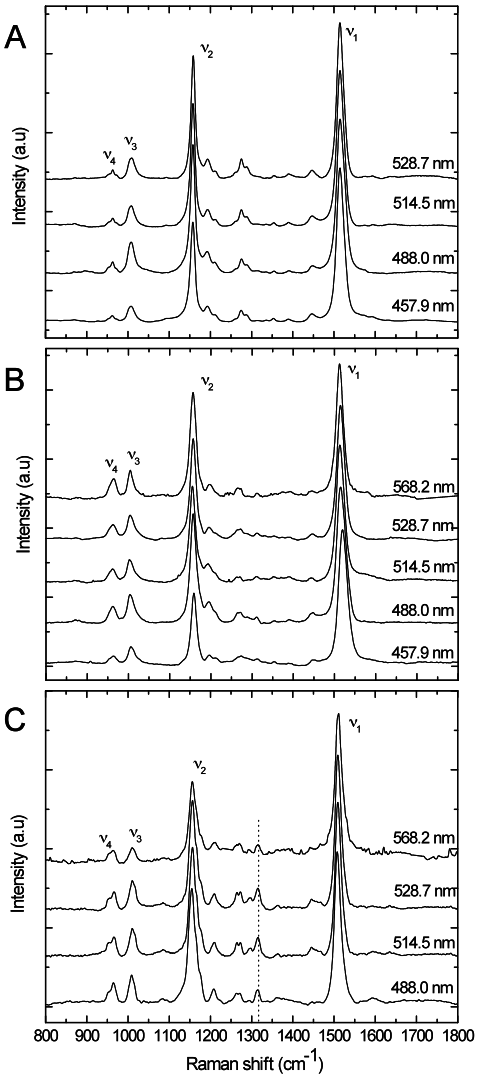

Figure 3.5. Resonance Raman spectra of the feathers. A: *P. rubra;* B: *E. ruber* and C: *I. isabellae*. The excitation wavelengths in nm units are indicated on the right hand side of the figure. The peak at ~ 1317 cm^{-1} in Figure 3.6C is not associated with a carotenoid (dashed line).

Table 3.1. Frequencies (cm^{-1}) of resonance Raman main bands observed in the feathers from *P. rubra*, *E. ruber* and *I. isabellae* (n.a: not applicable).

Excitation wavelength	resonance Raman band	*P. rubra*	*E. ruber*	*I. isabellae*
457.9 nm				
	ν_1	1514,3	1519,7	n.a.
	ν_2	1157,8	1159,1	n.a.
	ν_3	1007,5	1006,4	n.a.
	ν_4	972.2; 962.2; 952	963,1	n.a.
488.0 nm				
	ν_1	1514,3	1514,8	1507,5
	ν_2	1157,8	1157	1155; (1164.7,1174.5)
	ν_3	1007,5	1004,4	1008,7
	ν_4	972.2; 963.1; 952	963,1	965; 953.7
514.5 nm				
	ν_1	1514,3	1512,8	1508,6
	ν_2	1158,2	1155,3	1156.3; (1165,1175.7)
	ν_3	1007,5	1003,5	1009,8
	ν_4	972.2;963.1; 952	961,6	965; 954.9
528.7 nm				
	ν_1	1514,3	1514,1	1508,6
	ν_2	1158,6	1157	1156.3; (1165,1175.4)
	ν_3	1008,7	1004,4	1009,8
	ν_4	972.2; 963.1; 952	963,1	965; 954.9
568.2. nm				
	ν_1	n.a.	1521,1	1509,6
	ν_2	n.a.	1156,1	1156; (1165,1176.5)
	ν_3	n.a.	1004,4	1010,4
	ν_4	n.a.	964,6	964.3; 953.8

To examine further the effect of variation in carotenoid binding on the colors that birds perceive, we compared the reflectance spectra of *E. ruber, P. rubra,* and *I. isabellae* to the entire gamut of avian carotenoid plumages using a tetrachromatic model of avian color vision [3,37]. Since birds have four single cones- red, green blue, and violet/ultraviolet - their color perceptions can be modeled with a tetrahedral color space, or simplex [3,55]. In Figure 3.6, we show the total diversity of color perceptions produced by carotenoid plumages of more than 50 species in 23 avian families (gray circles and polyhedron, Figure 3.6). Using canthaxanthin pigment only, the plumage colors of *E. ruber* (red dots)*, P. rubra* (orange dots)*,* and *I. isabellae* (purple dot) span a huge range of the carotenoid plumage gamut. Using canthaxanthin pigments, the maximum span (the distance between *E. ruber* and *I. isabellae*) is 0.5342, compared to 0.6177, the maximum span of the entire known, avian carotenoid plumage gamut. Thus, canthaxanthin pigments in these three species achieve ~ 86% of the maximum span

achieved by all carotenoids. Given that the rest of these carotenoid colors set are produced by a wide diversity of molecules, these results show that the effect of carotenoid binding by feather proteins on plumage coloration perceived by birds can be at least as large as the effect on the spectra of the bound pigments induced by variation in the molecular structure itself.

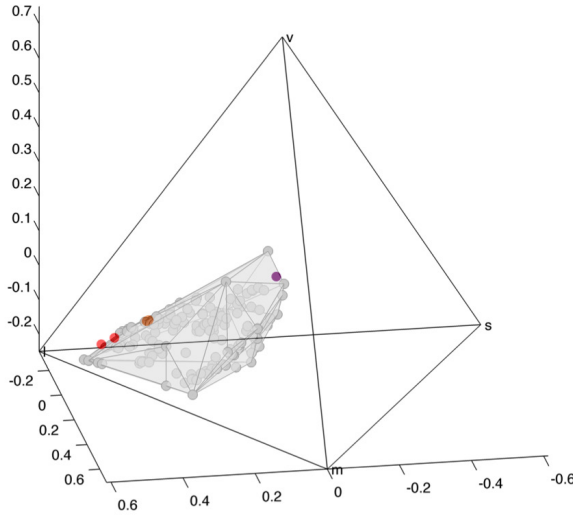

Figure 3.6. The plumage colors of *E. ruber* (red dots), *P. rubra* (orange dots), and *I. isabellae* (purple dot) modeled in a tetrahedral avian color space. The grey polyhedron represents the total diversity of color perceptions produced by carotenoid plumages of 145 plumage patches from 52 species in 23 avian families.

DISCUSSION

HPLC chromatographic analyses, chemical analysis and electronic reflectance and absorption spectroscopy carried out on differently colored feathers of *P. rubra*, *E. ruber* and *I. isabellae* indicate unambiguously that their color results from the same carotenoid pigment, canthaxanthin. We can also eliminate the possibility that the purple coloration is the result of a structural color. Small angle X-ray scattering (SAXS) data from Saranathan *et al*. [42] have shown that *I. isabellae* lacks any color producing nanostructure, and is indistinguishable from a random heterogeneous mixture of two materials with a well-defined interface [42]. Thus, the color of purple *I. isabellae* feathers is a distinctly pigmentary phenomenon, and is not the result of interference, or coherent scattering, of blue light wavelengths.

HPLC of extracted carotenoid molecules and the resonance Raman spectra of the feathers clearly indicate that canthaxanthin is present in in these feathers in an *all-trans* geometric isomeric configuration. Furthermore, in all resonance Raman spectra from feathers (Figure 3.6), the ν_4 band exhibits a well-structured lineshape and little variation with the excitation wavelength, indicating that the canthaxanthin molecules in each of the feathers have a single isomeric configuration; *i.e*. that they are all experiencing the same the out-of-plane distortions along the π-electron conjugated chain. Such distortions are determined by the interactions experienced by the carotenoid upon binding to the protein [20]. Therefore, we can conclude that canthaxanthin in the feathers within each species is not bound in a variable fashion within the protein matrix, but is bound in a highly consistent manner in each species.

However, the binding of canthaxanthin in the different feathers of the three species of birds varies substantially in a manner that is consistent with the observed differences in absorption and feather color. Specifically, the largest differences among the feather resonance Raman spectra were the substantial downshift of the ν_1 band in the purple feathers of *I. isabellae* in comparison to the red feathers of *P. rubra* or *E. ruber*, or to canthaxanthin in solution (Figures 3.4 and 3.5, Table 3.1). The frequency of the ν_1 band is functionally associated (*i.e*. correlates with the length of C=C bond conjugation) with the stretching of C=C double bonds [29,32,50]. The effective length of the C=C double bond chain of the carotenoid backbone also has a fundamental impact on the position of the allowed $S_0 \rightarrow S_2$ transition which produces the absorbance spectrum of carotenoid molecules. The effect on the absorption spectra due to differences in the length of the C=C double bond chain of carotenoid molecules is well-documented [46]. These results demonstrate that an extension of the π-electron C=C double bond chain length of a carotenoid molecule bound to feather protein can substantially affect the absorption of the pigment and the color produced. As previously mentioned, an X-ray structure analysis of canthaxanthin has revealed that the terminal rings in the molecule are twisted out of the plane of the conjugated double bond chain by ~ 55º which inhibits π-electron delocalization into the ring structures [53]. Thus, planarization of the terminal β-rings upon binding to the protein can lead to an extension of the C=C double bond chain length and produce a red-shift in the absorption of the molecule [47]. Thus, the

observed increase in the C=C double bond chain length in *I. isabellae* predicts the red-shift in absorption and, contributes to the violet color produced.

In solution, the position of the electronic absorption spectra of carotenoids depends on the polarizability of the environment (Figure 3.3). We documented this effect by measuring the resonance Raman spectrum of canthaxanthin in many different solvents and plotting the ν_1 values on the same graph with those obtained from the feathers (Figure 3.7). The data reveal a correlation between the measured frequency of the ν_1 band of canthaxanthin and the position of its electronic absorption transition, indicating that the electronic structure of the conjugated π-electron system in the ground state of canthaxanthin, which the ν_1 band probes, is sensitive to solvent polarizability. If we make the same correlation between the ν_1 band in feathers and the position of the lowest energy component of their absorption spectra, the slope of line associated with the canthaxanthin feathers is similar to, although slightly shallower than, the slope of the line obtained from canthaxanthin in various solvents and associated with changes in solvent polarizability (solid lines in Figure 3.7).

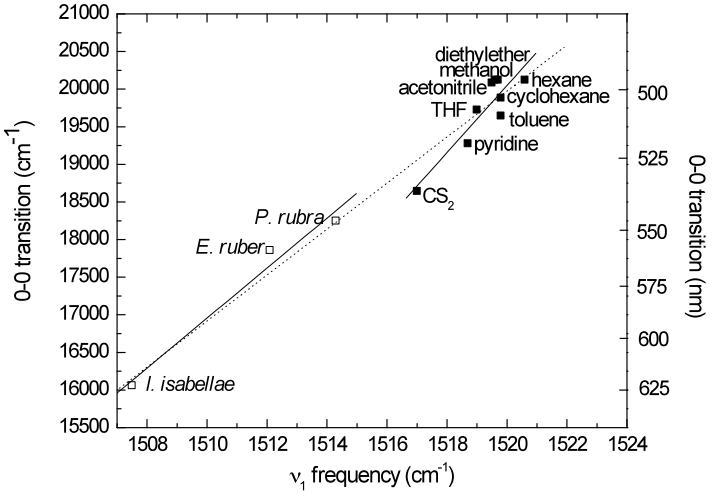

Figure 3.7. Correlation between the position of the (0-0) spectral origin of the $S_0 \rightarrow S_2$ transition and the ν_1 resonance Raman band of canthaxanthin in different solvents (solid squares) and in the feathers (open squares) of *P. rubra*, *E. ruber* and *I. isabellae*. Spectra in solvents were measured at 514.5 nm excitation wavelength; spectra of feathers correspond to the lowest frequency of the ν_1 Raman band observed for each feather. The solid lines represent a fit of the data to two independent linear functions. The dashed line represents a fit of the data to a single line.

It is important to note that the slope of this curve is characteristic from changes in polarizability. When other mechanisms tune the absorption of carotenoid molecules, such as changes in the conjugation length of the molecule, a shallower slope is obtained as seen in Chapter 2 (see also *e.g.* Araki G. and Murai T. [56], Angerhofer et *al*. [57]. Likewise, the difference in slope between canthaxanthin in solvents and in feathers could reflect additional properties of the binding of canthaxanthin in the feathers. However, it must be noted that it is possible to fit all the data (*i.e.* from both solvents and feathers) with a single line very close in slope to that determined for the feathers alone (dashed line in Figure 3.7) although canthaxanthin in CS_2 and in pyridine lie substantially off the line fitted to all the data (see the dashed line in Figure 3.7).

The results suggest that the position of the $S_0 \rightarrow S_2$ transition of canthaxanthin could be governed by the local polarizability of the carotenoid environment in the feathers. But, the likelihood of this hypothesis depends on the possibility of substantial variation in the refractive index of the protein binding site among species of birds. The refractive index of the β-keratin matrix in which the carotenoid molecules are embedded is fairly high at 1.58 [58] which corresponds to a polarizability, R(n), value of 0.333, typical of many solids at room temperature. An R(n) value of 0.333 predicts the position of the $S_0 \rightarrow S_2$ transition of keratin-bound canthaxanthin to be ~ 525 nm (Figure 3.3), which would be blue-shifted by ~ 11 nm compared to that observed for canthaxanthin in CS_2 (Figure 3.1B). Although the exact position of the spectral origin (0-0) band of canthaxanthin in feathers is difficult to assess accurately (Figure 3.1B), the (0-0) energies derived from the feather absorption lineshapes indicate a red-shift compared to that observed for canthaxanthin in CS_2 (Figure 3.7) not a blue-shift (hypsochromic or down- shift).

To obtain the observed (0-0) transition value of ~ 16,000 cm^{-1} for canthaxanthin in *I. isabellae* feathers (Figure 3.7) based on polarizability alone would require a value of ~ 0.6 for β-keratin (Figure 3.3), which corresponds to a refractive index of 2.3. That is an extraordinarily large, biologically impossible value that it is equivalent to many metals. Clearly, the data indicate that a change in polarizability alone cannot explain the variation in canthaxanthin absorption among feathers.

The analysis of the ν_4 bands further documents that the precise configuration of canthaxanthin is different between the feathers of different species. Two parameters are

important when considering the ν_4 bands: the frequencies of the observed components, which depend on the position of the out-of-plane distortion in the molecule, and their intensity which depends on the extent of the out-of plane distortion. In *P. rubra* feathers, the ν_4 band is slightly more intense compared to that of canthaxanthin in solvents, and about one fourth of that of the ν_3 band. This indicates that the binding of canthaxanthin to the feather protein induces a small, additional distortion of the π-electron conjugated chain that is not present in organic solvents. In *E. ruber,* the ν_4 band is nearly twice as intense as in *P. rubra*. Thus, carotenoid binding in *E. ruber* induces the same additional distortion to the molecule as in *P. rubra* but with a greater magnitude. Finally, in *I. isabellae*, the intensity of the ν_4 band reaches that of the ν_3 band, with two main components between 953.7 and 965.5 cm^{-1} (Table 3.1). These frequencies are only slightly higher than the corresponding ν_4 band frequencies observed for *P. rubra* and *E. ruber* feathers. From this we can conclude that the binding sites provided by the three feathers induce out-of-plane distortions of canthaxanthin around C-C single bonds of varying magnitudes, and that the most substantial distortion of canthaxanthin is observed in *I. isabellae* feathers. It is interesting to note that the more distorted canthaxanthin becomes compared to its structure in solvents, the redder is the absorption of the feathers.

Variation in the position and width of ν_1 band were observed with different excitation wavelengths in each of the three species. In *P. rubra,* variation in the ν_1 band with excitation wavelength was limited to a change in the fwhm of the peak. By contrast, in the feathers from *E. ruber* and *I. isabellae*, the ν_1 band shifted noticeably in frequency with excitation wavelength. More specifically, for *P. rubra* feathers, where only an increase in the width of the ν_1 resonance Raman band is observed, the absorption spectrum is broader as compared to that of canthaxanthin in solution. *E. ruber* feathers, for which ν_1 frequencies varied between 1512.1 and 1519.7 cm^{-1} (~ 7.5 cm^{-1}) with excitation wavelength, exhibit an even broader absorption band (Table 3.1). The range of ν_1 frequencies observed bracket the ν_1 peak of *P. rubra* (1514.3 cm^{-1}), and their absorption spectrum also extends beyond both ends of that observed from *P. rubra*.

Finally, for *I. isabellae*, the ν_1 frequency varies between 1507.5 and 1509.6 cm^{-1} (~ 2 cm^{-1}) depending on the excitation wavelength. This result correlates with a narrower absorption spectra for *I. isabellae* than observed in *E. ruber*.

Planarization of the terminal rings of canthaxanthin will extend the π-electron conjugation farther along the carbon chain. Lengthening the extent of π-electron conjugation is known to down-shift the resonance Raman ν_1 band and red-shift the absorption spectrum of carotenoids [32,59]. However, resonance Raman studies on carotenoids and polyenes having different π-electron conjugated chain lengths show that on average, there is ~ 15 nm of a red-shift in the absorption spectrum and ~ 6 cm^{-1} of a down-shift in the resonance Raman ν_1 band position for every added double bond [29,59]. Thus, the ~ 6-7 cm^{-1} down-shift in the ν_1 band observed in the feathers of *I. isabellae* compared to *P. rubra* (Table 3.1) is not enough to account for all of the ~ 75 nm red-shift occurring between their absorption spectra (Figure 3.7). Moreover, comparing the ν_1 band of canthaxanthin in hexane (1520.5 cm^{-1}) to that of the pigment in *I. isabellae* feathers (1508.6 cm^{-1}), both recorded using 514.5 nm excitation wavelength, shows a difference of 11.9 cm^{-1}. This would only amount to a difference of 11.9 cm^{-1} x (15 nm/6 cm^{-1}) ~ 30 nm between these two samples, which is clearly not enough to account for the violet purple color of *I. isabellae* feathers.

An additional factor that can influence carotenoid pigment absorption is the formation of molecular aggregates. Absorption and resonance Raman spectroscopic investigations of crystalline and aggregated samples of several *all-trans*-carotenoids [51,60,61] described the effect of close proximity of the pigments on their spectral properties. The data reveal that carotenoids packed in a head-to-tail arrangement, called J-aggregates in the molecular exciton coupling theory [62], undergo a significant red-shift in their absorption spectra. This is due to the fact that absorption into an energetically low-lying exciton state, formed when π-electron conjugated molecules are brought into close proximity, is red-shifted relative to the absorption bands associated with monomeric, unaggregated molecules. In fact, canthaxanthin undergoes a significant red-shift from 495 nm (20,202 cm^{-1}) in solution (monomeric) to 581 nm (17,202 cm^{-1}) in J-aggregate crystalline form [60]. Salares *et al*. [51] reported a 5 cm^{-1} down-shift of the ν_1 band of

canthaxanthin, from 1523 cm^{-1} in acetone to 1518 cm^{-1} for the aggregated molecule in 10% acetone-H_2O solution. Monomeric canthaxanthin in the eight different solvents used here has ν_1 values that span the range 1520.5 to 1517 cm^{-1} (using 514.5 nm excitation), and *I. isabellae* feathers have its ν_1 band at 1508.6 cm^{-1} (using the same excitation). This corresponds to an ~ 10 cm^{-1} down-shift, roughly twice that reported by Salares *et al*. [51] for carotenoid aggregates. This strongly suggests that carotenoid aggregation in the feathers is not the sole source of the spectral shift, but it appears to be an important factor, in addition to protein binding, needed to produce the violet color of *I. isabellae*. It is not difficult to envision that canthaxanthin may be taken up into the keratin protein fibers of feathers in a head-to-tail manner so that it forms J-aggregates or related aggregated species, which could themselves be sensitive to the properties of the local environment provided by keratin. However, additional work will be required to confirm the presence of molecular aggregates in the feather of *I. isabellae* and also to define whether the carotenoid binds directly to β-keratin or to another protein or molecule, and to assess the possibility of other interactions with the protein, *e.g.* via the C=O groups of canthaxanthin.

CONCLUSIONS

These results confirm that different species of birds have evolved differences in the carotenoid binding to feather keratin proteins. Our findings support the following conclusions:

(i) Different canthaxanthin binding modes among the three different species examined produces changes in feather reflectance spectrum that are perceived by birds as strikingly different colors. The effect of protein binding on plumage coloration can be at least as significant on plumage color as changes in molecular structure.

(ii) Canthaxanthin is bound in a consistent manner by feather proteins in each of the feathers from the three species analyzed, but each species induces a different degree of C=C double bond extension (ν_1) and out-of-plane twists of the carbon backbone (ν_4) of the bound pigment.

(iii) Different subpopulations of *all trans*-canthaxanthin molecules are present in each of the feathers, which may be distinguished on the basis of their resonance Raman

properties, particularly the frequency of their ν_1 band. These changes do not affect the general *all-trans* geometric structure of canthaxanthin, but qualitatively correlate with the width of the absorption of each of the feathers.

(iv) The degree of canthaxanthin distortion, especially the C=C double bond extension revealed through ν_1, correlates well with the red-shift in the absorption spectra exhibited by canthaxanthin in each of the three feathers studied. However, the entire extent of the red-shift cannot be explained by the refractive index/polarizability of the molecular environment nor by planarization of the canthaxanthin terminal β-rings alone, although those are contributing factors. Very likely, linear, end-to-end molecular aggregation of the carotenoid pigments is an additional important factor.

REFERENCES

[1] Blount, J. D., McGraw, K. J. 2008. Signal functions of carotenoid colouration. In: *Carotenoids vol 4: natural functions*. (eds. G. Britton, S. Liaaen-Jensen, H. Pfander), pp. 213-232. Basel, Switzerland; Boston, MA; Berlin, Germany: Birkhäuser.

[2] McGraw, K. J. 2006. Mechanics of carotenoid-based coloration. In: *Bird coloration vol 1: mechanisms and measurements*. (eds. G. E. Hill, K. J. McGraw), pp. 177-242. Cambridge, MA: Harvard University Press.

[3] Stoddard, M. C., Prum, R. O. 2011. How colorful are birds? Evolution of the avian plumage color gamut. *Behav. Ecol.* 22, 1042-1052

[4] Hill, G. E., McGraw, K. J. (eds). 2006. *Bird coloration, volume 1: mechanisms and measurements*. Cambridge, MA: Harvard University Press.

[5] Hill, G. E., McGraw, K. J., (eds). 2006. *Bird coloration, volume 2: function and evolution*. Cambridge, MA: Harvard University Press.

[6] Prum, R. O. 2006. Anatomy, physics, and evolution of avaian structural colors. In: *Bird coloration vol 1: mechanisms and measurements*. (eds. G. E. Hill., K. J. McGraw), pp. 295-353. Cambridge, MA: Harvard University Press.

[7] McGraw, K. J. 2006. Mechanics of melanin-based coloration. In: *bird coloration vol 1: mechanisms and measurements*. (eds. G. E. Hil, K. J. McGraw), pp. 243-294. Cambridge, MA: Harvard University Press.

[8] Prum, R. O., Torres, R. H., Williamson, S., Dyck, J. 1998. Coherent light scattering by blue feather barbs. *Nature* 396, 28-29.

[9] McGraw, K. J. 2003. Melanins, metals, and mate quality. *Oikos* 102, 402-406.

[10] Shawkey, M. D., Hill, G. E. 2005. Carotenoids need structural colours to shine. *Biol. Lett.* 1, 121-124.

[11] Stradi, R., Celentano, G., Rossi, E., Rovati, G., Pastore, M. 1995. Carotenoids in bird plumage: the carotenoid pattern in a series of *Paleartic Carduelinae. Comp. Biochem. Physiol.* 110B, 131-143.

[12] Goodwin, T. W. 1984. *The Biochemistry of Carotenoids. Volume II. Animals.* London,UK: Chapman and Hall.

[13] Schiedt, K. 1998. Absorption and metabolism of carotenoids in birds, fish and crustaceans. In: *Carotenoids vol 3: biosynthesis and metabolism*. (eds. G. Britton, S. Liaaen-Jensen, H. Pfander), pp. 285-358. Basel, Switzerland; Boston, MA; Berlin, Germany: Birkhäuser.

[14 Brush, A. H., Power, D. M. 1976. House finch pigmentation - Carotenoid metabolism and effect of diet. *Auk.* 93, 725-739.

[15] McGraw, K. J., Hill, G. E., Stradi, R., Parker, R. S. 2001. The influence of carotenoid acquisition and utilization on the maintenance of species-typical plumage pigmentation in the male American goldfinches (*Carduelis tristis*) and Northern cardinal (*Cadinalis cardinalis*). *Physiol. Biochem. Zool.* 74, 843-852.

[16] Stradi, R., Rossi, E., Celentano, G., Bellardi, B. 1996. Carotenoids in bird plumage: The pattern in three *Loxia* species and in *Pinicola enucleator*. *Comp. Biochem. Physiol.* 113B, 427-432.

[17] McGraw, K. J., Hill, G. E., Parker, R. S. 2005. The physiological costs of being colorful: nutritional control of carotenoid utilization in the American goldfinch, *Carduelis tristis*. *Anim. Behav.* 69, 653-660.

[18] McGraw, K. J., Hill, G. E., Parker, R. S. 2003. Carotenoid pigments in a mutant cardinal: Implications for the genetic and enzymatic control mechanisms of carotenoid metabolism in birds. *Condor* 105, 587-592.

[19] Hudon, J., Brush, A. 1992. Identification of carotenoid pigments in birds. In: *Carotenoids Part A: Chemistry, separation, quantitation, and antioxidation*. (ed. L. Packer), pp. 312-321. San Diego, CA: Academic Press.

[20] Britton, G., Helliwell, J. R. 2008. Carotenoid-protein interactions. In: *Carotenoids vol 4: natural functions* (eds. G. Britton, S. Liaaen-Jensen, H. Pfander), pp. 99-117. Basel, Switzerland; Boston, MA; Berlin, Germany: Birkhäuser.

[21] Brush, A. H. 1972. Correlation of protein electrophoretic pattern with morphology of normal and mutant feathers. *Biochem. Genet*. 7, 87-93.

[22] Brush, A. H. 1986. Tissue specific protein heterogeneity in keratin structures. *Biochem. Syst. Ecol.* 14, 547-551.

[23] Weesie, R. J., Jansen, F. J. H. M., Merlin, J. C., Lugtenburg, J., Britton, G., de Groot, H. J. M. 1997. 13C Magic angle spinning NMR analysis and quantum chemical modeling of the bathochromic shift of astaxanthin in α-Crustacyanin, the blue carotenoprotein complex in the carapace of the lobster *Homarus gammarus*. *Biochem.* 36, 7288-7296.

[24] Britton, G., Weesie, R. J., Askin, D., Warburton, J. D., Gallardo-Guerrero, L., Jansen F. J., Groot, H. J. M. D., Lugtenburg, J., Conrad, J. P., Merlin, J. C. 1997. Carotenoid blues: structural studies on carotenoproteins. *Pure Appl. Chem.* 69, 2075-2084.

[25] Cianci, M., Rizkallah, P. J., Olczak, A., Raftery, J., Chayen, N. E., Zagalsky, P. F., Helliwell, J. R. 2002. The molecular basis of the coloration mechanism in lobster shell: β-Crustacyanin at 3.2-Å resolution. *Proc. Natl. Acad. Sci. USA* 99, 9795-9800.

[26] Ilagan, R. P., Christensen R. L., Chapp, T. W., Gibson, G. N., Pascher, T., Polivka, T., Frank, H. A. 2005. A femtosecond time-resolved absorption spectroscopy of astaxanthin in solution and in α-crustacyanin. *J. Phys. Chem. A* 109, 3120-3127.

[27] Veronelli, M., Zerbi, G., Stradi, R. 1995. In-situ resonance Raman-spectra of carotenoids in birds feathers. *J. Raman Spectrosc.* 26, 683-692.

[28] Robert B., Horton P., Pascal, A. A., Ruban, A. V. 2004. Insights into the molecular dynamics of plant light-harvesting proteins *in vivo*. *Trends Plant Sci*. 9, 1360-1385.

[29] Koyama, Y. 1995. Resonance Raman spectroscopy. In: *Carotenoids vol 1B: Spectroscopy*. (eds. G. Britton, S. Liaaen-Jensen, H. Pfander), pp. 135-146. Basel, Switzerland; Boston, MA; Berlin, Germany: Birkhäuser.

[30] Robert, B. 1999. The electronic structure, stereochemistry and resonance Raman spectroscopy of carotenoids. In: *The photochemistry of carotenoids*. (eds. H. A. Frank, A. J. Young, G. Britton, R. J. Cogdell), pp. 189-201. Dordrecht, The Netherlands; Boston, MA; London, UK: Kluwer Academic Publishers.

[31] Ruban, A. V., Pascal, A. A., Robert, B., Horton, P. 2001. Configuration and dynamics of xanthophylls in light-harvesting antennae of higher plants: spectroscopic analysis of isolated light-harvesting complex of photosystem II and thylakoid membranes. *J. Biol. Chem*. 276, 24862-24870.

[32] Robert, B. 2009. Resonance Raman spectroscopy. *Photosynth. Res.* 101, 147-155.

[33] Fox, D. L., Hopkins, T. S. 1966. Carotenoid fractionation in the Scarlet Ibis. *Comp. Biochem. Physiol.* 19, 267-278.

[34] Fox, D. L. 1962. Carotenoids of the Scarlet Ibis. *Comp. Biochem. Physiol.* 5, 31-43.

[35] Hudon, J. 1990. Unusual carotenoid use by the Western Tanager (*Piranga ludoviciana*) and its evolutionary implications. *Can. J. Zool.* 69, 2311-2320.

[36] LaFountain, A. M., Kaligotla, S., Cawley, S., Riedl, K. M., Schwartz, S. J., Frank, H. A., Prum, R. O. 2010. Novel methoxy-carotenoids from the burgundy-colored plumage of the Pompadour Cotinga *Xipholena punicea*. *Arch. Biochem. Biophys.* 504, 142-153.

[37] Stoddard, M. C., Prum, R. O. 2008. Evolution of avian plumage color in a tetrahedral color space: A phylogenetic analysis of new world buntings. *Am. Nat*. 171, 755-776.

[38] Endler, J. A., Mielke, P. W. 2005. Comparing entire colour patterns as birds see them. *Biol. J. Linn. Soc.* 86, 405-431.

[39] Ödeen, A., Håstad, O. 2003. Complex distribution of avian color vision systems revealed by sequencing the SWS1 opsin from total DNA. *Mol. Biol. Evol.* 20, 855-861.

[40] Carvalho, L. S., Cowing, J. A., Wilkie, S. E., Bowmaker, J. K., Hunt, D. M. 2007. The molecular evolution of avian ultraviolet- and violet-sensitive visual pigments. *Mol. Biol. Evol* .24, 1843-1852.

[41] Britton, G., Liaaen-Jensen S., Pfander H. (eds). 2004. *Carotenoids handbook*, Basel, Switzerland; Boston, MA; Berlin,Germany: Birkhäuser.

[42] Saranathan, V., Forster, J. D., Noh ,H., Liew, S. F., Mochrie, S. G. J., Cao, H., Drusfene, E. R., Prum, R. O. 2012. Structure and optical function of amorphous photonic nanostructures from avian feather barbs: a comparative small angle X-ray scattering (SAXS) analysis of 229 bird species. *J. R. Soc. Interface* 75, 2563-2580.

[43] Noh, H., Liew, S. F., Saranathan, V., Prum, R. O., Mochrie, S. G. J., Dufrense E. R., Cao, H. 2010. Double scattering of light from biophotonic nanostructures with short-range order. *Opt. Expr.* 18, 11942-11948.

[44] Noh, H., Liew, S. F., Saranathan, V., Mochrie, S. G. J., Prum, R. O., Dufrense, E. R., Cao, H. 2010. How noniridescent colors are generated by quasi-ordered structures of bird feathers. *Adv. Mater.* 22, 2871-2880.

[45] Glatter, O., Kratky, O. 1983. *Small Angle X-ray Scattering*, 2nd edn. London,UK:Academic Press.

[46] Isler, O. 1971. *Carotenoids*, Basel, Switzerland: Birkhäuser.

[47] Bartalucci, G., Coppin J., Fisher, S., Hall, G., Helliwell, J. R., Helliwell, M. 2007. Unravelling the chemical basis of the bathochromic shift in the lobster carapace; new crystal structures of unbound astaxanthin, canthaxanthin, and zeaxanthin. *Acta Crystallogr. Sect. B: Struct Sci* B63, 328-337.

[48] Polívka, T., Frank, H. A. 2010. Molecular factors controlling photosynthetic light harvesting by carotenoids. *Acc. Chem. Res.* 43, 1125-1134.

[49] Renge, I., Sild, E. 2011. Absorption shifts in carotenoids-influence of index of refraction and submolecular electric fields. *J. Photochem. Photobiol. A* 218, 156-161.

[50] Koyama, Y., Kito, M., Takii, T., Saiki, K., Tsukida, K., Yamashita, J. 1982. Configuration of the carotenoid in the reaction centers of photosynthetic bacteria. Comparison of the resonance Raman spectrum of the reaction centers of *Rhodopseudomonas sphaeroides* G1C with those of *cis-trans* isomers of ß-carotene. *Biochim. Biophys. Acta* 680, 109-118.

[51] Salares, V. R., Young, N. M., Carey, P. R., Bernstein, H. J. 1977. Excited state (exciton) interactions in polyene aggregates. *J. Raman Spectrosc.* 6, 282-288.

[52] Lutz, M., Szponarski, W., Berger, G., Robert, B., Neumann, J. -M. 1987. The stereoisomerization of bacterial, reaction-center-bound carotenoids revisited: an electronic absorption, resonance Raman and NMR study. *Biochem. Biophys. Acta* 894, 423-433.

[53] Bart, J. C. J., MacGillavry, C. H. 1968. The crystal and molecular structure of canthaxanthin. *Acta Crystallog., Sect B* 24, 1587-1606.

[54] Ruban, A. V., Horton, P., Robert, B. 1995. Resonance raman spectroscopy of the photosystem II light-harvesting complex of green plants: A comparison of trimeric and aggregated states. *Biochem.* 34, 2333-2337.

[55] Cuthill, I. C. 2006. Color Perception. In: *Bird coloration, volume 1: mechanisms and measurements*. (eds. G. E. Hill, K. J. McGraw), pp. 3-40. Cambridge, MA: Harvard University Press.

[56] Araki, G., Murai, T. 1952. Molecular structure and absorption spectra of carotenoids. *Prog. Theor. Phys.* 8, 639-654.

[57] Angerhofer, A., Bornhauser, F., Gall, A., Cogdell, R. J. 1995. Optical and optically detected magnetic-resonance investigation on purple photosynthetic bacterial antenna complexes. *Chem. Phys.* 194, 259-274.

[58] Brink, D. J., van der Berg, N. G. 2004. Structural colours from the feathers of the bird *Bostrychia hagedash*. *J. Phys. D: Appl. Phys.* 37, 813-818.

[59] Koyama, Y., Fujii, R. 1999. *Cis-trans* carotenoids in photosynthesis: Configurations, excited-state properties and physiological functions. In: *The Photochemistry of Carotenoids*. (eds. H. A. Frank, A. J. Young, G. Britton, R. J. Cogdell), pp. 161-188. Dordrecht: Kluwer Academic Publishers.

[60] Mori, Y. 2001 Introductory studies on the growth and characterization of carotenoid solids: an approach to carotenoid solid engineering. *J. Raman Spectrosc.* 32, 543-550.

[61] Gruszecki, W. I. 1991. Structural characterization of the aggregated forms of violaxanthin. *J. Biol. Phys*. 18, 99-109.

[62] Gaier, K., Angerhofer, A., Wolf, H. C. 1991. The lowest excited electronic singlet states of all-trans β-carotene single crystals. *Chem. Phys. Lett*. 187, 103-109.

CHAPTER 4

MECHANISMS UNDERLYING CAROTENOID ABSORPTION IN OXYGENIC PHOTOSYNTHETIC PROTEINS

The electronic properties of carotenoid molecules underlie their multiple functions throughout biology, and tuning of these properties by their in vivo locus is of vital importance in a number of cases. This is exemplified by photosynthetic carotenoids, which perform both light-harvesting and photoprotective roles essential to the photosynthetic process. However, despite a large number of scientific studies performed in this field, the mechanism(s) used to modulate the electronic properties of carotenoids remain elusive. We have chosen two specific cases, the two β-carotene molecules in photosystem II reaction centers and the two luteins in the major photosystem II light-harvesting complex, to investigate how such a tuning of their electronic structure may occur. Indeed, in each case, identical molecular species in the same protein are seen to exhibit different electronic properties (most notably, shifted absorption peaks). We assess which molecular parameters are responsible for this in vivo tuning process, and attempt to assign it to specific molecular events imposed by their binding pockets.

This chapter is based on the following publication:
Mendes-Pinto, M. M., Galzerano, D., Telfer, A., Pascal, A. A., Robert, B., Ilioaia, C. 2013. *J. Biol. Chem.* 288, 18758-18765.

INTRODUCTION

Carotenoids are essential cofactors in the first steps of the photosynthetic process. They play a role as light-harvesters, complementing chlorophyll absorption in the blue-green range of the spectrum [see *e.g. 1*-4]. They also act as photoprotective molecules, through a number of different mechanisms. By quenching Chlorophyll triplet states they prevent the energy-transfer-mediated formation of singlet oxygen ($^1O_2$), one of the most harmful reactive oxygen species [5]. The latter chlorophyll triplet species are inevitably formed, with a low but significant yield, during excitation energy transfer in light-harvesting proteins and/or after charge recombination in reaction centers (RCs) [6-8]. They can additionally quench any $^1O_2$ that may nevertheless be formed. More recently it was shown that, in both plants and cyanobacteria, carotenoids play an essential role in regulating the amount of excitation energy reaching the reaction center in high-light environments, thus preventing damage due to overexcitation of these proteins [9-11].
Carotenoids achieve these functions through their electronic properties, which arise from their linear conjugated polyene chain. They exhibit a fairly simple structure built from the assembly of isoprenoid units (Figure 4.1) and a number of their electronic properties have been successfully predicted.

Figure 4.1. Molecular structures of β-carotene and lutein.

Their main absorption transition, which corresponds to a transition from the ground state to the second excited singlet state, $S_0 \rightarrow S_2$, tightly depends on the number of

conjugated C=C bonds present in this chain [12-16], and on the refractive index, *n*, of their local environment [17-22]. However, predicting the full electronic structure of carotenoid molecules has turned out to be extremely complex. Despite the intense level of research on carotenoid properties for four decades, several new, low-energy excited states have been proposed for these molecules in the last decade alone [23,24] and precise calculations of their electronic and vibrational properties still remain a challenge [25]. *In vivo*, protein binding sites provide a highly anisotropic environment to carotenoid molecules. In these conditions, it is extremely difficult to characterize the most important parameters which govern their electronic properties. However, determining these parameters would represent an important approach in our understanding of the role of the protein matrix in tuning the first steps of the photosynthetic process. Given that the role of carotenoids in other biological systems also generally involves their electronic properties (*e.g.* signaling functions, making specific use of their color), such an understanding should also prove more widely applicable throughout carotenoid research.

The combined use of electronic absorption and resonance Raman spectroscopies may help in determining the molecular parameters underlying the tuning of carotenoid electronic transitions. In resonance Raman spectra, the frequency of the C=C stretching mode of these molecules (the ν_1 band) gives direct access to the structure of the alternated system of their electronic ground state. As shown in Chapter 2 and as illustrated in Figure 4.2, a different relationship is observed between the frequency of the ν_1 band and the position of the $S_0 \rightarrow S_2$ transition, depending on the molecular mechanism tuning this transition. The frequency of the ν_1 band may thus yield direct indications on these mechanisms.

We have studied the absorption properties of β-carotene and lutein (Figure 4.1) bound to two photosynthetic proteins isolated from photosystem II (PSII) - the RC and the major light-harvesting complex (LHCII), respectively. The PSII-RC binds two β-carotene molecules, which at low temperature have their main absorption transition at 489 and 507 nm [26-28], the former being perpendicular and the latter parallel to the membrane plane [26,29-30]. These carotenoid molecules exhibit only limited singlet-singlet energy transfer to chlorophyll, and essentially no quenching of chlorophyll

triplets, but are both able to transfer an electron to the oxidized primary electron donor, albeit with very low efficiency [26,31-34]. LHCII is assembled into a trimeric form in the photosynthetic membrane, with each monomer containing two lutein molecules (lut1, lut2) whose binding sites are related by pseudo-symmetry. Whilst in LHCII monomers these luteins both absorb at 495 nm, in LHCII trimers one of them (lut2) has its absorption shifted to 510 nm (lut1 absorption remains at 495 nm; [3,35]). It has been proposed that one of these two luteins (lut1) is involved in quenching chlorophyll singlet excited states during the pH-dependent phase of non-photochemical quenching [9], the central mechanism that regulates excitation transfer in PSII.

In this work, we determine the factors which underlie differences in the electronic properties of these carotenoid molecules. In addition, we attempt to relate these differences to the three-dimensional structures of these proteins, as determined by X-ray crystallographic studies [30,36-38]. We propose a mechanism by which their binding pockets may impose specific conformations on carotenoids to modulate their electronic structure, in order to tune their absorption spectra.

MATERIAL AND METHODS

Carotenoids

β-carotene (β,β-carotene synthetic type I, C-9750) was obtained from Sigma-Aldrich (St. Louis, MO, USA). Lutein (β,ε-carotene-3,3'-diol) was isolated and purified as previously described [39]. The molecular structure of these molecules is shown in Figure 4.1.

Solvents

The solvents used in this study were all purchased from Sigma-Aldrich (St. Louis, MO, USA): tetrahydrofuran (THF), hexane, cyclohexane and acetonitrile (all absolute grade, ≥ 99.5 % GC), toluene, methanol and pyridine (anhydrous, 99.8 %), chloroform and carbon disulphide (CS_2) (anhydrous, ≥ 99 %), diethylether (≥ 99.8 % GC) and nitrobenzene (≥ 99.5 % GC).

Sample preparation

LHCII complexes were prepared from *Spinacia oleracea* PSII-enriched particles by isoelectric focusing (IEF), followed by sucrose gradient centrifugation [40]. These trimeric complexes contain two lutein molecules, one neoxanthin and only negligible amounts of violaxanthin per monomer [40]. PSII-RCs with two bound β-carotenes were isolated following the method described in Telfer *et al*. 2003 [34]. Prior to use, LHCII trimers and PSII-RC were concentrated using Centricon 30 K and 100 K cut-off concentrating tubes, respectively, to a final optical density > 5 OD at 675 nm.

Spectroscopy

Absorption spectra were collected using a Varian Cary E5 double-beam scanning spectrophotometer. The $S_0 \rightarrow S_2$ electronic transition of carotenoid molecules displays three vibrational levels; the 0-0 level (the red-most band) was used to determine the position of this transition. Resonance Raman spectra were recorded with 90° signal collection using a two-stage monochromator (U1000, Jobin Yvon, Longjumeau, France) equipped with a front-illuminated, deep-depleted CCD detector (Jobin Yvon, Longjumeau, France). Excitation wavelengths were provided by a 24 W Sabre laser (Coherent, Palo Alto, CA, USA); typically, less than 20 mW reached the sample, and sample integrity was verified by following resonance Raman spectral evolution during the experiment. Measurements at low temperature (77 K) were performed using a nitrogen-flow cryostat (Air Liquide, Sassenage, France).

RESULTS AND DISCUSSION

Isolated β-carotene and lutein

The position of the $S_0 \rightarrow S_2$ transition of carotene molecules tightly depends on their molecular structure, and in particular on the length of the π-electron conjugated system. Increasing this length induces a progressive loss of the double bond character of the C=C double bonds. This double bond character can be directly probed by resonance Raman spectroscopy, as it influences the frequency of the ν_1 Raman band. As a result, for a given solvent, a linear correlation between this frequency and the position of the $S_0 \rightarrow S_2$ transition exists, when expressed as a function of the length of the carotenoid

conjugated chain (Figure 4.2, black line). The frequency of the ν_1 Raman band for lutein and β-carotene does not correspond to that expected for carotenoids with 10 and 11 double bonds, respectively, while they nevertheless show the same relationship between ν_1 frequency and absorption position (Figure 4.2). These cyclic carotenoids, when isolated in solvents, actually display effective conjugation lengths of 9.3 and 9.6, respectively. This result was attributed to rotation of the conjugated end cycles out of the plane, such that the ring C=C's are only partially-conjugated (see Chapter 2). The position of the main absorption transition of carotenoid molecules also tightly depends on the properties of the solvent they are dissolved in, and particularly on its refractive index [17-22]. Again, there is a correlation between the position of the $S_0 \rightarrow S_2$ absorption transition and the frequency of the ν_1 Raman band for a given carotenoid molecule, when expressed as a function of solvent polarizability. This correlation is plotted in Figure 4.2 for β-carotene and lutein (red lines), and displays a different slope to that for different carotenoids in the same solvent (black), as already observed and discussed for several carotenoid molecules.

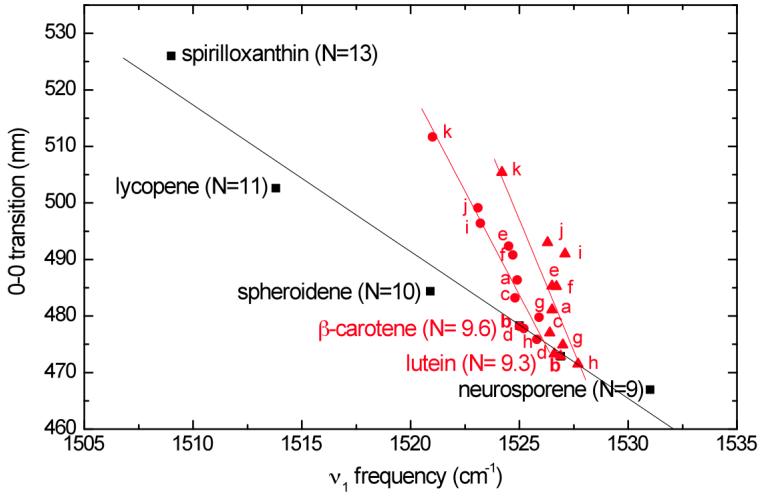

Figure 4.2. Correlation between the $S_0 \rightarrow S_2$ electronic transition and the frequency of the ν_1 Raman band for linear carotenoids with different conjugation length, N (performed in hexane; black line), compared to the same correlation for β-carotene (red line, circles) and lutein (red line, triangles) as a function of solvent polarizability (solvents: a- THF; b- hexane; c- cyclohexane; d- diethylether; e- toluene; f- chloroform; g- acetonitrile; h- methanol; i- pyridine; j- nitrobenzene; k- CS_2).

β-*Carotene in PSII-RCs*

At low temperature, PSII-RCs exhibit two main peaks in the carotenoid transition region at 489 and 507 nm (Figure 4.3). Linear dichroism experiments showed that these peaks correspond to distinct carotenoid molecules, with different orientations relative to the membrane plane [26] and, considering their position, they must be attributed to the 0-0 level of the absorption transition of each molecule. Although the resolution between these peaks becomes much lower at room temperature (RT), the overall position of the carotenoid absorption transition appears not to shift by more than 2 nm between low temperature and room temperature (Figure 4.3). This is not specific to PSII and was already observed in other photosynthetic complexes. For instance, in light-harvesting complexes from purple bacteria it was shown that, in general, the absorption transitions of the bound carotenoid molecules are very poorly dependent on temperature [41].

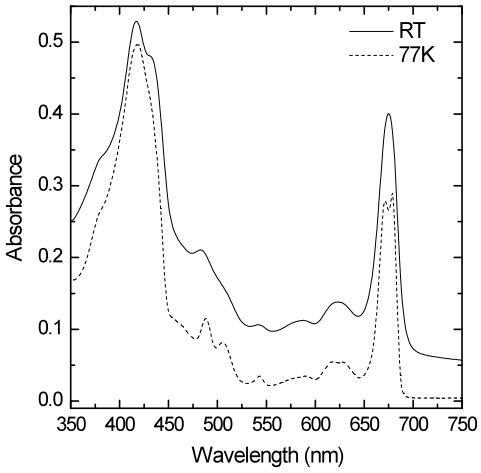

Figure 4.3. Absorption spectra of PSII-RC particles at RT (solid line) and 77 K (dashed line).

Figure 4.4 panel A displays resonance Raman spectra of PSII-RCs obtained at RT with 514.5 and 488.0 nm excitation wavelengths, chosen to be selective for the 507 and 489 nm absorbing β-carotenes respectively. They contain four main groups of bands, denoted ν_1 to ν_4, typical of carotenoid molecules. The ν_1 band ~ 1520 cm^{-1} arises from stretching vibrations of C=C double bonds. As mentioned above, its frequency depends

on the length of the π-electron conjugated chain and on the carotenoid conformation. The ν_2 band at 1160 cm^{-1} arises from stretching vibrations of C-C single bonds coupled with C-H in-plane bending modes. This region may be used as a fingerprint for the assignment of carotenoid configurations (*trans-cis*). The ν_3 band at ~ 1000 cm^{-1} arises from in-plane rocking vibrations of the methyl groups attached to the conjugated chain, coupled with in-plane bending modes of the adjacent C-Hs. Finally, the ν_4 band ~ 960 cm^{-1} arises from C-H out-of-plane wagging motions coupled with C=C torsional modes (out-of-plane twists of the carbon backbone). When the conjugated system of the carotenoid is symmetric and the molecule is planar, these out-of-plane modes will not be coupled with the electronic transition. As a result, these bands will not be resonance-enhanced upon excitation and will exhibit very low intensity in the resonance Raman spectra. However, distortions around C-C single bonds will increase the coupling of these modes with the electronic transition, resulting in an increase in resonance enhancement - *i.e.* ν_4 gains intensity. Although both spectra are globally similar and typical for *all-trans*-β-carotene, at 514.5 nm the ν_1 frequency is down-shifted by 6 cm^{-1} compared to 488.0 nm while ν_3 and ν_4 are both slightly narrower. These differences are also observed at 77 K (Figure 4.4, panel B; see also [34]) indicating that the detailed structure of each β-carotene molecule is the same at both temperatures. It is worth noting that the increase at 488.0 nm in the width of ν_3 at RT is translated into a splitting of this band into two components at 77 K.

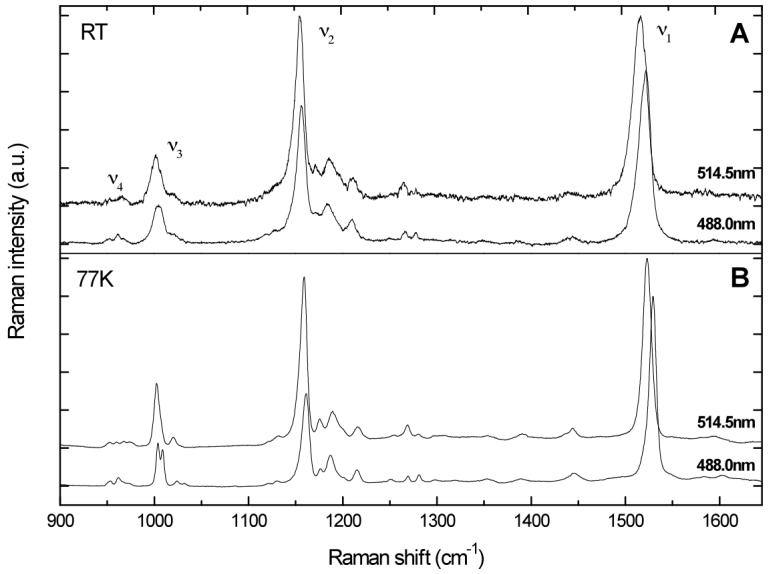

Figure 4.4. Resonance Raman spectra of PSII-RC recorded with 488.0 and 514.5 nm excitation wavelengths at RT (panel A) and 77 K (panel B).

In Figure 4.5 we plot the ν_1 frequencies and absorption positions of the two β-carotenes from PSII-RC's at RT (filled diamonds), as compared with the frequencies and positions of different-length carotenoid molecules (black line) and of β-carotene in various solvents (red line) taken from Figure 4.2. The values obtained for the blue-absorbing carotene fit on the blue slope, suggesting that the position of this absorption transition is mainly governed by the local polarizability of its binding site. It may be noted that the binding site of this molecule exhibits a rather low local polarizability (equivalent to that found in chloroform- blue open circle labeled f- with a polarizability, R(*n*), value of 0.266). On the other hand, the difference in ν_1 frequency of the two β-carotene molecules accompanying the shift in their $S_0 \rightarrow S_2$ transition is much too large (see dashed lines in Figure 4.5) to be accounted for by changes in the local polarizability of their protein binding sites. In this case, considering the difference in the position of their electronic transition, a change of ν_1 frequency of ~ 2 cm^{-1} should be expected, *i.e.* three times smaller than actually observed. The 6 cm^{-1} change seen here corresponds to a sizeable change of the apparent length of the conjugated chain, probably through

perturbation of its alternated system. Such a change in the alternated system (observed upon increasing the length of the conjugated chain) would actually up-shift the position of the carotenoid absorption by ~ 17 nm, *i.e.* it is sufficient to explain the difference in absorption between the two PSII-RC-bound β-carotene molecules. Thus the dashed line connecting these two points is parallel to the black line, which relates carotenoid of different chain length in the same solvent (Figure 4.5).

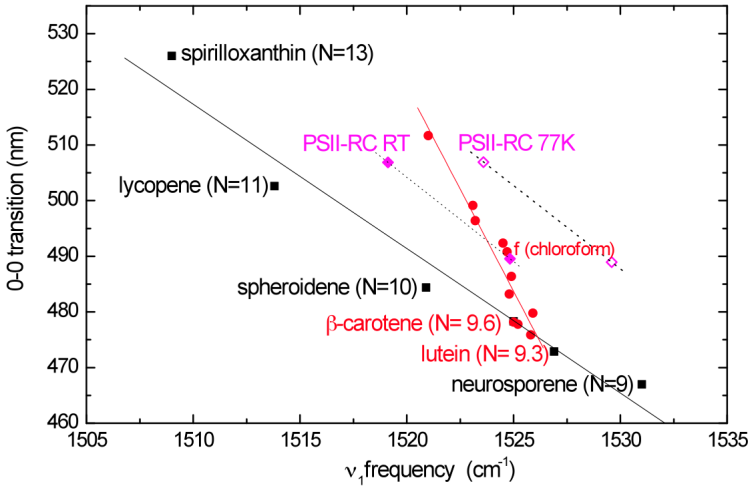

Figure 4.5. Correlation between the $S_0 \rightarrow S_2$ electronic transition and the frequency of the ν_1 Raman band for the two β-carotene molecules in PSII-RC at RT (filled diamonds) and 77 K (empty diamonds). For comparison, the relationship between carotenoids of different conjugation length in the same solvent (hexane) and the relationship expressed as a function of solvent polarizability for β-carotene are also shown (*c.f.* Figure 4.2.).

The same relationship between absorption position and ν_1 frequency is also shown for measurements of the PSII-RC at 77 K (Figure 4.5, empty diamonds). The dashed line between these two points exactly parallels that obtained at RT, but at the lower temperature there is a shift of ~ 5 cm^{-1} in the ν_1 frequency for both β-carotene molecules. Exactly the same shift for this Raman band, between room and low temperature, has recently been described in resonance Raman spectra of carotenoids in solution, and was explained by an intrinsic sensitivity of the Raman frequency to temperature (for details see [42]).

Lutein molecules in LHCII

The absorption spectrum of LHCII trimers in the carotenoid region is rather complicated, as these complexes bind up to four carotenoid pigments per monomer, namely two luteins, one 9-*cis* neoxanthin and usually one violaxanthin/zeaxanthin (present in negligible amounts in our sample). Indeed, the position of the individual absorption transitions could only be determined through second derivative analyses of absorption spectra obtained at 4 K [3]. However, as in PSII, comparing the absorption spectra of LHCII at low temperature and RT suggests that the main band positions of the LHCII-bound carotenoid molecules are very poorly sensitive to temperature (Figure 4.6).

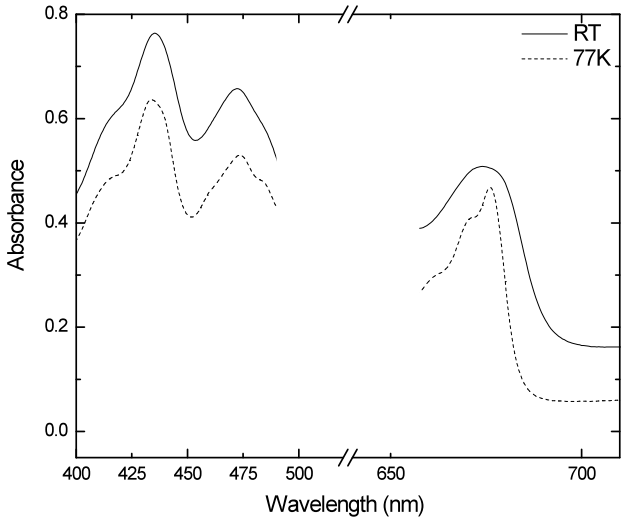

Figure 4.6. Absorption spectra of LHCII trimers at RT (solid line) and 77 K (dashed line).

Resonance Raman spectra of the LHCII-bound luteins at 77 K are displayed in Figure 4.7, panel B. As extensively documented in the literature [3,43,44], at this temperature 496.5 and 514.5 nm excitation wavelengths yield resonance Raman spectra dominated by contributions from lut1 (absorbing at 495 nm) and lut2 (absorbing at 510 nm), respectively. The frequency of the ν_1 band, which arises from the C=C stretching modes of lutein molecules, is observed at 1531 and 1527 cm^{-1} for lut1 and lut2, respectively. In

the ν_3 region (~ 1000 cm^{-1}), lut1 (at 496.5 nm) exhibits two overlapping components of similar amplitude, at 1003 and 1007 cm^{-1}. The same two bands are seen for lut2 (514.5 nm excitation wavelength), but the intensity of the higher-frequency component is less than a third that of the lower-frequency one. The ν_4 region exhibits higher intensity and structure for lut2 than for lut1 (514.5 and 496.5 nm excitation wavelengths, respectively), indicating a higher degree of distortion for lut2 in its LHCII binding site (as previously concluded; [3,43]). At RT, the broadening of the carotenoid electronic transitions must, at least in part, impair selective excitation of each carotenoid. In RT spectra obtained using excitation at 514.5 nm (Figure 4.7, panel A, upper trace), the ν_1 is quite narrow (fwhm ~ 16 cm^{-1}) and the structure of the ν_4 region is very similar to that observed at the same excitation in low temperature spectra. We may safely conclude that this excitation still ensures selective excitation of the lut2 molecule at the higher temperature, and also that the distortion of this molecule, up to now only observed at low temperature, is also present in LHCII at RT. Thus this distortion does not result from temperature-induced reorganization of the binding site. In this spectrum the position of the ν_1 band is at 1522 cm^{-1}. As in PSII-RC, we thus observe a 5 cm^{-1} shift between experiments conducted at 77 K and RT. In contrast, the spectrum at 496.5 nm exhibits significant broadening of ν_1 when the measurement is taken at RT (Figure 4.7, panel A, lower trace; fwhm ~ 18 cm^{-1}). The contributions of more than one carotenoid are thus present in this spectrum, due to a reduction in resonance selectivity as a result of broadening of the carotenoid absorption transitions at the higher temperature. Indeed, in the ν_2 region a small but significant increase in intensity is observed for the shoulder at ~ 1130 cm^{-1}. This is consistent with an increase in neoxanthin contributions to the spectrum, as bands on the low frequency side of ν_2 are quite typical for 9-*cis* carotenoids. Contributions of lut1 thus cannot be selectively observed in resonance Raman spectra at RT. Indeed, this was found to be difficult even at 77 K, where a "pure" lut1 spectrum was only obtained after removing the neoxanthin contribution from the spectra by differential analysis [44].

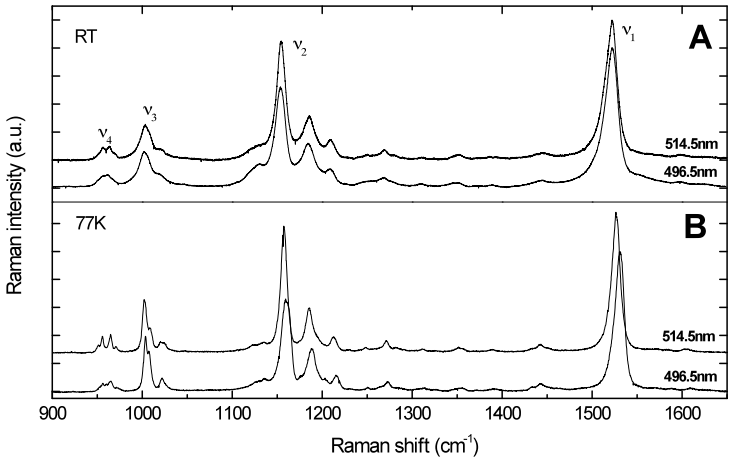

Figure 4.7. Resonance Raman spectra of LHCII trimers recorded with 496.5 and 514.5 nm excitation wavelengths at RT (panel A) and 77 K (panel B).

In Figure 4.8, the absorption position and ν_1 frequency of luteins in LHCII are compared to those obtained for lutein in various solvents (red line) and with the frequencies and positions of different-length carotenoid molecules (black line). A large shift is observed in ν_1 frequency between the two luteins at low temperature (4 cm^{-1}). As for β-carotene in PSII-RC, this shift, which reflects a change in the alternation of the conjugated C=C chain, is enough to account for the energy difference between their $S_0 \rightarrow S_2$ absorption transitions. As in PSII-RC, the ν_1 frequency of lut2 at RT (the only one we could safely extract from the resonance Raman spectra) is shifted by ~ 5 cm^{-1} as compared to its low temperature value. By analogy, we can deduce the expected ν_1 frequency of lut1 at RT, by shifting its low temperature value by 5 cm^{-1}. The resulting value fits perfectly with the *in vitro* relationship between the lutein ν_1 frequency and the position of its $S_0 \rightarrow S_2$ transition according to the polarizability of the solvent (Figure 4. 8, red line), tending to validate this approach. As in PSII-RC, we may conclude that the position of the electronic transition of this molecule is mainly governed by the local polarizability of its binding site. However, the deduced polarizability for this lutein is much higher than that calculated for the blue β-carotene in PSII-RC, as it corresponds to a value slightly higher than that for nitrobenzene (j, red triangle; Figure 4.8) with a polarizability, R(*n*), value of 0.319.

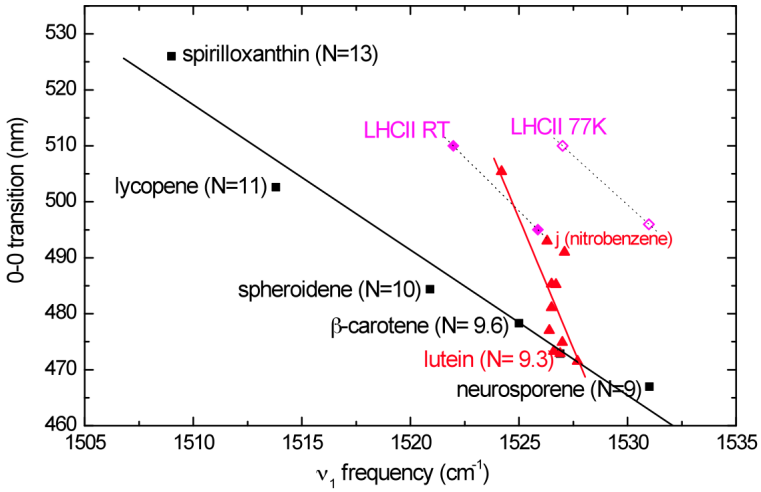

Figure 4.8. Correlation between the $S_0 \rightarrow S_2$ electronic transition and the frequency of the ν_1 Raman band for the two lutein molecules in LHCII trimers (filled diamond- RT; empty diamond- 77 K). For comparison, the relationship between carotenoids of different conjugation length in the same solvent (hexane) and the relationship expressed as a function of solvent polarizability for lutein are also shown (*c.f.* Figure 4.2).

Mechanisms tuning carotenoid absorption in PSII-RC and LHCII

In both PSII-RC and LHCII, resonance Raman spectroscopy unambiguously shows that the position of the absorption transition of the blue-absorbing carotenoid molecule is mainly governed by the polarizability provided by the protein environment. Indeed, the position of this transition and the frequency of the ν_1 mode of these molecules strictly obey the correlation obtained for both β-carotene and lutein according to solvent refractive index. The deduced average value of the environment polarizability of the blue-absorbing β-carotene in PSII-RC is lower than that of lutein. This is consistent with the environment deduced by the analysis of X-ray crystallographic structures [29,30,36]. In PSII-RCs, carotenoids are mainly surrounded by amino acids and are quite distant from other cofactors- they exhibit only low rates of energy transfer to PSII-RC chlorophyll molecules [26,32,33]. On the other hand, the luteins in LHCII are in very close contact with the LHCII-bound chlorophyll molecules, both at the levels of their end cycles and of the conjugated C=C chain [36]. Some of these chlorophylls, such

as Chl *a*-603, are nearly in *van der Waals* contact with lut1 (closest distance 3.83 Å) and are likely to provide an environment of higher polarizability.

By contrast, it is quite clear that the energy shifts between the blue- and the red-absorbing carotenoid molecules in both studied complexes are not induced by a variation in polarizability of their binding sites. If so, the position of the absorption transition of these carotenoids and their frequency would obey a correlation similar to the red lines in Figure 4.2, whereas it is clear that they deviate from these lines (see Figures 4.5 and 4.8). Again, this conclusion is consistent with the description of the environment of these molecules provided by the crystallographic structures of the two pigment-protein complexes - the blue and red luteins in LHCII, as well as the blue and red β-carotene molecules in PSII-RC, are embedded in quite similar protein environments, which are unlikely to display large changes in average polarizability (indeed in LHCII, the two binding pockets are related by the local two-fold symmetry of the complex). Instead, the absorption transition of these molecules and the frequency of their ν_1 Raman band behave as if the conjugated chain of the carotenoid molecules was increased by nearly one C=C double bond at constant polarizability (Figures 4.5 and 4.8). The apparent length of the conjugated chain of the red-absorbing lutein and β-carotene in LHCII and PSII-RC (at RT) become 10 and 10.2, respectively (Figures 4.5 and 4.8). The external parameters susceptible to induce such changes are not documented in the literature and, again, there is no dramatic change in the environment of these pigments which could be at the origin of such a change. It was shown that the luteins of LHCII and the β-carotenes in PSII-RC experience different distortions at low temperature [3,34] and we show in this work that these distortions actually also exist at RT. However, small distortions around C-C single bonds are expected to have little influence on the structure of the C=C conjugated chain and while in LHCII the red-absorbing lutein is distorted [45], in PSII it is the blue-absorbing carotenoid which exhibits the larger distortion [34].

However, lutein and β-carotene both exhibit shorter conjugation length in solvents than expected from their chemical structure (9.3 and 9.6 respectively), probably due to an out-of-plane rotation of the conjugated end-cycles of these molecules (a hypothesis recently confirmed by molecular modeling, unpublished data). Bringing one of these

end-cycles back into the plane of the C=C conjugated chain should accordingly result in a net increase of the effective conjugation length of these molecules of about 0.6 - 0.7, exactly as observed here for the red-absorbing lutein and β-carotene in LHCII and PSII-RC. We thus propose that these proteins are able to tune the absorption of their red-absorbing carotenoid via the rotation of conjugated end-cycles towards the conjugated plane of the molecule, this rotation being imposed by their binding pocket through steric hindrance. As lutein only has one conjugated end-cycle it must be this β-ring that is implicated in LHCII, while for β-carotene in PSII-RC this rotation may involve one or both end-cycles.

The initial crystallographic structure of LHCII led to the conclusion that the lutein end-rings were all in a conformation perpendicular to the C=C chain [36], a conformation which would induce a further shortening of the C=C chain of the lutein molecules. This is at variance with the present vibrational analysis of these pigments, and with the position of their electronic transitions. However, a more recent analysis led to the conclusion that these molecules display different conformations, with lut2 being more distorted than lut1 [38]- fully in agreement with our previous conclusions [3]. The progressive distortion of lut2 occurring from C9 to C13, as observed in the latter analysis, brings one of the end-rings back into the plane of the C=C chain. Such a phenomenon could indeed account for the results obtained in this work - assuming this ring contains the (partially-) conjugated C=C double bond (*i.e.* that it is the β-ring) then it would become more conjugated as a result of this distortion. It would also explain why the red-shift of lut2 absorption only occurs when this molecule is distorted - in LHCII monomers, where the lut2 conformation is relaxed, its absorption transition coincides with that of lut1 (495 nm; [3]).

Similarly, in the most recent crystallographic structure of photosystem II, a clear difference appears between the cycle geometries of the two β-carotenes bound to the PSII reaction center [30]. Both cycles of the (blue-absorbing) β-carotene perpendicular to the membrane plane (Bcr645 in PDB structure 3ARC) make a large angle with the conjugated C=C chain (dihedral angles 59 and 68°). This is quite different for the (red-absorbing) β-carotene parallel to the membrane (Bcr651), where one of the cycles makes a dihedral angle of only 12° with the plane of the C=C chain while the other,

though lying out of this plane, still makes a smaller angle than those measured for the blue-absorbing carotenoid (48°). Such a structural difference is perfectly in line with the conclusions of this study, and would account for the difference in conjugation length measured by Raman between these two molecules.

It is worth noting that, in the resonance Raman spectra of the red-absorbing β-carotene bound to PSII, only a single, narrow contribution is seen in the ν_3 region, whereas for the blue-absorbing β-carotene ν_3 is relatively broad at RT and even splits into two components at 77 K (Figure 4.4). Although this tendency is not so clear for LHCII, it is nevertheless seen- the red-absorbing lutein exhibits one major component with a satellite at higher frequency, while this higher-frequency component is more prominent for the blue-absorbing lutein (Figure 4.7). ν_3 arises from in-plane rocking vibrations of the methyl groups attached to the conjugated chain, coupled with in-plane bending modes of the adjacent C-H's. In resonance Raman spectra of fucoxanthin the ν_3 band is similarly composed of two components, which was attributed to differences in the methyl nearest neighbors in the fucoxanthin chemical structure [46]. Along the same lines, the splitting of this band observed in the blue-absorbing carotenoid may reflect the out-of-plane rotation of the end cycles, as this rotation is likely to perturb the rocking frequency of the neighboring methyl group. It is striking that in lutein, where only one rocking mode should be concerned, the intensity of the additional component is weaker than in β-carotene (where potentially two methyl groups may be concerned). In solvents, where it was concluded that the end cycles are at least partially out of the plane, the ν_3 is also observed to be broader in resonance Raman spectra at RT (see Chapter 2). The structure of this band could thus be a direct indication of the conformation of the end cycles in both β-carotene and lutein, representing a probe for this mechanism of conjugation-length modulation.

Finally, it is striking that Nature has generally used carotenoids with conjugated end cycles in oxygenic photosynthesis. Our results show that by playing on the conformation of these cycles, the position of the absorption transitions of these cyclic carotenoid molecules may be tuned by up to 15 nm per ring. It may be that this property explains the recruitment of carotenoid molecules with conjugated end cycles in the

photosynthetic process, allowing for an optimization of the excitation energy cascade in these complex light-transducing structures.

REFERENCES

[1] Cogdell, R. J., Gillbro, T., Andersson, P. O., Liu, R. S. H., Asato, A. E. 1994. Carotenoids as accessory light-harvesting pigments. *Pure Appl. Chem.* 66, 1041-1046.

[2] Horton, P., Ruban, A. V., Walters, R. G. 1996. Regulation of light harvesting in green plants. *Annu. Rev. Plant Physiol. Plant Molec. Biol.* 47**,** 655-684.

[3] Ruban, A. V., Pascal., A. A., Robert B. 2000. Xanthophylls of the major photosynthetic light-harvesting complex of plants: identification, conformation and dynamics. *FEBS* 477, 181-185.

[4] Polivka, T., Frank, H. A. 2010. Molecular factors controlling photosynthetic light-harvesting by carotenoids. *Accounts Chem. Res.* 43**,** 1125-1134.

[5] Foote, C. S. 1976. Photosensitized oxidation and singlet oxygen: consequences in biological systems. In: *Free radicals in biology.* (ed. William Pryor), pp. 85-133. New York, NY: Academic Press.

[6] Britton, G., Liaaen-Jensen, S., Pfander, H. 2008. *Carotenoids: natural fucntions, vol. 4* Basel, Switzerland; Boston, MA; Berlin, Germany: Birkhäuser.

[7] Truscott, T. G., Land, E. J., Sykes, A. 1973. *In-vitro* photochemistry of biological molecules. 3. Absorption-spectra, lifetimes and rates of oxygen quenching of triplet-states of β-carotene, retinal and related polyenes. *Photochem. Photobiol.* 17**,** 43-51.

[8] Niyogi, K. K., Bjorkman, O., Grossman, A. R. 1997. The roles of specific xanthophylls in photoprotection. *Proc. Natl. Acad. Sci. USA* 94**,** 14162-14167.

[9] Ruban, A. V., Berera, R., Ilioaia, C., van Stokkum, I. H. M., Kennis, J. T. M., Pascal, A. A., van Amerongen, H., Robert, B., Horton, P., van Grondelle, R. 2007. Identification of a mechanism of photoprotective energy dissipation in higher plants. *Nature* 450, 575-578.

[10] Ahn, T. K., Avenson, T. J., Ballottari, M., Cheng, Y. C., Niyogi, K. K., Bassi, R., Fleming, G., R. 2008. Architecture of a charge-transfer state regulating light harvesting in a plant antenna protein. *Science* 320**,** 794-797.

[11] Wilson, A., Punginelli, C., Gall, A., Bonetti, C., Alexandre, M., Routaboul, J. M., Kerfeld, C. A., van Grondelle, R., Robert, B., Kennis, J., T., M., Kirilovsky, D. 2008. A photoactive carotenoid protein acting as light intensity sensor. *Proc. Natl. Acad. Sci. USA* 105, 12075-12080.

[12] Araki, G., Murai, T. 1952. Molecular structure and absorption spectra of carotenoids. *Prog. Theorec. Phys*. 6, 639-654.

[13] Dale, J. 1954. Empirical relationships of the minor bands in the absorption spectra of polyenes. *Acta Chem. Scand.* 8, 1235-1256.

[14] Susuki, H. Mizuhash, S. 1964. π-electronic structure and absorption spectra of polyenes. *J. Phy*s. Soc. *Jpn*. 19, 724-738.

[15] Hemley, R., Kohler, B. E. 1977. Electronic-structure of polyenes related to visual chromophore. A simple model for the observed band shapes. *Biophys. J.* 20**,** 377-382.

[16] Christensen, R. L., Barney, E. A., Broene, R. D., Galinato, M. G. I., Frank, H. A. 2004. Linear polyenes: models for the spectroscopy and photophysics of carotenoids. *Arch. Biochem. Biophys.* 430, 30-36.

[17] Le Rosen, A. L., Reid, C. E. 1952. An investigation of certain solvent effect in absorption spectra. *J. Chem. Phys* 20, 233-236.

[18] Hirayama, K. 1955. Absorption spectra and chemical structure. II. Solvent effect. *J. Am. Chem. Soc.* 77, 379-381.

[19] Andersson, P. O., Gillbro, T., Ferguson, L., Cogdell, R. J. 1991. Absorption spectral shifts of carotenoids related to medium polarizability. Photochem. Photobiol. 54, 353-360.

[20] Kuki, M., Nagae, H., Cogdell, R.J., Shimada, K., Koyama, Y. 1994. Solvent effect on spheroidene in nonpolar and polar solutions and the environment of spheroidene in the light-harvesting complexes of *Rhodobacter sphaeroides* 2.4.1 as revealed by the energy of the $^1Ag^- \rightarrow {}^1Bu^+$ absorption and the frequencies of the vibronically coupled C=C stretching Raman lines in the $^1Ag^-$ and 2^1Ag^- states. *Photochem. Photobiol.* 59, 116-124.

[21] Chen, Z. G., Lee, C., Lenzer, T., Oum, K. 2006. Solvent effects on the S_0 (1^1Ag^-) $\rightarrow S_2$ (1^1Bu^+) transition of beta-carotene, echinenone, canthaxanthin, and astaxanthin in supercritical CO2 and CF_3H. *J. Phys. Chem. A* 110, 11291-11297.

[22] Renge, I., Sild, E. 2011. Absorption shifts in carotenoids-influence of index of refraction and submolecular electric fields. *J. Photochem. Photobiol. A- Chem.* 218, 156-161.

[23] Papagiannakis, E., Kennis, J. T. M., van Stokkum, I. H. M., Cogdell, R. J., van Grondelle, R. 2002. An alternative carotenoid-to-bacteriochlorophyll energy transfer pathway in photosynthetic light harvesting. *Proc. Natl. Acad. Sci. USA* 99, 6017-6022.

[24] Wang, P., Nakamura, R., Kanematsu, Y., Koyama, Y., Nagae, H., Nishio, T., Hashimoto, H., and Zhang, J. P. 2005. Low-lying singlet states of carotenoids having 8-13 conjugated double bonds as determined by electronic absorption spectroscopy. *Chem. Phys. Lett.* 410, 108-114.

[25] Wirtz, A. C., van Hermert, M. C., Lugtenburg, J., Frank, H. A., Groen, E. J. J. 2007. Two stereoisomers of spheroidene in the *Rhodobacter sphaeroides* R26 reaction center: A DFT analysis of resonance Raman spectra. *Biophys. J.* 93, 981-991.

[26] Van Dorssen, R. J., Breton, J., Plijter, J. J., Satoh, K., van Gorkom, H. J., Amesz, J. 1987. Spectroscopic properties of the reaction center and of the 47 kDa chlorophyll protein of photosystem II. *Biochim. Biophys. Acta* 893, 267-274.

[27] Kwa, S. L. S., Newell, W. R., Vangrondelle, R., Dekker, J., P. 1992. The reaction center of photosystem-II studied with polarized fluorescence spectroscopy. *Biochim. Biophys. Acta* 1099, 193-202

[28] Tomo, T., Mimuro, M., Iwaki, M., Kobayashi, M., Itoh, S., and Satoh, K. 1997. Topology of pigments in the isolated photosystem II reaction center studied by selective extraction. *Biochim.. Biophys. Acta-Bioenerg.* 1321, 21-30.

[29] Loll, B. Kern, J., Saenger, W., Zouni, A., Biesiadka, J. 2005. Towards complete cofcator arrangement in 3.0 Angstrom resolution structure of photosystem II. *Nature* 438, 1040-1044.

[30] Umena, Y., Kawakami, K., Shen, J. R., Kamiya, N. 2011. Crystal structure of oxygen-evolving photosystem II at a resolution of 1.9Å. *Nature* 473, 55-60.

[31] Takahashi, Y., Hansson, O., Mathis, P., Satoh, K. 1987. Primary radical pair in the photosystem II reaction center, *Biochim. Biophys. Acta* 893**,** 49-59.

[32] Durrant, J. R., Giorgi, L. B., Barber, J., Klug, D. R., Porter, G. 1990. Characterization of triplet-states in isolated photosystem II reaction centers - Oxygen quenching as a mechanism for photodamage. *Biochim. Biophys. Acta.* 1017, 167-175.

[33] Mimuro, M., Tomo, T., Nishimura, Y., Yamazaki, I., Satoh, K. 1995. Identification of a photochemically inactive pheophytin molecule in the spinach D-1-D-2-cyt b(559) complex. *Biochim. Biophys. Acta-Bioenerg.* 1232, 81-88.

[34] Telfer, A., Frolov, D., Barber, J., Robert, B., Pascal, A. A. 2003. Oxidation of the two β-carotene molecules in the photosystem II reaction center. *Biochem.* 42, 1008-1015.

[35] Caffarri, S., Croce, R., Breton, J., Bassi, R. 2001. The major antenna complex of photosystem II has a xanthophyll binding site not involved in light harvesting. *J. Biol. Chem.* 276**,** 35924-35933.

[36] Liu, Z., Yan, H., Wang, K., Kuang, T., Zhang, J., Gui, L., An, X., Chang, W. 2004. Crystal structure of spinach major light-harvesting complex at 2.72 Å resolution. *Nature* 418, 287-292.

[37] Standfuss, R., van Scheltinga, A. C. T., Lamborghini, M., Kühlbrandt, W. 2005. Mechanisms of photoprotection and nonphotochemical quenching in pea light-harvesting complex at 2.5 Å resolution. *Embo J.* 24**,** 919-928.

[38] Yan, H., Zhang, P., Wang, C., Liu, Z., Chang, W. 2007. Two lutein molecules in LHCII have different conformations and functions: insights into the molecular mechanism of thermal dissipation in plants. *Biochem. Biophys. Res. Commun.* 355, 457-463.

[39] Phillip, D., Ruban, A. V., Horton, P., Asato, A., Young, A. J. 1996. Quenching of chlorophyll fluorescence in the major light-harvesting complex of photosystem II: a systematic study of the effect of carotenoid structure. *Proc. Natl. Acad. Sci. US A* 93, 1492-1497.

[40] Ruban, A. V., Lee, P. J., Wentworth, M., Young, A. J., Horton, P. 1999. Determination of the stoichiometry and strength of binding of xanthophylls to the photosystem II light harvesting complexes. *J. Biol. Chem.* 274**,** 10458–10465.

[41] Gall, A., Robert, B. 1999. Characterization of the different peripheral light-harvesting complexes from high- and low-light grown cells from Rhodopseudomonas palustris. *Biochem.* 38, 5185-5190.

[42] Andreeva, A., Apostolova, I., Velitchkova, M. 2011. Temperature dependence of resonance Raman spectra of carotenoids. *Spectrochim. Acta Part A: Mol. Biomol. Spectrosc.* 78, 1261-1265.

[43] Robert, B., Horton, P., Pascal, A. A., Ruban, A. V. 2004. Insights into the molecular dynamics of plant light-harvesting proteins in vivo. *Trends in Plant Science*. 9, 385-390.

[44] Ilioaia, C., Johnson, M. P., Liao, P. N., Pascal, A. A., van Grondelle, R., Walla, P. J., Ruban, A. V., Robert, B. 2011. Photoprotection in plants involves a change in lutein 1 binding domain in the major light-harvesting complex of photosystem II. *J. Biol. Chem.* 286**,** 27247-27254.

[45] Ruban, A.V., Pascal, A. A., Robert, B., Horton, P. 2001. Configuration and dynamics of xanthophylls in light-harvesting antennae of higher plants - Spectroscopic analysis of isolated light-harvesting complex of photosystem II and thylakoid membranes. *J. Biol. Chem.* 276, 24862-24870.

[46] Premvardhan, L., Bordes, L., Beer, A., Buchel, C., Robert, B. 2009. Carotenoid structures and environments in trimeric and oligomeric fucoxanthin chlorophyll a/c(2) proteins from Resonance Raman Spectroscopy. *J. Phys. Chem. B* 113, 12565-12574.

CHAPTER 5

CAROTENOID BREAKDOWN PRODUCTS- THE NORISOPRENODS- IN WINE AROMA

In recent years there has been much interest in the role that products of carotenoid breakdown- the norisoprenoids- may play in wine aroma. The basis for this interest is that norisoprenoids have very low olfactory perception thresholds and so have a high sensorial impact on wine aroma. The norisoprenoids can be formed by direct degradation of carotenoids such β-carotene and neoxanthin or they can be stored as glycoconjugates, which can then release their volatile aglycone during fermentation via enzymatic and acid hydrolysis processes. The norisoprenoids identified in wine with important sensory properties are: TCH (2,2,6-trimethylcyclohexanone), β-damascenone, β-ionone, vitispirane, actinidiol, TDN (1,1,6-trimethyl-1,2-dihydronaphthalene), riesling acetal and TPB (4-(2,3,6-trimethylphenyl)buta-1,3-diene). The grape carotenoid profile, fermentation process and wine storage conditions, are determinant factors for the aroma of wine. The mechanisms involved in overall aroma development from grapes through fermentation to wine are yet to be defined. Progress in this area is reviewed.

This chapter is based on the following publication:
Mendes-Pinto, M. M. 2009. *Arch. Biochem. Biophys*. 483, 236-245.

Carotenoid compounds involved in wine aroma

Carotenoids in grapes

Research on carotenoids in grapes has been extensively reported in the literature. The major carotenoids (85% of the total) are β-carotene and lutein, in the range of mg/Kg; the remaining fraction is represented at levels of μg/Kg by other xanthophylls, including neochrome, neoxanthin, violaxanthin, luteoxanthin, flavoxanthin, lutein-5,6-epoxide and zeaxanthin, and *cis* isomers of lutein and β-carotene [1-8]. The carotenoids suggested to be directly involved in the aroma of wine are β-carotene and neoxanthin though lutein and violaxanthin can also be considered because they also undergo breakdown reactions that may produce norisoprenoid compounds [9,10]. A comprehensive book [9] provides extensive information about norisoprenoids and other metabolite compounds derived from carotenoids which have aroma properties in Nature.

Both the qualitative and quantitative profiles of carotenoids in grapes are affected by several factors including plant variety, climatic conditions, stage of maturity, soil characteristics and viticulture practices. The combination of these multiple parameters affects the quality of the grapes and therefore the quality of wine [11-16]. Termed *terroir* by the French, these interactions are strongly considered to be responsible for the making of a unique wine.

Type of variety: a study performed with 13 different French varieties showed that the level of carotenoid in the matured grapes ranges between 0.8 and 2.5 mg/Kg [1]. The presence of neochrome and *cis* isomers of both lutein and β-carotene has been identified only in some Portuguese varieties [8].

Sun/Shade exposure: Light is one the environmental factors with greatest influence on the growth and development of higher plants, which make use of the sun light for photosynthesis. Light is also the main factor responsible for the changes in the biosynthesis and in the regulation of carotenoids as consequence of the environmental alterations [9,17-20]. In general the highest carotenoid levels occurred in hot regions of the world. However, the temperature effect on grape composition is complex and should not be dissociated from the different degree of sunlight exposure. It seems that light

promotes the increase of carotenoids in the unripe grapes, *i.e.* before veraison, compared to shaded grapes; during maturity, grapes exposed to sunlight show a significant decrease of carotenoids compared to grapes under shade conditions [4,-6,9,21-23].

Stage of maturity: Carotenoids are synthesized mostly from the first stage of fruit formation until veraison and then degrade till the end of maturity [23]. Numerous works on the evolution of carotenoids during the maturation of grapes have revealed that the levels of β-carotene, lutein, flavoxanthin and neoxanthin decrease drastically after veraison until maturation [4,-6,21]. This is apparently related to chemical and enzymatic degradation, as will be considered further, or it may be due to processes of bioconversion of these compounds into others, for example the formation of violaxanthin from β-carotene as a consequence of the activation of the xanthophylls cycle at the end of maturation [20-23]. Violaxanthin, lutein 5,6-epoxide and luteoxanthin only appear when the sugar concentration in the grape reaches the level of 160g/Kg, while neochrome is characteristic of green grapes. Carotenoids are generally concentrated in the skin of mature grapes at levels 2-3 times higher than in the pulp [1,2,5,20,24]. A recent work on the tissue-specific mRNA expression profiling in grape berry tissue using an extensive array of genes demonstrated that the genes encoding carotenoid biosynthesis (and catabolism) showed mostly skin-specific expression patterns [25]. The observed differences in carotenoid levels from the beginning till the end of maturation have been strongly suggested as an indication of the formation of C_{13} norisoprenoids, *i.e*. the varietal aromas, responsible for the typical aromas of some grape varieties [2,9,13,23,26-30]. In fact, the biogeneration of C_{13} norisoprenoid compounds from carotenoids in grapes via a proposed biogenetic pathway was remarkably studied by Baumes and coworkers [23].

Soil characteristics and viticulture practices: Knowledge of the influence of both soil and viticulture practices on carotenoid profile in grapes is quite limited. There are, though, some studies that indicate that irrigation, for instance, have lower influence on carotenoid profile than the type of soil and its water retention capacity, showing that low water retention capacity soil can result in an increase of carotenoid concentration [31]. On a molecular basis, it was shown that water-deficit stress irrigation, which leads to significant changes in the organoleptic properties of grapes, have strong effect on the

mRNA expression patterns in the grapes [25]. Another recent study showed that different irrigation treatments do affect the size of the berry and the levels of sugar and organic acids, thus affecting directly the growth of the plant and the maturation of the grape [32]. Regarding soil composition, there are no reported studies on the assessment of carotenoid levels. However, a study with a soil that was subjected to long-term nitrogen fertilization showed that the norisoprenoids respond differentially under such soil conditions [33], which can be a possible indication of the effect on carotenoids in such grapes. Different pruning techniques, which affect the canopy of the grapes, have an impact on the yield of grapes [34], but it has not been demonstrated whether these practices influence carotenoid profile in grapes. Knowing that different light intensities can be associated with a higher or lower degree of shading of the grape bunches by the canopy, it is reasonable to speculate about a potential effect of pruning techniques on carotenoid levels.

Carotenoids in musts and wines

So far carotenoids have only been reported in must and wines of Port from the Douro Valley, northern Portugal [24,35,36]. In samples of must (macerated grapes with skin in contact with seeds and pulp) of Port winemaking cultivars from two different vinification conditions (stainless steel tank and foot-trodden "lagar") taken on an industrial scale, β-carotene and lutein were present in the range of μg/L with a different behaviour according to the vinification conditions [35]. In Port wines, the qualitative profile of carotenoids is similar to that of the corresponding grapes but at lower concentrations; the highest values found for β-carotene and lutein were 358 and 106 μg/L, respectively. Carotenoid concentrations seem to be dependent on the age of wines, with higher total carotenoid levels found in new than in aged Ports [35,36]. Carotenoids have not been reported in juice of white grapes (pressed grapes without skin contact). The fact that carotenoid molecules exist in Port wines and not in red and white table wines is probably related to the winemaking process. As Port is a naturally sweet wine produced by interrupting alcoholic fermentation by addition of brandy, some compounds of the grape matrix can remain intact in the respective wines. This is

probably the main reason that carotenoids persist in Port wines. Moreover, the addition of brandy (up to 20% v/v ethanol) may facilitate the solubilization of these molecules.

Role of carotenoids as precursors of norisoprenoids

Carotenoids are unstable compounds because of the typical highly conjugated double-bond structure. Thus, carotenoids undergo chemical and enzymatic reactions generating several compounds, some of which have powerful aroma properties*, i.e.*, carotenoids are precursors of norisoprenoids [9,10,23,37-42]. These breakdown products of carotenoids are carbonyl compounds with 13, 11, 10 or 9 carbon atoms, and retaining the terminal group of their carotenoid parent as illustrated in Figure 5.1.

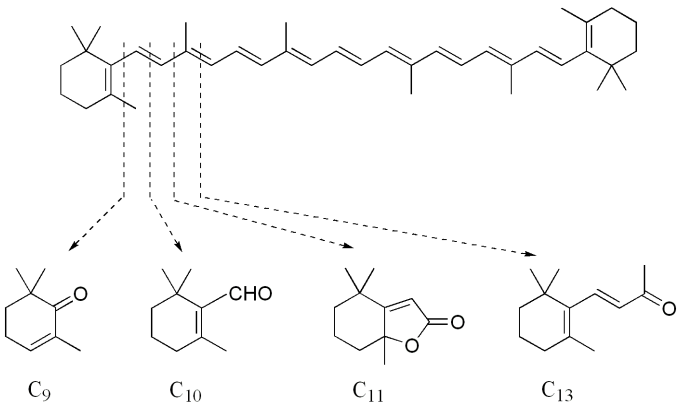

Figure 5.1. Formation of C_9, C_{10}, C_{11} and C_{13} norisoprenoid compounds from β-carotene [3].

The C_{13} compounds are the most abundant norisoprenoids in Nature. They can be divided into (i) compounds with the megastigmane structure, including the family of ionones and damascones with oxygen at different positions, *e.g.* with a keto group at C(9) as in β-ionone or at C(7) as in β-damascenone and (ii) compounds with the megastigmane structure but without oxygen in the lateral chain, *e.g.* (*E,E*)-megastigma-4,6,8-triene [9,10] (Figure 5.2). Compounds such as 2,2,6-trimethylcyclohexen-1-one, β-cyclocitral and DHA (dihydroactinidiolide) are examples of C_9, C_{10}, C_{11} norisoprenoids, respectively (Figure 5.1) [9,10]. As the breakdown products of

carotenoids that participate in wine aroma are norisopenoid compounds, the term 'norisoprenoids' is used throughout this chapter.

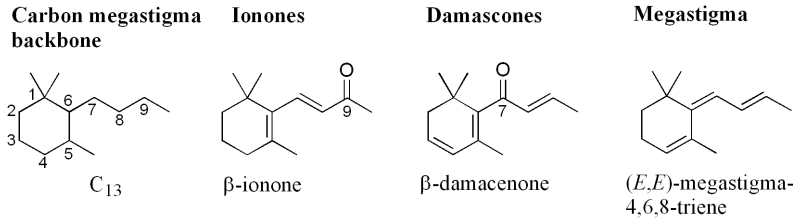

Figure 5.2. Chemical structures of carotenoid-derived norisoprenoids with the megastigma carbon backbone [9].

Norisoprenoids with high impact on the aroma of wines

Several norisoprenoids have been reported in both white and red wines, including Ports, Madeira, Rioja, Grenache, Merlot, Fiano, Rieslings, Chardonnay, Chenin blanc, Shiraz, Semillon, Cabernet Sauvignon, Sauvignon blanc and Pinot noir [9,13,15,23,34,35,43-57]. Those compounds that have been considered important to the aroma of wines are: TCH (2,2,6-trimethylcyclohexanone), β-damascenone [(2,2,6-trimethyl-1,3-cyclohexadien-1-yl)-2-buten-1-one)], β-ionone [(2,2,6-trimethyl-1,3-cyclohexen-1-yl)-3-buten-2-one)], vitispirane (2,10,10-trimethyl-6-methylene-1-oxa-spiro[4.5]dec-7-ene), actinidiol, TDN (1,1,6-trimethyl-1,2-dihydronaphthalene) and Riesling acetal (2,2,6,8-tetramethyl-7,11-dioxatricyclo [6.2.1.$0^{1,6}$]undec-4-ene). With the exception of TCH, which is a C_9 compound with a "rock-rose-like" descriptor (*Cistus ladaniferus*), and is found only in Ports, occurring at 50-400 ng/L in young wines, with an odour threshold in water of 44.3 μg/L [48], and reaching a concentration of 2.7 μg/L in aged wines [49], all the other described norisoprenoids in wine are C_{13} compounds. β-Damascenone was isolated from Bulgarian rose (*Rosa damascena*) oil by Demole *et al*. [58] and first identified in grapes and wines by Schreier and Drawert [59]. This norisoprenoid ketone is a ubiquitous compound and has a descriptor of "cooked apple/floral/quince" with an extremely low odour threshold of 2 ng/L in water [9,60]. In sweet white wines this value is estimated at 4.5 μg/L [61] with a very wide range of odour thresholds in red wines depending on the wine matrix [57], and a value of 50 ng/L in a model wine [47];

concentrations of β-damascenone in red wines can reach 4000 ng/L [15]. The other ketone, β-ionone, was isolated in 1929 from *Boronia megastigma* and identified some decades later in wines of white grapes by Schreier *et al*. [61]. It has a descriptor of "violet/woody/raspberry" and an odour threshold of 7 ng/L in water [9,62]. Levels of β-ionone in wines from Bordeaux are higher than or close to its odour threshold of 90 ng/L determined in a model wine solution [56]. Vitispirane has a "camphorous/eucalyptus" descriptor [63] and was first identified in wines by Simpson *et al*. [64], with an initial odour threshold of 800 µg/L, a value presumably obtained for a natural vitispirane compound of unknown stereochemistry [64]. Vitispirane has two chiral carbons and therefore can exist in four stereoisomeric forms. The synthesis of each of the pairs of diastereoisomers showed that they have different aroma: the pair (2*R*,5*R*) and (2*S*,5*S*) has an intensively fresher flowery-fruity note compared to the strong notes of exotic flowers and earthy-woody undertone of the pair (2*S*,5*R*) and (2*R*,5*S*) [65]. Determination of the four stereoisomers of vitispirane in Riesling wines revealed that the four enantiomers are present in different proportions [66]. Another study in which the vitispirane concentration was determined as the total of the four stereoisomers, in 17 commercial wines (Riesling, Chardonnay, Sauvignon blanc, Cabernet sauvignon and Pinot noir), showed that vitispirane was present in concentrations as low as 500 ng/L [50]. These levels are significantly lower than the reported odour threshold of 800 µg/L which, it is suggested, represents the sum of the four stereoisomers [50]. The individual odour threshold for the different vitispirane stereoisomers has not been reported. The norisoprenoid acinidiol was isolated in 1967 from the essential oil of the leaves of *Actinidia polygama* [67]. It has a descriptor of "camphoraceous or woody and resinous" [68] and also has four stereoisomers present in different proportions, which were determined later by Dimitriadis *et al*. [68] after the initial synthesis [69]. Actinidiol and its isomers are present in several different wines at higher levels than β-damascenone, vitispirane and TDN, and also in aged wines, with the exception of Riesling [9,61,66,70]. The odour threshold is still undefined. TDN (1,1,6-trimethyl-1,2-dihydronaphthalene) has received particular interest and has been the most studied norisoprenoid in wine [71]. This is probably related to the "kerosene/petrol like" descriptor of this compound with an odour threshold of 20 µg/L,

[72]. TDN is often mentioned as typical aroma of aged Riesling wines, where concentrations can reach 200 μg/L and is potentially negative for the quality of wine [9,45,73-77]. The norisoprenoid Riesling acetal has a fruity aroma descriptor and its odour threshold has not been reported [9,76,77]; high levels are also found in aged Rieslings along with TDN [9,76,77].

In addition to these norisoprenoids reported over the past decades, a new compound has recently been described by Sefton and co-workers: 4-(2,3,6-trimethylphenyl)buta-1,3-diene (TPB) [78-80]. This compound, detected in Semillon, Chardonnay and Riesling wines has a descriptor of "green or cut grass" at low concentrations and "pungent or chemical" when present in higher concentrations [79]. Concentrations range from 50-210 ng/L and the odour threshold in wine has not been established, though in a neutral white wine the reported value is 40 ng/L [78]. The structures of these norisoprenoid compounds are illustrated in Figure 5.3.

Figure 5.3. Structures of norisoprenoids important to the aroma of wine. (1) TCH (2,2,6-trimethylcyclohexanone); (2) β-damascenone; (3) β-ionone; (*4*) vitispirane; (5) actinidiol; (6) TDN (1,1,6-trimethyl-1,2-dihydronaphthalene); (7) Riesling acetal; (8) TPB (4-(2,3,6-trimethylphenyl)-buta-1,3-diene).

The contribution of other norisoprenoids, for instance vomifoliol, β-cyclocitral and α-ionone, among many others, to the wine aroma is still uncertain, because sensory studies have not yet been reported. This is also the case with other norisoprenoids identified as constituents of oak wood [81].

Interactions of norisoprenoids with the chemical composition of wine

The aroma of wine is complex. Along with norisoprenoids, more than 800 other compounds, belonging to different classes of aroma compounds such as thiols, amines, esters, lactones and alcohols, all contribute to the wine aroma at concentrations ranging from ng/L to mg/L, as widely reported in the literature. Moreover the aroma descriptor and aroma perception of a given compound are influenced by its concentration as well as by interactions with the biological matrix of wine [46,47,57,82,83]. While most of the works on such interactions that can change, decrease or increase the aroma properties of the volatile compounds in wines have been made with polyphenols [84-86], metoxypirazines and others [87-89], only recently some researchers have been focused on these interactions involving norisoprenoids. A study with various French red wines shows that β-damascenone enhances some fruity aromas and masks the herbaceous aroma of methoxypyrazine, and is suggested to have more an indirect than a direct sensorial impact on these red wines [57]. The enhancement of fruity aroma by both β-damascenone and β-ionone was also observed in wines from Uruguay [90]. In Spanish aged red wines, the fruity aroma depends on the levels of β-damascenone while β-ionone odour perception seems to be affected by some volatile alcohols [91]; in young white wines, β-damascenone does not affect the aroma [92]. In a model wine, the concentration of β-damascenone was decreased by SO_2, but not affected by small changes in pH [93]. This complexity of the wine aroma makes it complicated to predict the aroma properties of a wine from a given compound alone, because its perception can be affected by other wine volatile compounds.

Breakdown reactions of carotenoids

The breakdown reactions responsible for the formation of norisoprenoids that participates in the aroma of wine are yet to be defined. The mechanisms reported in the literature based on model assays *in vitro* and chemical synthesis, and involving β-carotene and neoxanthin as initial carotenoid precursors and some megastigmane structures as intermediates, have been taken as realistic proposals for the possible biochemical pathways for the norisoprenoid wine biological matrix since the pioneering

work of Isoe *et al.* in 1969 [39]. The proposed mechanisms for the formation of the described norisoprenoids will be illustrated, with the exception of actinidiol, a compound that is reported to be involved in the formation of TPB; there is no proposed pathway for its formation in wine. These mechanisms consider two types of reactions [9,10]: (a) enzymatic, catalysed by dioxygenases, as a one-step direct carotenoid degradation, or via glycosylation and breakdown of stored glycosides by glycosidase enzymes and (b) non-enzymatic reactions, involving one or several steps of carotenoid degradation, stimulated by light, oxygen, temperature and acid hydrolysis.

Carotenoid degradation: formation of norisoprenoids

Carotenoids can degraded by enzymatic or non-enzymatic reactions yielding norisoprenoids [9,10,23,37-42]. However, these norisoprenoids can arise either by direct degradation of carotenoids or via glycosylated intermediates [9,10,30,94-96]. Those that are in the non-glycosylated (free) fraction constitute the C_{13} varietal aromas in grapes; the others that are glycoconjugated (bound fraction) are stored and can then release their volatile aglycone during the fermentation, via enzymatic and acid hydrolysis [9,10,30,94-96] (Figure 5.4). While for a long time the involvement of regiospecific enzymatic cleavage by 9,10,(9',10')-carotenoid cleavage dioxygenase (CCD) in the formation of C_{13} norisoprenoids in grapes was a hypothesis, albeit supported by negative correlations between carotenoids and C_{13} norisoprenoids levels during grape maturation, the recent discovery of the carotenoid cleavage dioxygenase gene in grapes by Mathieu and co workers [97,98] constitutes a significant step in elucidating the effective role of these enzymes on the biosynthesis of C_{13} norisoprenoids in grapes.

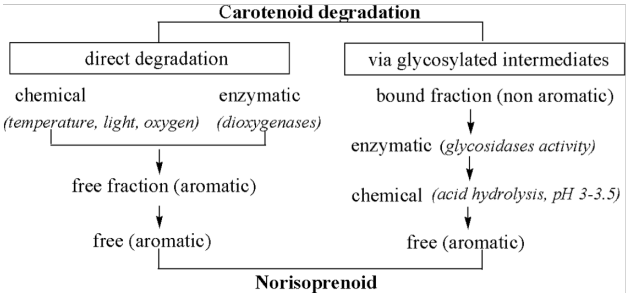

Figure 5.4. Formation of norisoprenoids either via direct carotenoid degradation or via glycosylated intermediates.

Proposed realistic mechanisms

General mechanism: the formation of β-damascenone from neoxanthin: The general mechanism for the formation of norisoprenoids in plants requires three steps [9]: (i) initial dioxygenase cleavage, (ii) enzymatic transformation of the primary cleavage products to give the non-aroma intermediate metabolites and (iii) acid catalysed conversion of these non-aroma intermediates into the aroma compounds. The formation of β-damascenone from neoxanthin by both enzymatic and non-enzymatic reactions, proposed by Isoe *et al*. in 1973 [41] is illustrated in Figure 5.5. The 'grasshopper ketone', an allenic ketodiol isolated from the defensive secretions of a flightless grasshopper [99], is the primary oxidative product) which undergoes enzymatic reduction to the allenic triol megastigma-6,7-diene-3,5,9-triol followed by conversion into the aroma ketone β-damascenone by acid catalysis at pH 3 [9]. The observation that grasshopper ketone derivatives are present in both grapes and wines [27,43,74] gives support to this mechanism for β-damascenone generation in grapes and wines.

Figure 5.5. (Left) General mechanism for the conversion of carotenoids into norisoprenoid aroma compounds in plants. (Right) the formation of β-damascenone from neoxanthin [9].

Enzymatic reactions: Carotenoid biodegradation is assumed to be catalysed by a 9,10,(9',10')-carotenoid cleavage dioxygenase (CCD) that is not specific for any particular carotenoid end group. The formation of β-ionone from β-carotene (in rose flowers) proposed by Eugster and Marki-Fischer in 1991 [100] is shown in Figure 5.6. A second molecule of β-ionone is proposed to be formed together with the C_{14} -diapocarotenoid rosafluene, by subsequent oxidative degradation of the C_{27} alcohol, 10'-apo-β-caroten-10'-ol. The common occurrence of β-ionone and rosafluene in garden roses supports this consideration [10]. β-Ionone is then considered to be the primary product of β-carotene by 9,10,(9',10')-carotenoid cleavage dioxygenase activity [10]. The study of carotenoid cleavage enzymes in plants has been the focus of researchers for a long time. In spite of the contribution of studies with enzymes purified from quince (*Cydonia oblonga*) and star fruit (*Averrhoa carambola*) [9,10,101], the knowledge of carotenoid cleavage enzymes is still limited [9].

Figure 5.6. Cleavage of β-carotene by 9,10,(9',10')-carotenoid cleavage dioxygenases with the formation of two molecules of β-ionone and the C_{14} rosafluene. (Adapted from [10]).

Chemical reactions (photo-oxygenation, thermal degradation in aqueous medium and acid hydrolysis of intermediate megastigma precursors): The oxidation of β-carotene under light exposure was also proposed by Isoe *et al*. in 1969 for the generation of a β-ionone and also DHA [39] (Figure 5.7). The extent of this photo-oxygenation reaction

depends on the levels of oxygen and light intensity. Knowing that light exposure is one of the natural environmental conditions that affect the carotenoid profile during grape maturation (see section Carotenoids in grapes) the photo-oxygenation of β-carotene is thus a reasonable proposal as a pathway that contributes to the presence of β-ionone in grapes *in vivo*.

Figure 5.7. Photo-oxygenation of β-carotene to generate β-ionone and DHA (dihydroactinidiolide) [39].

Thermal degradation of β-carotene in aqueous medium leads to the formation of β-ionone and TCH, 2,2,6-trimethylcyclohexen-1-one, β-cyclocitral, DHA and other reaction products. The reaction at 97°C for 3 hours involves initially epoxidation and furanoid rearrangement. The mechanism illustrated in Figure 5.8 was proposed by Kanasawud and Crouzet in 1990 [38]. The extent of β-carotene degradation is strongly dependent on temperature and time of reaction [9,38].

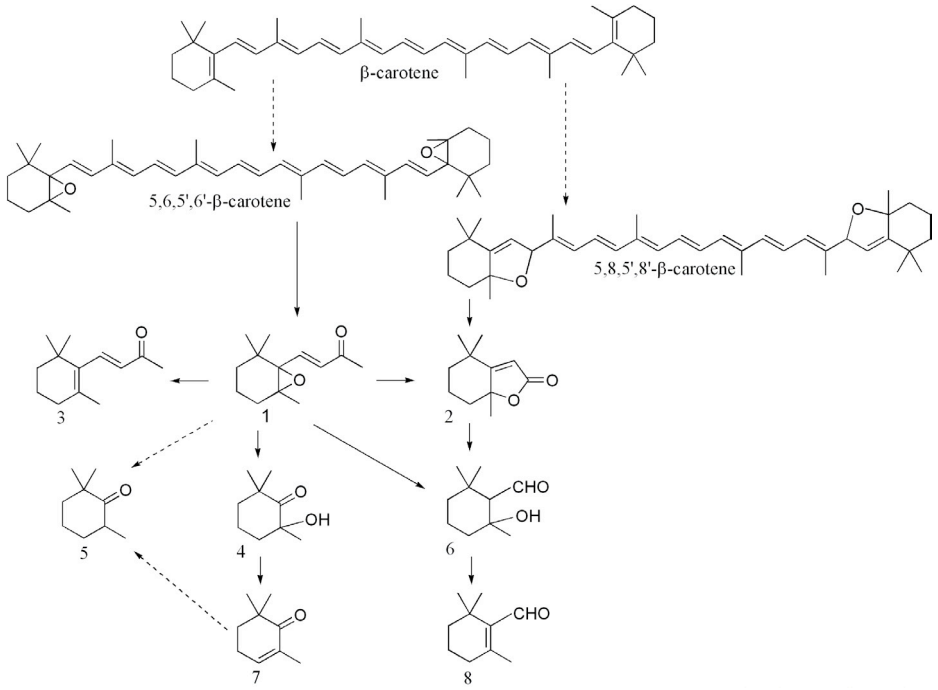

Figure 5.8. Thermal degradation products of β-carotene. (1) DHA (dihydroactinidiolide); (2) 5,6-epoxy-β-ionone; (3) β-ionone; (4) 2-hydroxy-2,6,6-trimethylcyclohexanone; (5) TCH (2,2,6-trimethylcyclohexanone; (6) 2-hydroxy-2,6,6-trimethylcyclohexane-1-carboxaldehyde; (7) 2,6,6-trimethylcyclohex-2-en-1-one; (8) β-cyclocitral. (Adapted from [38]).

It is important to take into consideration that the model systems studied for thermal degradation of β-carotene require extreme temperature over a long period of time, sometimes in the presence of organic solvents such as ethanol and benzene [9,38]. Although these conditions are not representative of the natural conditions that can contribute to the degradation of carotenoids and norisoprenoids formation, they are valid studies because they can be indicators of the naturally occurring reactions. The formation of TDN and Riesling acetal by acid hydrolysis of megastigmane structures as intermediates has been proposed by Winterhalter *et al*. in 1991 [76]. The existence of multiple possible precursors for TDN, vitispirane and also of β-damascenone, was observed in heated juice of Riesling grapes [30]; the glycosylated forms were hydrolysed to release the corresponding aroma norisoprenoids. In Riesling wines, TDN, vitispirane and Riesling acetal were formed in high concentrations by acid hydrolysis of

the glycosylated precursors [74]. While the precursor of β-damasenone has already been suggested (megastigma-6,7-dien-3,5,9-triol) the precursors of TDN and Riesling acetal were proposed later [76]; the glycosylated form of 2,6,10,10-tetramethyl-1-oxaspiro[4.5]dec-6-ene-2,8-diol (structure 1a) identified in wines was considered as a natural precursor of TDN after acid hydrolysis, while 1,4-dihydroxy-7,8-dihydro-β-ionone (structure 1b) was considered as the precursor of Riesling acetal [75]. This work also provided evidence of multiple precursors of TDN as previously suggested in related work with the same Riesling wine [73]. The reaction sequence for the formation of these aroma compounds is shown in Figure 5.9. Vitispirane seems also to have multiple gltcoconjugated precursors in grapes and wines [73]; acid hydrolysis of these generates various vitispirane species [102,103]. Glycosylated derivatives of megastigm-5-ene-3,4,9-triol and 3-hydroxytheaspirane that were identified in grapes and wine could be some of the precursors of vitispirane [101,102]. Figure 5.10 represents mechanisms for the formation of isomeric vitispiranes in Riesling wine proposed by Waldmann and Winterhalter in 1992 [103].

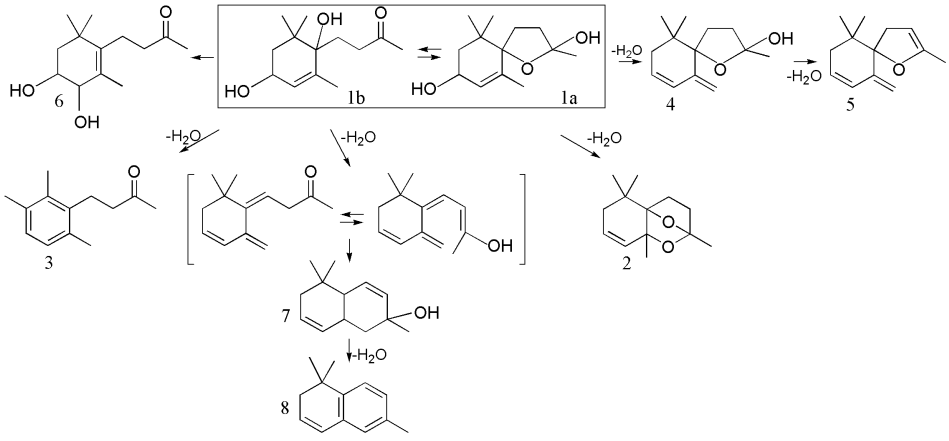

Figure 5.9. Proposed mechanism for the formation of TDN (1,1,6-trimethyl-1,2-dihydronaphtalene) and Riesling acetal. (1a) 6,10,10-trimethyl-2-oxaspiro[4.5]dec-6-ene-2,8-diol; (1b) 3,6-dihydroxy- 4,5-didehydro-5,6,7,8-tetrahydro-β-ionone; (2) Riesling acetal; (3) 4-(2,3,6-trimethylphenyl)-butan-2-one; (4) 10,10-dimethyl-6-methylene-2-oxaspiro[4.5]dec-7-en-2-ol; (5) 10,10,dimethyl-2-oxaspiro[4.5]dec-2,7-diene; (6) 3-4-dihydroxy-7,8-dihydro-β-ionone; (7) 6-hydroxy-1,1,6-trimethyl-1,2,5,6-tetrahydronaphthalene; (8) TDN. (Adapted from [76]).

Figure 5.10. Proposed mechanism for the formation of vitispirane. (1) megastigma-4-ene-3,6,9-triol; (2) and (3) (3-β-D)- and (9-β-D)- glycosylated forms of (1). (4) glycosylated megastigma-5-ene-3,4,9-triol; (5) glycosylated 3,5-diene-6,9-diol; (6) glycosylated 3-hydroxytheaspirane; (7) vitispirane. (Adapted from [103]).

The generation of the newly identified norisoprenoid with sensory wine properties, TPB, was proposed by Cox *et al*. in 2005 [80] to occur by acid hydrolysis of intermediate megastigma precursors, namely 3,6,9-trihydroxymegastigma-4,7-diene and 3,4,9-trihydroxymegastigma-5,7-diene and isomeric actinidiols (Figure 5.11). Significant levels of TPB were produced by chemical synthesis from these precursors at wine pH conditions and at both ambient temperature (25°C) and 45°C. Glycosylated forms of these compounds are suggested to be responsible for the presence of TPB observed in crude glycosidic extracts of various red and white grapes [80].

Figure 5.11. Proposed mechanism for formation of TPB (4-(2,3,6)trimethylphenyl)-buta-1,3-diene). (1) 3,6,9-trihydroxymegastigma-4,7-diene; (2) 3,4,9-trihydroxymegastigma-5,7-diene; (3) 4-(4-hydroxy-2,6,6-trimethylcyclohex-2-enyl)-2,3-dihydroxybut-4-ene; (4) actinidiol; (5) 4-(2,2,6-trimethylcyclohexa-3,5-dienyl)-2,3-dihydroxybut-4-ene; (6) 4-(2,3,6-trimethylphenyl)-2-hydroxybut-3-en; (7) TPB. (Adapted from [80]).

Though no mechanism has been proposed for its formation, actinidiol is known to be derived from actinidiolide, a compound related to DHA [67]. Free and glycosylated megastigmatriol structures found in Riesling leaves are suggested to be involved in the formation of isomeric actinidiols [104,105].

The work developed since 1969 by Isoe *et al*. on the formation of carotenoid breakdown products by direct degradation has been widely cited for the different possibilities of norisoprenoids formation and the aroma of wine. However, the formation of β-damascenone by thermal oxidation of neoxanthin was recently proposed [106]. This model system study with a highly purified and labelled carotenoid precursor provides accurate and precise evidence for the direct formation of β-damascenone from neoxanthin by a non-enzymatic process. Another recent study on the degradation of β-

carotene and lutein and the formation of β-damascenone, β-ionone and β-cyclocitral in both model wine solution and wines, may have provided misleading information because commercial carotenoid samples were used without further purification (β-carotene and lutein were 95% and 70% purity level, respectively) and stable istotopic labelling was not used [107]. These are vital requirements if new insights are to be gained into the relationship between carotenoid degradation and norisoprenoids in biological samples.

Overall contribution of norisoprenoids to the wine aroma: from grapes to aged wine

The overall contribution of norisoprenoids to the aroma of wine is made by norisoprenoids that occur free in the grapes, by norisoprenoids released by enzymatic or acid hydrolysis during fermentation and finally by the chemical reactions that can occur during wine aging and storage.

Grapes. The carotenoid breakdown reactions that occur during the maturation of grapes and the subsequent formation of norisoprenoids, as C_{13} varietal aromas, provide the contribution of the free fraction of norisoprenoids to the wine aroma [2,9,13,23,26-30]. This contribution can be more or less relevant to the final aroma of wine depending on the viticulture conditions, which affect the carotenoid profile of the grape. It is worth mentioning though, that the several viticulture conditions or parameters should not be studied individually but as interacting effects, as is the case of light exposure and temperature [13].

Fermentation. The release of glycosylated intermediates by acid hydrolyses occurs during fermentation and has been suggested to make a major contribution to the concentration of the aroma active norisoprenoids in wine [9,10,30,94-96]. The study of glycoconjugated norisoprenoids and the formation of the aroma compounds by glycosidase activity has been the focus of much work [26,27,30,94-96,105]. Some of this gives information about the glycoconjugate composition of grapes of several red and white cultivars, and shows that levels of both glycoconjugated and released compounds vary greatly among the different grapes. [27,93,105,108-112]. Different fermentation processes are used according to the type of wines. Microvinification with

different conditions of mild acid hydrolysis (temperature, maceration techniques, alcohol content and levels of sugar, yeast and bacteria activity) has been used as a small-scale winemaking process [113-115].

Aged wine. In young wines, the aroma norisoprenoids composition comprises compounds arising directly from grapes and those released during the fermentation process, but the wine storage conditions, particularly temperature and oxygen, can also affect the development of aroma in wines. The wine aging process, both in oak and in bottles, and the development of aroma properties under storage conditions has been a great concern and subject of study during the past two decades. The information related to norisoprenoids is still very limited, however [35,44,49,74,107,115-117]. In order to understand the behaviour of aroma compounds in wine, accelerated-aging protocols with different temperatures and oxygen concentrations have been used to obtain an indication of the chemical reactions responsible for the evolution of the wine aroma bouquet [35,44,49,74,107,115-117]. It has been observed that, in general, high oxygen intake and high temperatures stimulate the formation of norisoprenoids in wines. This is in agreement with the high levels of some norisoprenoids typically found in aged wines, in particular in aged Rieslings [30,74] and in Ports [35,49]

Port wine is a particular case. Ports contain considerable levels of carotenoids [24,35,36]. Because important norisoprenoids identified in ports are TCH, β-damascenone, β-ionone and TDN [48,49], which have been proposed as carotenoid breakdown products, it can be considered that the carotenoids in ports are chemically degraded and thus have a role in the evolution of aroma during the wine aging process. Moreover, the long period of aging of ports (more than 4 years both for bottle-aged "vintage category" and barrel-aged "tawny category") potentially also leads to chemical reactions with the norisoprenoid and other constituents of oak woods [81].

Challenge for carotenoid research/wine aroma- some considerations

The relationship between carotenoid compounds and norisoprenoids in wine is extremely complex. During the past decades, research on norisoprenoids and wine aroma has been widely reported and significant advances have been made in the field of carotenoid breakdown products with aroma impact in wine quality. Important research

has been developed principally in Europe, United States, South Africa and Australia, where the production of wine in the different Demarcated Regions imposes a standard level of quality of the wine and is thus closely concerned with the market demand and consumer preferences. The contribution to the present state of knowledge has been remarkable. However, future research work should lead to an improved understanding of the behaviour and the biochemical pathways for formation of carotenoid breakdown products that contribute to the aroma of wine. Therefore, some challenges, which require an interdisciplinary approach are proposed: (a) analytical chemistry with purified standards and isotopic labelling assays both *in vivo* and in model systems to allow the monitoring and assessment of compounds present in trace amounts; (b) molecular biology for the characterization of the genes coding for the enzymes of norisoprenoid biosynthesis, which may involve carotenoids other than β-carotene and neoxanthin; (c) sensorial analysis involving different types of panels for better consistency of the descriptors and for establishing, when possible, the different threshold levels of a given compound in a particular wine, as well as the determination of the sensory properties of the many other norisoprenoids detected in wines and their interactions; (d) development of statistical and sensorial models to correlate the chemical composition with aroma properties of the wine, with the aim of predicting these properties from the chemical composition.

A main goal is to have research outcomes that can give guidance to viticulturists and winemakers. From their perspectives, it is essential to identify the viticulture practices that can lead to a good balance of the varietal aromas and link this to the knowledge of fermentation conditions that will enhance the release of these aromas, and ultimately combine this with the knowledge of the appropriate storage for the aging of the wine. There is thus a need for strong knowledge which can be translated into a priority of the wine research and industry: to produce wine with quality.

REFERENCES

[1] Razungles, A., Bayonove, C. L, Cordonnier, R. E., Baumes, R. 1987. Étude des caroténoides du raisin à maturité. *Vitis* 26, 183-191.

[2] Razungles, A., Bayonove, C. L, Cordonnier, R. E, Sapis, J. C. 1988. Grape carotenoids: changes during the maturation period and localization in mature berries. *Vitis* 39, 44-48.

[3] Marais J., van Wyk , C. J., Rapp, A. 1989. Carotenoids in grapes. In: *Flavors and off-flavors, Proc. 6th Int. Flavor Conference Rethymnon, Crete, Greece* (ed. G. Charalambous), pp. 71-85. Amsterdam, The Netherlands: Elsevier.

[4]Marais, J., van Wyk, C. J., Rapp, A. 1991. Carotenoid levels in maturating grapes as affected by climatic regions, sunlight and shade. 1991. S. *Afr. J. Enol. Vitic*. 12, 64-69.

[5] Razungles, A., Babic, I., Sapis, J. C., Bayonove, C. L. 1996. Particular behaviour of epoxy xanthophylls during véraison and maturation stage. *J. Agric. Food Chem*. 44, 3821-3825.

[6] Bureau, S. M., Razungles, A., Baumes, R. L., Bayonove, C. L. 1998. Effect of vine or bunch shading on carotenoid composition in *Vitis vinifera L.* berries. I. Syrah grapes. *Vitic. Enol. Sci*. 53, 64-71.

[7] Bureau, S. M., Razungles, A., Baumes R. L., Bayonove, C. L. 1998. Effect of vine or bunch shading on carotenoid composition in *Vitis vinifera L.* berries. II. Muscat of Frontignan grapes. *Vitic. Enol. Sci*. 53, 72-78.

[8] Mendes-Pinto, M. M., Silva Ferreira, A. C., Oliveira, M. B. P. P, Guedes de Pinho, P. 2004. Evaluation of some carotenoids in grapes by reversed- and normal-phase liquid chromatography. *J. Agric. Food Chem.* 52, 3182-3188.

[9] Winterhalter, P., Rouseff, R. (eds). 2001. *Carotenoid-derived aroma compounds*. ACS, Symp. Ser. 802. Am. Chem. Soc. Washington DC, USA.

[10] Wahlberg, I. Eklund, A. -M. Degraded carotenoids. 1998. In: *Carotenoids Vol. 3: Biosynthesis and metabolism* (eds. G. Britton, S. Liaasen-Jensen, H. Pfander), pp. 195-216. Basel, Switzerland; Boston, MA; Berlin, Germany: Birkhäuser.

[11] Jones, G. V., Davis, R. E. 2000. Climate influences on grapevine phenology, grape composition and wine production and quality for Bordeaux, France. *Am. J. Enol. Vitic.* 51, 249-261.

[12] van Leeuwen, C., P. Friant, P., Chone, X., Tregoat, O., Koundouras, S., Bubourdieu, D. 2004. Influence of climate, soil and cultivar on terroir. *Am. J. Enol. Vitic.* 55, 207-217.

[13] Lee, S. -H., Seo, M. -J., Cotta, J. P., Block, D. E., Dokoozlian, N. K., Ebeler, S. 2007. Vine microclimate and norisoprenoid concentration in Cabernet sauvignon grapes and wines. *Am. J. Enol. Vitic*. 58, 291-301.

[14] Falcao, L. D., de Revel, G., Perello, M. C., Moutsiou, A., Zanus, M., Bordignon-Luiz, M. T. 2007. A survey of seasonal temperatures and vineyard altitude influences on 2-methoxy-3-isobutyl pyrazine, C13-norisoprenoids, and the sensory profile of Brazilian Cabernet sauvignon wines. *J. Agric. Food Chem.* 55, 3605-3612.

[15] Sabon, I., de Revel, G., Kosteridis, Y., Bertrand, A. 2002. Determination of volatile compounds in Grenache wines in relation with different terroirs in the Rhone valley. *J. Agric. Food Chem*. 50, 6341-6345.

[16] Marais, J., Calitz, F., Haasbroek , P. D. 2001. Relationship between microclimatic data, aroma compound concentrations and wine quality parameters in the prediction of Sauvignon blanc wine quality. *S. Afri. J. Enol. Vitic.* 13, 22-26.

[17] Young, A. J. 1993. Ocurrence and distribution of carotenoids in photosynthetic systems. In: *Carotenoids in photossinthesis* (eds. A. J. Young, G. Britton), pp. 16-72. London, UK: Chapman and Hall.

[18] Young, A. J., Britton, G. 1990. Carotenoids and stress. In: Stress responses in plants: adaptation and acclimation mechanism. (eds. R. G. Alscher, J. R. Cumming), pp. 87-112. New York, USA: Wiley-Liss.

[19] Goodwin, T. W. 1980. *The Biochemistry of the carotenoids, Vol 1. Plants.* London, UK: Chapman and Hall.

[20] During, H. 1999. Photoprotection in leaves of grapevines: responses of the xanthophylls cycle to alterations of light intensity. *Vitis*. 38, 21-24.

[21] Razungles, A. J., Bureau, S., Bayonove, C., Baumes, C.R. 1999. Effect de l'ensoleillement sur les teneurs en precurseurs d'arome des baies de Syrah. *OIV*. 2, 382-388.

[22] Oliveira, C., Silva Ferreira, C., Costa, P., Hogg, T., Guedes de Pinho, P. 2004. Effect of some viticultural parameters on the grape carotenoid profile. *J. Agric. Food. Chem*. 52, 4178-4184.

[23] Baumes, R., Wirth, J., Bureau, S. Gunata, Y., Razungles, A. 2002. Biogeneration of C13-norisoprenoid compounds: experiments supportive for an apo-carotenoid pathway in grapevines. *Anal. Chim. Acta* 458, 3-14.

[24] Guedes de Pinho, P., Silva Ferreira, A. C., Mendes Pinto, M., Benitez, J. C., Hogg, A. T. 2001. Determination of carotenoid profile in grapes, musts and fortified wines from Douro varieties of *Vitis vinifera*. *J. Agric. Food Chem*. 49, 484-5488.

[25] Grimplet, J., Deluc, L. G., Tillett, R., Wheatley, M. D., Schlauch, K. A., Cramer, G. R., Cushman, J. C. 2007. Tissue-specific mRNA expression in grape berry tissues. *BMC Genomics* 187, 187-200.

[26] Sefton, M. A., Skouroumounis, G. K., Massy-Westropp, R. A., Williams, P. J. 1989. Norisoprenoids in *Vitis vinifera* white wine grapes and the identification of a precursor of damascenone these fruits. *Aust. J. Chem.* 42, 2071-2084.

[27] Sefton, M. A., Francis, I. L., Williams, P. J. 1993. The volatile composition of Chardonnay juices: a study by flavour precursor analysis. *Am. J. Enol. Vitic.* 44, 359-370.

[28] Francis, I. L., Sefton, M. A., Williams, P. J. 1992. Sensory descriptive analysis of the aroma of hydrolysed precursor fractions from Semillon, Chardonnay and Sauvignon blanc grape juices. *J. Sci. Food Agric.* 59, 511-520.

[29] Marais, J., van Wyk, C. J., Rapp, A. 1992. Effect o sunlight and shade on norisoprenoid levels in maturating Weisser Riesling and Chenin blanc wine quality. *S. Afr. J. Enol. Vitic*. 13, 23-32.

[30] Strauss, C. R., Wilson, B., Anderson, R., Williams, P. J. 1987. Development of precursors of C13-norisoprenoids flavorants in Riesling grapes. *Am. J. Enol. Vitic*. 38, 23-27.

[31] Oliveira, C., Silva Ferreira, A. C., Mendes Pinto, M. M., Hogg, T., Alves, F., Guedes de Pinho, P. 2003. Carotenoid compounds found in grapes and their relationship to plant water status. *J. Agric. Food. Chem*. 51, 5967-5971.

[32] Intrigliolo, D. S, Castel, J. R. 2008. Effect of irrigation on the performance of grapevine c.v. Tempranillo in Requena, Spain. *Am. J. Enol. Vitic*. 59, 30-38.

[33] Linsenmeier, A. W., Lohnertz, O. 2007. Changes in norisoprenoid levels with long-term nitrogen fertilization in different vintages of *Vitis vinifera var*. Resling wines. *S. Afr. J. Enol. Vitic*. 28, 17-24.

[34] Main, G. L., Morris, J. R. 2008. Impact of pruning methods on yield compounds and juice and wine composition of Cynthiana grape. *Am. J. Enol. Vitic*. 59, 179-187.

[35] Mendes Pinto, M. M. 2003. *Carotenoids profile in grapes, musts and Port wines*. Master thesis, University of Porto, Porto.

[36] Mendes-Pinto, M. M, Silva Ferreira, A. C., Caris-Veyrart, C., Guedes de Pinho, P. 2005. Evaluation of some carotenoids in grapes by reverse- and normal-phase liquid chromatography: a qualitative analysis. *J. Agric. Food Chem*. 53, 10034-10041.

[37] Mordi, C. M., Walton, J. C, Burton, B. G., Hughes, L., Ingold, U. K., Lindsay, D. A. 1991. Exploratory study of β-carotene auto-oxidation. *Tetrahedron Lett*. 32, 4203-4206.

[38] Kanasawud, P., Crouzet, J. C. 1990. Mechanisms of formation of volatile compounds by thermal degradation of carotenoids in aqueous medium. 1. β-Carotene degradation. *J. Agric. Food Chem*. 38, 237-243.

[39] Isoe, S., Hong, B. S., Sakan, T. 1969. Photooxygention of carotenoids I. The formation of dihydroactinidiolide and β-ionone from β-carotene. *Tetrahedron Lett.* 4, 279-281.

[40] Isoe, S., Hong, B. S., Katsumura, S., Sakan, T. 1972. Photooxygention of carotenoids II. The absolute configuration of loliolide and of dihydroactinidiolide. *Tetrahedron Lett.* 25, 2517-2520.

[41] Isoe, S., Hong, B. S., Katsumura, S., Sakan T. 1973. The synthesis of damascenone and β-damascone and the possible mecahnism of their formation from carotenoids. *Helv. Chim. Acta*, 56, 1514-1516.

[42] Lutz, A., Winterhalter, P. 1992. Isolation of additional carotenoid metabolites from quince fruit (Cydonia oblonga Mill.). *Tetrahedron Lett*. 33, 5169-5172.

[43] Aznar, M., Lopez, R., Cacho, J. F,. Ferreira, V. 2001. Identification and quantification of impact odorants of aged red wines from Rioja. GC-olfatometry, quantitative GC-MS and odor evaluation of HPLC fractions. *J. Agric. Food Chem*. 49, 2924-2929.

[44] Leino, M., Francis, I. L, Kallio, H., Williams, P. J. 1993. Gas-chromatographic headspace analysis of Chradonnay and Semillon wines after thermal processing. Z. *Lebensm. Unters. Forsch.* 197, 29-33.

[45] Marais, J. Versini J., van Wyk, C. J., Rapp, A. 1992. Effect of region on free and bound monoterpene and C13-norisoprenoid concentration in Weisser Riesling wines. *S. Afr. J. Enol. Vitic*. 13, 71-77.

[46] Guth, H. 1997. Identification of characteristic impact odorants of different white wines varieties. *J. Agric. Food Chem*. 45, 3022-3026.

[47] Guth, H. 1997. Quantification and sensory studies of characteristic impact odorants of different white wines varieties. *J. Agric. Food* Chem. 45, 3027-3032.

[48] de Freitas, V. A. P, Ramalho, P. S., Azevedo, Z., Macedo, A. 1999. Identification of some volatile descriptors of the rock rose-like aroma of fortified red wines from Douro demarcated region. *J. Agric. Food Chem*. 47, 4327-4331.

[49] Silva Ferreira, A. C., de Pinho, P. G. 2004. Nor-isoprenoids profile during port wine ageing- influence of some technological parameters. *Anal. Chim. Acta* 513, 169-176.

[50] Eggers, N. J., Bohna, K., Dooley, B. 2006. Determination of vitispirane in wines by stable isotope dilution assay. *Am. J. Enol. Vitic*. 57, 226-232.

[51] Fang, Y., Qian, M. C. 2006. Quantification of selected aroma-active compounds in Pinot noir wines from different grape maturities. *J. Agric. Food Chem*. 54, 8567-8573.

[52] Alves, R. F., Nascimento, A. M. D., Nogueira, J. M. F. 2005. Characterization of the aroma profile of Madeira wine by sorptive extraction technique. *Anal. Chim. Acta* 546, 11-21.

[53] Ferreira, V., Ortin, N, Escudero, A., Lopez, R. Cacho, J. 2003. Chemical characterization of the aroma of Grenache rose wines, aroma extract dilutions analyses, quantitative determination and chemometry study. *J. Agric. Food Chem.* 50, 4048-4054.

[54] Genovese, A., Gambuti, A., Piombino, P., Moio, L. 2007. Sensory properties and aroma compounds of sweet Fiano wine. *Food Chem.* 103, 1228-1236.

[55] Boido, E., Lloret, A., Medina, K, Farina L., Carrau F., Versini G., Dellacassa, E. 2003. Aroma composition of *Vitis vinifera* cv Tannat: the typical red wine from Uruguay. *J. Agric. Food Chem. 51*, 5408-5413.

[56] Kotseridis, Y., Baumes, R. L, Bertrand, A., Skouroumounis, G. K. 1999. Quantitative determination of β-ionone in red wines and grapes of Bordeaux using a stable isotope diluton assay. *J. Chromatogr. A* 848, 317-325.

[57] Pineau, B., Barbe, J. C., van Leeuwen, C., Dubourdieu, D. 2007. Which impact of b-damascenone on red wines aroma? *J. Agric. Food Chem*. 55, 4103-4108.

[58] Demole, E., Enggist, P., Sauberli, U., Stoll, M., Kovats, E. 1970. Structure et synthèse de la damascénone (trymethyl-2,6-6-trans-crotonoyl-1-cyclohexadiène-1,3), constituant odorant de l´essence de rose bulgare (rosa damascena Mill.). *Helv. Chim. Acta* 53, 541.

[59] Schreier, P., F. Drawert, F. 1974. Investigation of volatile components in wine by gas chromatography and mass-spectrometry. I. Non polar compounds of wine flavour white wines. *Z. Lebensm. Unters. Forsch.* 154, 273-278.

[60] Buttery, R. G, Teranish, R., Ling, L. C, Turbaugh, J. G. 1990. Quantitative and sensory studies on tomato paste volatiles. *J. Agric. Food Chem.* 38, 336-340.

[61] Schreier, P. Drawert, F, Junker, A. Z. 1976. GLC-mass-spectrometrical investigation of the volatile compounds of wines. IV. Aroma compounds of Tojak aszu wines. a) neutral compounds. Z. *Lebensm. Unters. Forsch.* 161, 249-258.

[62] Etievant, P. X. 1991. Wine. In: *Volatile compounds in Food and Beverages*, *TNO-CIVO, Food Analysis* Institute Zeist (ed. H. Maarse), 483-546. The Netherlands.

[63] Rapp, A., Mandery, H. 1986. Wine aroma. *Experimentia* 42, 873.

[64] Simpson, R. F., Strauss, C. R, Williams, P. J. 1977. A C13 spiro-ether in the aroma volatiles of grape juices, wines and destilled grape spirits. *Chem. Ind*. 15, 663-664.

[65] Schulte-Elte, K. H, Gautschi, F., Renold, W., Hauser, A., Franhauser, P., Limacher, J., Ohloff, G. 1978. Vitispiranes, important constituents of vanilla aroma. *Hev. Chim. Acta* 61, 1125-1133.

[66] Full, G., Winterhalter, P. Application of on-line coupled mass spectrometric techniques to the study of isomeric vitispiranes and precursors of grapevine c.v. Riesling. 1994. *Vitis* 33, 241-244.

[67] Sakan, T, Isoe, S., Hyeon, S. B. 1967. The structure of actinidiolide, dihydroactniolide and actinidol. *Tetrahedron Lett*. 8, 1623-1627.

[68] Dimitriadis, E., Strauss, C. R, Wilson, B., Williams, P. J. 1985. The actnidiols: nor-isoprenoid compounds in grapes, wines and spirits. *Phytochem.* 24, 767-770.

[69] Isoe, S., Hyeon, S. B., Ichikawa H., Katsumura, H., Sakan, T. 1968. The synthesis of actiniolide, dihydroactniolide and actinidol. *Tetrahedron Lett.* 9, 5561-5563.

[70] Williams, P. J., Sefton, M. A., Wilson, B. 1989. Nonvolatile conjugates of secondary metabolites as precursors of varietal flavour compounds. In: *Flavour Chemistry-Trends and Developments* (eds. R. Teranishi, R. G. Buttery, F. Shahidi), pp. 35-48. *ACS*, Symp. Ser. 802. Am. Chem. Soc. Washington DC, USA.

[71] Simpson, R. F. 1978. Aroma and compositional change in wine with oxidation, storage and aging. *Vitis* 17, 274-287.

[72] Simpson, R. F. 1978. 1,1,6-Trimethyl-1,2-dihydronaphthalene- important contribution to bottle aged bouquet of wine. *Chem. Ind.* 1, 37.

[73] Simpson, R. F., Miller, G. C. 1983. Aroma composition of aged Riesling wine. *Vitis* 22, 51-63.

[74] Winterhalter, P., Sefton, M. A., Williams, P. J. 1990. Volatile C13-norisoprenoid compounds in Riesling wine are generated from multiple precursors. *Am. J. Enol. Vitic*. 41, 277-283.

[75] Marais, J. van Wyk, C. J., Rapp, A. 1992. Effect of storage time, temperature and region on the levels of 1,1,6-trimethyl-1,2-dihydronaphthalene and other volatile and on quality of Weisser Riesling wines. *S. Afr. J. Enol. Vitic*. 13, 33-44.

[76] Winterhalter, P. 1991. 1,1,6-Trimethyl-1,2-dihydronafthalene (TDN) formation in wine. Studies of the hydrolysis of 2,6,10,10-tetramethyl-1-oxaspiro[4,5]dec-6-ene-2,8-diol rationalising the origin of TDN and related C13-norisoprenoids in Riesling wine. *J. Agric. Food Chem*. 39, 1825-1829.

[77] Winterhalter, P., Sefton, M. A., Williams, P. J. 1990. A new C13-norisoprenoid intramolecular acetal in Riesling wines. *Chem. Ind.* 463-464.

[78] Janusz, A., Capone, D. L., Puglisi, C. J., Perkins, M. V., Elsey, G. M., Sefton, M. A. 2003. (*E*)-1-(2,3,6-Trimethylphenyl)buta-1,3-diene: a potent grape-derived odorant in wine. *J. Agric Food Chem*. 51, 7759-7763.

[79] Cox, A., Capone, D. L., Elsey, G. M., Perkins, M. V., Sefton, M. A. 2005. Quantitative analysis, occurrence and stability of (*E*)-1-(2,3,6-trimethylphenyl)buta-1,3-diene in wine. J. *Agric. Food Chem*. 53, 3584-3591.

[80] Cox, A., Skouroumounis, G. K., Elsey, G. M., Perkins, M. V., Sefton, M. A. 2005. Generation of *E*)-1-(2,3,6-trimethylphenyl)buta-1,3-diene from C13-norisoprenoid precursor. *J. Agric. Food Chem*. 53, 6777-6783.

[81] Sefton, M. A., Francis, I. L., Williams, P. J. 1990. Volatile norisoprenoid compounds as constituent of oak woods used in wine and spirit maturation. *J. Agric. Food Chem*. 38, 2045-2049.

[82] Kotseridis, Y., Baumes, R. 2000. Identification of impact odorants in Bordeaux red grape juice, in the commercial yeast used for its fermentation and in the produced wine. *J. Agric. Food Chem*. 48, 400-406.

[83] Jung, D. M., Ebeler, S. E. 2003. Headspace solid-phase microextraction method for the study of the volatility of selected flavour compounds. *J. Agric. Food Chem*. 41, 200-205.

[84] Aronsona, J., Ebeler, S. 2004. Effect of polyphenol compounds on the headspace volatility of flavours. *Am. J. Enol. Vitic.* 55, 13-21.

[85] Gawel, R., Francis, L., Waters, L. J., 2007. Statistical correlations between the in-mouth textural characteristics and the chemical composition of Shiraz wines. *J. Agric. Food Chem.* 55, 2683-2687.

[86] Cortell, J. M., Sivertsen, H. K., Kennedy, J. A., Heymann, H. 2008. Influence of vine vigor on Pinot noir fruit composition, wine chemical analysis, and wine sensory attributes. *Am. J. Enol. Vitic.* 59, 1-10.

[87] Preston, L. D., Block, D. E., Heymann, H., Soleas, G., Noble, A. C., Ebeler, S. E. 2008. Defining vegetal aromas in Cabernet sauvignon using sensory and chemical evaluation. *Am. J. Enol. Vitic*. 59, 137-145.

[88] Campo, E., Ferreira, V., Escudero, A., Cacho, J. 2005. Prediction of the wine sensory properties related to grape variety from dynamic-headspace gas chromatography-olfatometry data. *J. Agric Food Chem*. 53, 5682-5690.

[89] Roussis, I. G., Sergiantis, S. 2008. Protection of some aroma volatile in a model wine medium by sulphur dioxide and mixtures of glutathione with caffeic acid or gallic acid. *Flavour Frag. J.* 23, 35-39.

[90] Escudero, A., Campo, E., Farina, L., Cacho, J., Ferreira, V. 2007. Analytical characterization of the aroma of five premium red wines. Insights into the role of odour families and the concept of fruitness wines. *J. Agric. Food Chem*. 55. 4501-4510.

[91] Aznar, M., Lopez, R., Cacho, J., Ferreira, V. 2003. Prediction of aged red wine aroma properties from aroma chemical composition. *J. Agric. Food Chem*. 51, 2700-2707.

[92] Escudero, A., Gogorza, B., Melus, M. A., Ortin, N., Cacho,J., Ferreira, V. 2004. Characterization of the aroma of a wine from Maccabeo key role played by compounds with low odour activity values. *J. Agric. Food Chem*. 52, 3516-3524.

[93] Daniel, M. A., lsey, G. M., Capone, D. L., Perkins, M. V., Sefton, M. A. 2004. Fate of damascenone in wine: the role of SO_2. *J. Agric. Food Chem*. 52, 8127-8131.

[94] Gunata, Y. Z., Bayonove, C. L., Baumes, R. L., Cordonnier, R. E. 1985. The aroma of grapes. I. Extraction and determination of free and glycosidically bound fraction of some grape aroma components. *J. Chromatogr. A* 331, 83-90.

[95] Skouroumounis, G. K., Massy-Westropp, R. A., Sefton, M. A., Williams, P. A. 1992. Precursors of damascenone in fruit juices. *Tetrahedron Lett.* 33, 3533-3536.

[96]Stefano, R. D., Bottero, S., Pigello, R., Borsa, D., Bazzo, G., Corno, L. 1988. Glycosilated aroma precursors in red winemaking grape cv. *Enotecnico* 34, 63-74.

[97] Mathieu, S., Terrier, N., Procureur, J., Bigey, Gunata, Z. 2005. A carotenoid cleavage dioxygenase from *Vitis vinifera L. J. Exp. Botany* 56, 2721-2731.

[98] Mathieu, S., Bigey, F., Procureur J., Terrier, N., Gunata, Z. 2007. Production of recombinant carotenoid cleavage dioxygenase from grape and enzyme assay in water-miscible organic solvents. *Biotechnol. Lett.* 29, 837-841.

[99] Isoe, S., Katsumura, S., Hong, B. S., Sakan, T. 1971. Biogenetic type synthesis of grasshopper ketone and ioliolide and a possible biogenis of allenic carotenoids. *Tetrahedron Lett.* 16, 1089-1971.

[100] Eugster, C. H., Marki-Fischer, E. 1991. The chemistry of rose pigments. *Angew. Chem. Int*. 30, 654-658.

[101] Fleischmann, P., Studer, K., Winterhalter, P. 2002. Partial purification and kinetic characterization of a carotenoid cleavage enzyme from quince fruit (Cydonia oblonga). *J. Agric. Food Chem*. 50, 1677-1680.

[102] Winterhalter, P., Sefton, M. A., Williams, P. J. 1990. Two dimensional GC-DCCC analysis of the glycocomjugates of monoterpenes, norisoprenoids, and shikinate-derived metabolites from Riesling wines. *J. Agric. Food Chem*. 38, 1041-1048.

[103] Waldmann, D., Winterhalter, P. 1992. Identification of a novel vitispirane in Riesling wine. *Vitis* 31, 169-174.

[104] Strauss, C. R., Dimitriadis, E., Wilson, B., Williams, P. J. 1986. Studies of the hydrolysis of two megastigma- 3,6,9-triols rationalizing the origins of some volatile C13-norisoprenoids of *Vitis vinifera* grapes. *J. Agric. Food Chem*. 34, 145-149.

[105] Skouroumounis, G. K., Winterhalter, P.1994. Glycosidically bound morisoprenoids from *Vitis vinifera cv.* Rielsing leaves. *J. Agric. Food Chem*. 42, 1068-1072.

[106] Bezman, Y., Bilkis, I., Winterhalter, P., Fleischmann, P., Rouseff, R. L., Baldermann, S. Naim, M. 2005. Thermal oxidation of 9'-*cis*-neoxanthin in a model system containing peroxyacetic acid leads to the potent odorant β-damascenone. *Agric. Food Chem.* 53, 9199-9206.

[107] Silva Ferreira, A. C, Monteiro, J., Oliveira, C., de Pinho, P. G. 2008. Study of major aromatic compounds in port wines from carotenoid degradation. *Food Chem.* 110, 83-87.

[108] Kotseridis, Y., Baumes, R. L., Skouroumounis, G. K. 1999. Quantitative determination of free and hydrotically liberated β-damascenone in red grapes and wines using isotope dilution assay. *J. Chromatogr. A* 849, 245-254.

[109] Camara, J. S., Herbet, P., Marques, J. C., Alves, M. A. 2004. Varietal flavour compounds of four grape varieties producting Madeira wines. *Anal. Chim. Acta* 513, 203-207.

[110] Lopez, R., Ezpeleta, E., Sanchez, I., Cacho, J, Ferreira, V. 2004. Analysis of the aroma intensities of volatile compounds released from wild acid hydrolisates of odourless precursors extracted from Trempanillo and Grenache using gas chromatography-olfatometry. *Food Chem.* 88, 95-103.

[111] Oliveira, C., Barbosa, A., Silva Ferreira, A. C., Guerra, J., de Pinho, P. G. 2006. Carotenoid profile in grapes related to aromatic compounds in wines from Douro region. *J. Food Sci.* 71, S001-S007.

[112] Ugliano, M. Moio, L. 2008. Free and hydrolytically released volatile compounds of *Vitis vinifera L. cv*. Fiano grapes as odour-active constituents of Finao wine. *Anal. Chim*. *Acta* 621,79-85.

[113] Esti, M., Tamborra, P. 2006. Influence of winemaking techniques on aroma precursor. *Anal. Chim. Acta* 563, 173-179.

[114] Pogorzelski, E., Wilkowska, A. 2007. Flavour enhancement through the enzymatic hydrolysis of glycosidic aroma precursors in juices and wine beverages: a review. *Flavour Fragr. J*. 22, 251-254.

[115] Zoecklein, B. W., Hackney, C. H., Duncan, S. E., Marcy, J. E. 1999. Effect of fermentation, aging and thermal storage of total glycosides, phenol-free glycosides and volatile compounds of white Riesling (*Vitis vinifera L.*). *J. Ind. Microb. Biotchnol*. 22, 100-107.

[116] de La Presa-Owens, C., Noble, A. C. 1997. Effect of storage at elevated temperature on aroma of Chardonnay wines. *Am. J. Enol. Vitic*. 48, 310-316.

[117] Ferreira, V., Aznar, M, Cacho, J. 2001.Quantitative gas chromatography-olfatometry carried out at different dilutions of an extract. Key differences in the odour profile of flavour high-quality Spanished aged red wines. *J. Agric. Food Chem.* 49, 4818-4824.

SUMMARY

Biological functions of carotenoids involving interaction with light, such as coloration and in photosynthesis, are determined by the electronic properties of the conjugated polyene chain that is characteristic of carotenoid molecules. Molecular interactions with proteins *in vivo,* in the specific environment of the carotenoid binding pocket, can tune the electronic properties of the carotenoid, thereby changing the light absorption properties so that a spectral red-shift is observed relative to the molecule *in vitro*. Understanding how these properties are tuned *in vivo* is essential for understanding the mechanisms underlying carotenoid function, and is a major challenge for carotenoid research.

This challenge is addressed in this thesis, which aims to investigate the possible molecular factors that determine or contribute to the absorption spectral shifts *in vivo*. This study has used resonance Raman spectroscopy associated with electronic absorption spectroscopy to characterize the structure of the electronic ground state of the carotenoid molecule *in vivo* by the selective enhancement of the vibrational modes coupled to the $S_0 \rightarrow S_2$ electronic transition.

In Chapter 2, the electronic properties of nine relatively simple linear and β-ring cyclic carotenoids molecules are addressed. A systematic investigation *in vitro* of the correlations between the position of the $S_0 \rightarrow S_2$ electronic transition, the frequency of ν_1 Raman band and the conjugation chain length N is presented. Excellent correlations were found for linear carotenoids. For the β-ring cyclic carotenoids, whereas the two spectroscopic parameters also exhibit an excellent correlation, a deviation from the linear correlations with the nominal conjugation chain length N was observed, consistent with the conclusion that β-carotene and β-ring cyclic carotenoids display an effective conjugation chain length shorter than that expected from their formal chemical structure, due to twisting of the β-ring out of the plane.
Furthermore, the effect of solvent properties on the two spectroscopic parameters for four molecules was also addressed. Linear correlations between these parameters and

solvent polarizability, expressed as $R(n) = (n^2-1) / (n^2+2)$, where n = refractive index, were observed. No such correlation was found as a function of solvent polarity (ε, dielectric constant). The correlations obtained between the position of the $S_0 \rightarrow S_2$ electronic transition and the frequency of the ν_1 Raman band expressed as (i) function of change in the effective conjugation chain length (different carotenoids in same solvent(in hexane) or (ii) function of solvent polarizability (same carotenoid in different solvents), exhibit very different slopes. Such different correlations can be useful to distinguish between these two mechanisms as possible causes of the shifts in $S_0 \rightarrow S_2$ electronic transition, the absorption shifts, *in vivo*. Consequently, this information was applied to the example of the absorption shifts of carotenoid bound to light-harvesting (LH) proteins in photosynthetic purple bacteria. The average polarizability of the protein environment, predicted to be similar for these three LH proteins, can fully account for the spectral shifts of these carotenoids.

This chapter provides groundwork for the spectroscopic studies of carotenoid absorption properties *in vivo* presented in the following Chapters 3 and 4, which represent two very different biological systems of carotenoid interactions with proteins.

Chapter 3 present a spectroscopic study of feathers from the brilliant red scarlet ibis (*Eudocimus ruber,* Threskiornithidae), the orange-red summer tanager (*Piranga rubra,* Cardinalidae) and the violet-purple feathers of the white-browed purpletuft (*Iodopleura isabellae,* Tityridae). All these plumage patches contain canthaxanthin as their major carotenoid. In order to investigate the structural changes and molecular interactions, responsible for the different colors of canthaxanthin in these feathers, a comparative study was made between the resonance Raman and electronic absorption spectra deduced from reflectance spectra of canthaxanthin bound *in situ,* and data recorded from canthaxanthin in solution. The results show that canthaxanthin binds differently to the feather keratin proteins in the different species of birds. A significant variation was observed in the frequency of the ν_1 Raman band among the birds, and this correlates well with the red-shifts in the absorption spectra exhibited by canthaxanthin in each of the feathers. The most significant of these is seen in *I. isabellae.* The entire extent of the red-shift in the violet feathers, however, cannot be explained by the

polariability/refractive index of the binding site nor by the coplanarity of the β-rings. It is proposed that, along with these two factors, a head-to-tail molecular aggregation of the bound carotenoid molecules is likely to be an important additional factor responsible for the violet color of *I. isabellae*. Additional work will be required to confirm the presence of molecular aggregates in this feather and also to define whether the carotenoid binds directly to β-keratin or to another protein or molecule and to assess the possibility of other interactions with the protein, *e.g.* via the C=O groups of canthaxanthin.

In Chapter 4, the absorption shifts of the two β-carotenes in PSII-RC and those of the two luteins in LHCII were investigated. The evaluation of the molecular factors underlying these absorption shifts was complemented by the structural information on the carotenoid binding pocket provided by the three-dimensional structure of these proteins as determined by X-ray crystallography. The results show that the carotenoid molecules with lowest absorption maximum, here named blue-absorbing carotenoids, are mainly influenced by the local environment associated with the protein, since they fit on the linear correlations obtained for β-carotene and lutein expressed as function of solvent polarizability. This observation is shown to be consistent with the structural information of the binding sites. Concerning the red-absorbing molecules (with relatively highest absorption maximum), the shift in the $S_0 \rightarrow S_2$ electronic transition is proposed to be due to an increase of the effective conjugation chain length N due to coplanarization of the β-end rings with the polyene chain induced by local steric hindrances.

The research work presented in this thesis represents a considerable contribution to the understanding of how the electronic properties of carotenoids *in situ* may be tuned by the conditions of the protein binding site *in vivo*. Addressing the possible factors responsible for the absorption behaviour of carotenoids in birds and higher plants may help in the elucidation of absorption tuning in other living organisms, and provide useful information on how the electronic properties of carotenoid molecules are tuned to optimise their different functions.

In addition, a general survey of the existing knowledge on the carotenoid breakdown products- the norisoprenoids- and their higly sensorial impact on wine aroma, is reviewed and presented in Chapter 5. Key information extensively reported in the literature for the last decades is considered. Particular focus is given on the several parameters that affect both qualitative and quantitative profile of carotenoids in grapes, the relevance of norisoprenoids to the wine aroma, their chemical and sensorial characterization, and the proposed realistic mechanisms for their formation involving β-carotene and neoxanthin as norisoprenoids precursors. The overall contribution to the wine aroma and some of the open challenges for carotenoid research and wine aroma were proposed.

SAMENVATTING

Inzicht in moleculaire mechanismes van eigenschappen van carotenen

De biologische functies van carotenen die met de interactie van licht te maken hebben, bijvoorbeeld kleur en fotosynthese, worden bepaald door elektronische eigenschappen van de karakteristieke geconjugeerde polyeen keten van carotenen. Moleculaire interacties met eiwitten *in vivo*, in de specifieke omgeving van de bindingspocket van het caroteen, kunnen de elektronische eigenschappen van het caroteen veranderen. Daardoor veranderen de lichtabsorptie eigenschappen zodat een roodverschuiving optreedt ten opzichte van het molecuul *in vitro*. Begrijpen hoe deze eigenschappen *in vivo* veranderen is essentieel voor het begrijpen van de mechanismes onderliggend aan de functies van caroteen en is een grote uitdaging voor caroteenonderzoek.

Dit proefschrift gaat over deze uitdaging en heeft tot doel het onderzoeken van mogelijke moleculaire factoren die bepalend zijn voor of bijdragen aan de absorptieverschuivingen *in vivo*. In dit onderzoek is Raman spectroscopie samen met elektronische absorptie spectroscopie gebruikt om de structuur van de elektronische grondtoestand van het caroteen molecuul *in vivo* te karakteriseren door middel van selectieve versterking van de vibrationele modi gekoppeld aan de elektronische $S_0 \rightarrow S_2$ overgang.

In Hoofdstuk 2 worden de elektronische eigenschappen van negen relatief eenvoudige lineaire en β-ring cyclische caroteen moleculen behandeld. Een systematisch onderzoek *in vitro* van de correlaties tussen de positie van de elektronische $S_0 \rightarrow S_2$ overgang, de frequentie van de ν_1 Raman band en de conjugatie lengte N wordt gepresenteerd. Zeer goede correlaties werden gevonden voor lineaire carotenen. Voor de en β-ring cyclische carotenen, waar de twee spectroscopische parameters ook een zeer goede correlatie vertonen, is een afwijking van de lineaire correlatie met de conjugatie lengte N waargenomen. Dit is consistent met de conclusie dat β caroteen en β-ring cyclische carotenen effectief een kortere conjugatielengte hebben dan verwacht zou worden op basis van de chemische structuur; dit omdat de β-ring uit het vlak draait.

Daarnaast is het effect van eigenschappen van het oplosmiddel op de twee spectroscopische parameters onderzocht voor vier moleculen. Lineaire correlaties

werden gevonden tussen deze parameters en oplosmiddel polarizeerbaarheid, uitgedrukt als $R(n) = (n^2-1)/(n^2+2)$, waar n = refractie-index. Een dergelijke correlatie werd niet gevonden als functie van de polariteit (ε, diëlectrische constante). De correlaties die werden gevonden tussen de positie van de elektronische $S_0 \rightarrow S_2$ overgang en de frequentie van de ν_1 Raman band uitgedrukt als (i) functie van verandering in de effectieve conjugatie lengte (verschillende carotenen in hetzelfde oplosmiddel, hexaan) of (ii) functie van oplosmiddel polarizeerbaarheid (zelfde caroteen in verschillende oplosmiddelen), tonen verschillende richtingscoëfficiënten. Zulke verschillende correlaties kunnen nuttig zijn om onderscheid te maken tussen deze twee mechanismes als mogelijke oorzaken van de verschuiving in de elektronische $S_0 \rightarrow S_2$ overgang, de absorptieverschuiving, *in vivo*. Vervolgens is deze informatie toegepast bij de absorptieverschuivingen in caroteen gebonden aan light-harvesting (LH) eiwitten in fotosynthetische paarse bacteriën. De gemiddelde polarizeerbaarheid van de eiwitomgeving, die vergelijkbaar wordt geschat voor deze drie LH eiwitten, kan de spectrale verschuivingen van deze carotenen volledig verklaren.

Hoofdstuk 3 toont een spectroscopisch onderzoek van veren van de felrode rode ibis (*Eudocimus ruber,* Threskiornithidae), de oranjerode zomertangare (*Piranga rubra,* Cardinalidae) en de paarse veren van de witkeeldwergcotinga (*Iodopleura isabellae,* Tityridae). Al deze verendekken bevatten canthaxanthin als belangrijkste caroteen. Om de structuurveranderingen en moleculaire interacties die verantwoordelijk zijn voor de verschillende kleuren van canthaxanthin in deze veren te bestuderen, werd een vergelijkend onderzoek gedaan tussen de resonantie Raman en elektronische absorptie spectra, afgeleid van reflectie spectra van gebonden canthaxantin *in situ* en van canthaxantin data gemeten in oplossing. De resultaten tonen dat canthaxanthin verschillend bindt aan de keratine eiwitten in de veren van de verschillende vogelsoorten. Een significante variatie werd waargenomen in de frequentie van de ν_1 Raman band van de verschillende vogels. Dit heeft een goede correlatie met de roodverschuivingen in de absorptiespectra van canthaxantin in de verschillende veren. Het meest significante voorbeeld hiervan is *I. isabellae*. De roodverschuivingen in de paarse veren kunnen echter niet volledig worden verklaard door verschillen in poralizeerbaarheid of refractie-index van de bindingssite, noch door het coplanair zijn

van de β-ringen. De suggestie wordt gedaan dat, naast deze twee factoren, een moleculaire kop-staart aggregatie van de gebonden carotenen waarschijnlijk een belangrijke factor is bij de paarse kleur van *I. isabellae*. Vervolgonderzoek zal nodig zijn om de aanwezigheid van moleculaire aggregaten te bevestigen en ook om te bepalen of het caroteen direct bindt aan β-keratine of aan een ander eiwit of molecuul en om de mogelijkheid van andere interacties met het eiwit, bijvoorbeeld via de C=O groepen van canthaxantin te onderzoeken.

In Hoofdstuk 4 worden the aborptieverschuivingen van de twee β-carotenen in PSII-RC en de β-carotenen in LHCII onderzocht. De evaluatie van moleculaire factoren die ten grondslag liggen voor deze verschuivingen werd aangevuld met structurele informatie over de caroteen bindingspocket uit de driedimensionale structuur van deze eiwitten uit röntgenkristallografie. De resultaten tonen dat de caroteenmoleculen met het laagste absorptiemaximum, hier blauw-absorberend genoemd, voornamelijk beïnvloed worden door de lokale omgeving van het eiwit, omdat deze passen in de lineaire correlaties die werden gevonden voor β-caroteen en luteïne als functie van polarizeerbaarheid van het oplosmiddel. Deze waarnemen blijkt in overeenstemming met de structurele informatie van de bindingssites. Betreffende de rood-absorberende moleculen (met het hoogste absorptiemaximum), wordt gesuggereerd dat de verschuivingen in de elektronische $S_0 \rightarrow S_2$ overgang het gevolg is van een toenemende effectieve conjugatielengte N vanwege coplanarizatie van de β-ringen aan het einde van de polyeenketen vanwege sterische hinder.

Het onderzoek dat in dit proefschrift wordt gepresenteerd draagt bij aan het begrijpen van hoe elektronische eigenschappen van carotenen *in situ* veranderd kunnen worden door de omstandigheden van de eiwitbindingssite *in vivo*. Het bestuderen van de verschillende factoren die verantwoordelijk zijn voor het absorptiegedrag van carotenen in vogels en hogere planten kan helpen in het ontrafelen van absorptieverschuivingen in andere levende organismes en kan waardevolle informatie geven over hoe de elektronische eigenschappen van caroteenmoleculen geoptimaliseerd worden voor verschillende functies.

Hiernaast wordt in Hoofdstuk 5 een overzicht gegeven van de bestaande kennis over afbraakproducten van caroteen- de norisoprenoïdes- en hun grote invloed op de aroma

van wijn. Belangrijke informatie die in de afgelopen tientallen jaren is gerapporteerd in de literatuur wordt beschouwd. De parameters die zowel kwalitatief als kwantitatief het profiel van carotenen in druiven bepalen worden uitgelicht, de relevantie van norisoprenoïdes voor wijn aroma, chemische- en waarnemingskarakterisatie en het voorgestelde realistische mechanisme voor de vorming daarvan met β-caroteen en neoxanthin als precursor. De bijdrage aan wijnaroma en een aantal openstaande uitdagingen voor caroteenonderzoek en wijnaroma worden benoemd.

ACKNOWLEDGMENTS

I would like to thank, first of all, Prof. Bruno Robert, for believing that I could do a PhD thesis in Biophysics, in a field where almost the only recognizable thing to me was the carotenoid molecules. I thank him for his supervision, enthusiasm and for having shared with me his admirable perception of science, always with bright thinking and curiosity.

My gratitude goes also to Prof. Harry Frank and Amy LaFountain for their interest and strong commitment during the valuable collaboration in the study involving the bird feathers.

For the coauthors of the papers my thanks for their contribution to the work, in particular to my group colleagues.

To Janneke Ravensbergen for have kindly translated both title and summary into Dutch.

To all the persons I met during my stay at CEA-iBiTec-S\SB2SM, my thanks for their kindness and help. To those I treasure as friends, my sincere thanks for lighting up my days with your smiles and care, specially when I needed the most.

To Dr. George Britton, my special thanks for his endless support and for all that I have been learning from him.

Finalmente, agradeço do fundo do coração aos meus amigos e á minha família, por todo o apoio e carinho e por acreditarem sempre que lhes digo que tem que valer a pena. Parafraseando Fernando Pessoa, "*Tudo vale a pena quando a alma não é pequena*".